

**ANNUAL REPORT OF THE
FRAUNHOFER-INSTITUTE FOR
MICROELECTRONIC CIRCUITS
AND SYSTEMS
IMS DUISBURG 2011**

PREFACE

For Fraunhofer IMS the year 2011 was characterized by the stabilization of the high level reached in the previous year. With an increasing number of employees in comparison to the previous year, the operating budget in 2011 amounted to 25,8 million euros. Therefore the good results of 2010 could be increased slightly.

Project cooperations and alliances

Fraunhofer IMS could gain the first multinational project within the HTA – Heterogeneous Technology Alliance. The HTA is an alliance of four great European application-oriented research institutes: The CEA Leti (France), the Fraunhofer Group of Microelectronics (Germany), the CSEM (Switzerland) and VTT (Finland). The main target of the HTA cooperation is to build up application oriented partnerships with the European industry.

The business unit “High-temperature electronics” acquired further chip design projects in 2011. Our SOI CMOS processes are an excellent technology platform for high temperature applications with operating temperatures up to 250 °C.

The successful cooperation with ELMOS in the area of CMOS processes as well as with Infineon in the area of SOI high voltage components could be expanded in 2011.

In February 2011 Dr. Trieu resigned from Fraunhofer IMS and responded the call of the Hamburg University of Technology, where he directs the institute of microsystems technology. We are looking forward to cooperate with Professor Trieu also in future.

According to the standards ISO 13485 and IEC62304 for medical devices the TÜV Süd audited a hard- and software development of the Fraunhofer IMS. That marks a further development step for this medical application.



Under the direction of Dr. Tom Zimmermann the working group "Biohybrid Systems" has been enlarged. In this area the engineers link biological and biochemical parameters with electronics. The development of biohybrid systems enables completely new approaches to the markets: Life Sciences, Medicine, Chemistry, Environment, Food Industry and Safety engineering.

Events 2011

In the 26th year of Fraunhofer IMS the Microsystems Technology Lab has been completed and officially opened on June 22nd. Minister Schulze, State Secretary Rachel and the Fraunhofer Research Senior Vice President Professor Buller were our guests of honor at the opening of the new MST Lab&Fab. In the MST Lab&Fab the conventional CMOS technology is expanded by Post-Processing. Additional layers of different materials are added to the conventional CMOS wafers, which enables a variety of supplementary functions and by these new fields of application. By this further strategic development Fraunhofer IMS aims at the development of new markets in medical engineering, building technology and industrial electronics.

The celebration of the 10-years-existence of the Fraunhofer-inHaus-Center was another highlight in 2011. At the inHaus-Center the potentials and competences of several Fraunhofer institutes and more than 80 commercial partners are successfully combined to develop, to test and to bring future-oriented product components and system solutions for residential and commercial buildings to the market.

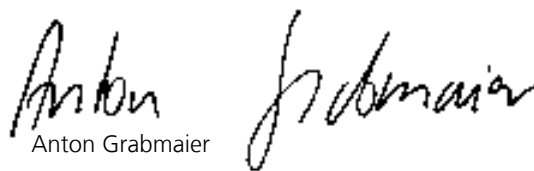
At the user forum for wireless sensor technology in industry and logistics in November the question was handled how production and logistic processes in the industry can be optimized in future and which advantages wireless technologies in comparison to wired systems have.

On the basis of precise application examples more than 50 participants talked about technical challenges and their solutions.

Also in November the inHaus-forum "The energy turnaround in buildings – trends and solutions for future energy systems" took place. The main topic "energy efficiency" in rooms and buildings was addressed to service providers, suppliers, the housing and real estate industry, the manufacturers of building services engineering of all kinds, architects, expert planners and craftsmen, but also to interested persons from research, politics and the fields of application of real estates like office, hospital, nursing home, hotel.

I would like to thank all our business partners for the trustful cooperation in the last year.

My special thanks go to our employees who have enabled the economic and scientific success in 2011 by their dedicated work. Despite the recent European currency turmoil and the associated difficult market prospects we are well prepared for the future.


Anton Grabmaier

CONTENTS

Profile	7
Fraunhofer IMS Business Fields and Core Competencies	11
Development of the IMS	21
Selected Projects of the year 2011	
I CMOS Devices and Technology	
Photodiodes Reducing the Impact of Process Variations on the Sensitivity of CMOS F. Hochschulz, S. Dreiner, H. Vogt, U. Paschen	26
Intelligent Nano-modified 3d-Electrodes A. Jupe, A. Hoeren, A. Goehlich, H. Vogt	30
Radiation-hard CMOS Image Sensor Process J. Fink, F. Hochschulz	33
II Silicon Sensors and Microsystems	
Test of Uncooled Passive IRFPAs in Batch-Production A. Utz, L. Gendrisch, S. Kolnsberg, F. Vogt	36
A Far Infrared Uncooled VGA-IRFPA for Automotive Applications D. Weiler	40
Intravascular Monitoring System for Hypertension M. Görtz, P. Fürst	43
CMOS Pixels for Pulsed 3D Time-of-Flight Sensors D. Durini, A. Spickermann	47
CMOS High-Frame-Rate HDTV Sensor G. Varga, D. Durini	50

III CMOS Circuits

Interface for OLEDs on CMOS Circuits 53
S. Weyers

High Temperature Embedded Microcontroller for Harsh Environments 55
H. Kappert

Mixed-Signal/Analog Signal Conditioning Circuitry
for Wide Temperature Range Applications 57
A. Schmidt

IV Wireless Chips and Systems

Digital Radio Receiver for an UHF RFID System With an
Undersampling Digitalization Scheme 61
S. Grey, G. vom Bögel

Radio Frequency Powering of Microelectronic Sensor Modules 67
G. vom Bögel, F. Meyer, M. Kemmerling,

Wireless Integrated Pressure Sensor for Quality Control of Vacuum Insulation Panel 73
G. vom Boegel, M. Goertz, M. Kemmerling

A New Indoor Localization System With Improved Multipath Mitigation 78
M. Marx

V Systems and Applications

Building Automation: Building and Infrastructure Services 81
H.-J. Schliepkorte

List of Publications and Scientific Theses 2011	87
Chronicle 2011	97
Preis des Bundespräsidenten „Ort der Idee 2011“ B. Tenbosch, K. Scherer	98
The Opening of the New Microsystems Technology Lab&Fab S. van Kempen, M. van Ackeren, H. Vogt	99
CONLIFE and REHACARE B. Tenbosch, K. Scherer	100
IVAM Round Table S. van Kempen, M. van Ackeren, H. Vogt	101
The User Forum for Wireless Sensor Technology S. van Kempen, M. van Ackeren, G. vom Bögel	102
Fairs and Exhibitions S. van Kempen, M. van Ackeren	103
inHaus-Forum 2011 B. Tenbosch, K. Scherer	104
Press Review	105

PROFILE



FRAUNHOFER IMS IN DUISBURG

The Fraunhofer Institute for Microelectronic Circuits and Systems (IMS) was established in Duisburg in 1984. The Fraunhofer IMS is, through continued growth and innovative research and development, one of the leading institutes in Germany for applied research and development in microelectronics and CMOS-technology.

Fraunhofer IMS

Employees	260
Budget	25,8 Mio. Euro
Industrial Projects	50 % of Budget
Public Projects	25 % of Budget
Fraunhofer Projects	25 % of Budget

Infrastructure

Fraunhofer IMS offers a wide range of services and production of in silicon based devices and systems.

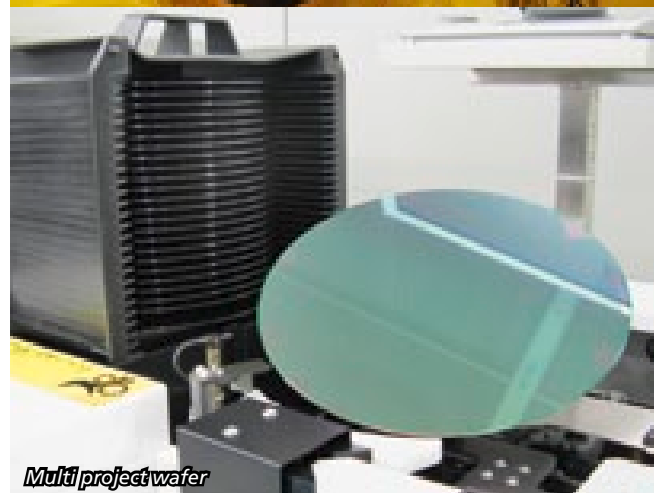
The fabrication takes place in class ten cleanrooms, wafer-testing rooms and an assembly-line with together more than 2500 square meters.

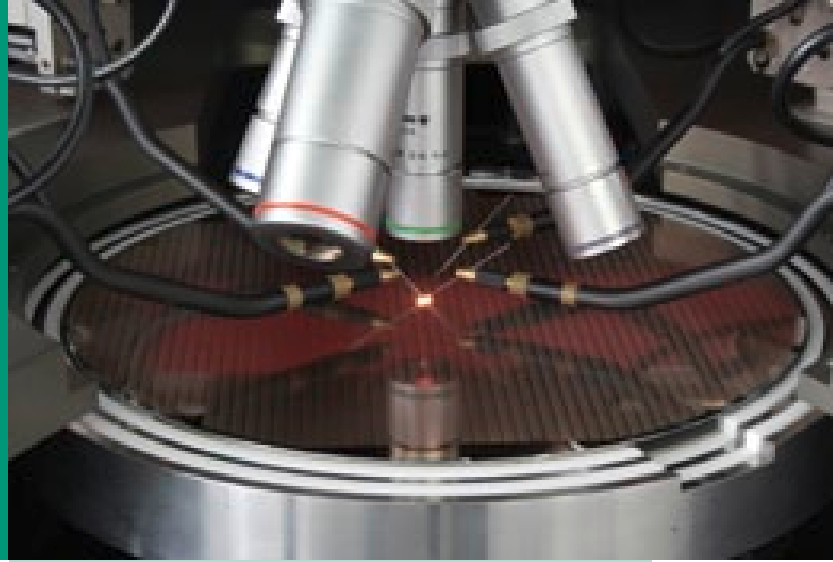
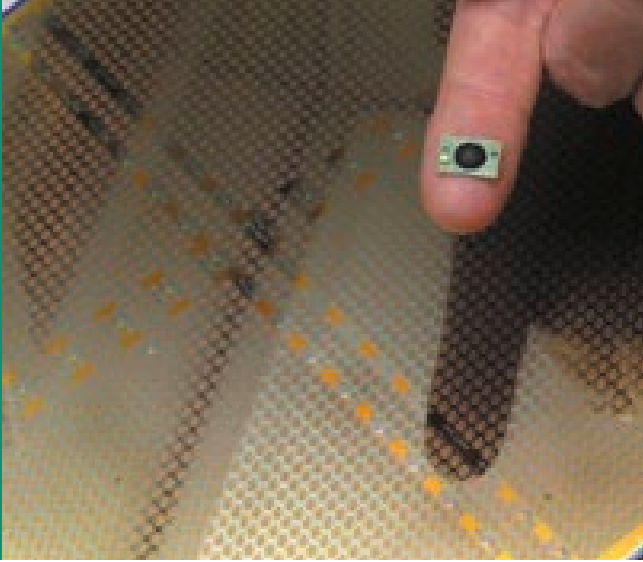
Fraunhofer IMS CMOS Wafer Fab

Wafer size	200 mm (8 inches, 0.35 μ m)
Cleanroom area	1300 square meters
Cleanroom class	10
Employees	app. 120 in 3 shifts 7 days a week
Capacity	> 70.000 wafer/year

IMS Production and Development

Fraunhofer IMS develops, produces and assembles smart sensors, integrated circuits and discrete elements (ICs and ASICs). It also offers the fabrication of devices on a professionally managed CMOS production line in small to medium quantities.





In the new microsystems technology lab (MST-Lab&Fab, 600 square meters) we integrate different micro- and nanofunctions directly on top of the signal processing CMOS circuits. This procedure is called post-processing.

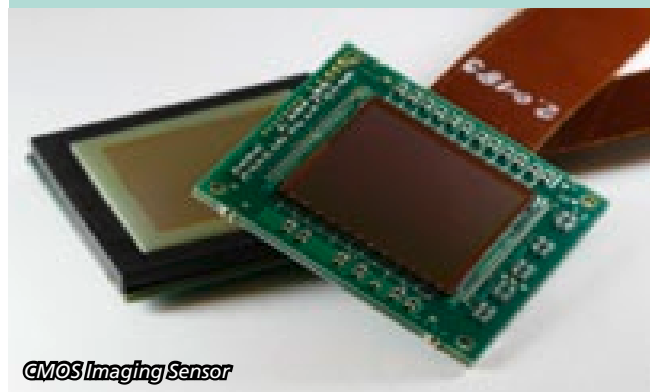
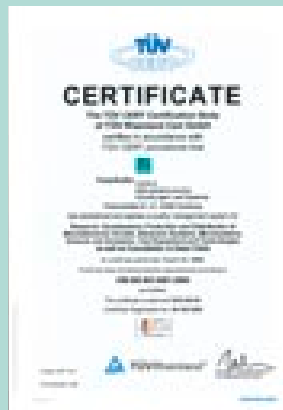
The ICs are assembled in the cleanroom (400 square meters) of Fraunhofer IMS assembly facility. This facility supports the production of ICs in ceramic packages or as COB (Chip on board, COB). COB assembly is available from small quantities to several million units per year.

Supply and Service

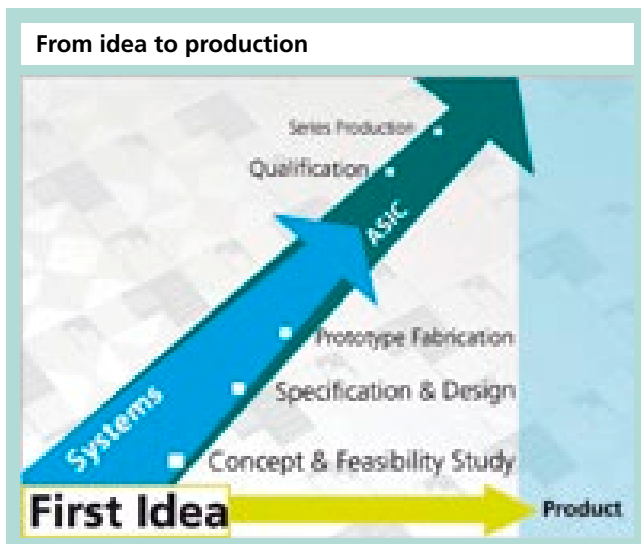
The Fraunhofer IMS offers R&D services tailored to our customer needs, providing efficient solutions ranging from the initial studies to the series products.

Cooperation possibilities:

- Studies and feasibility studies
- Consulting and concept development
- Demonstrator and prototype development
- Chip production (ASIC Production)
- Development of soft- and hardware



CMOS Imaging Sensor



RFID System



FRAUNHOFER IMS BUSINESS FIELDS AND CORE COMPETENCIES

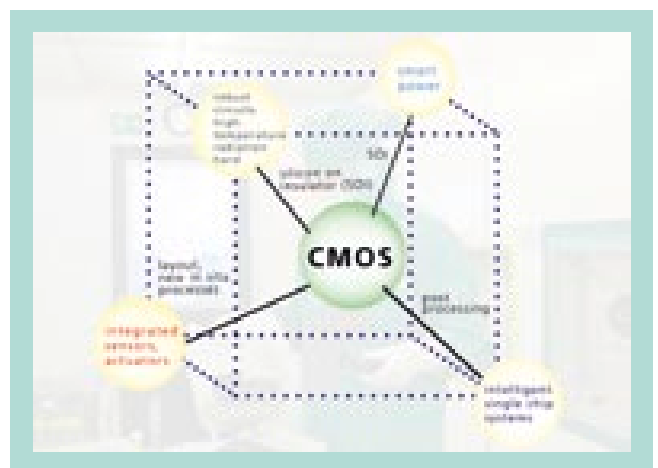
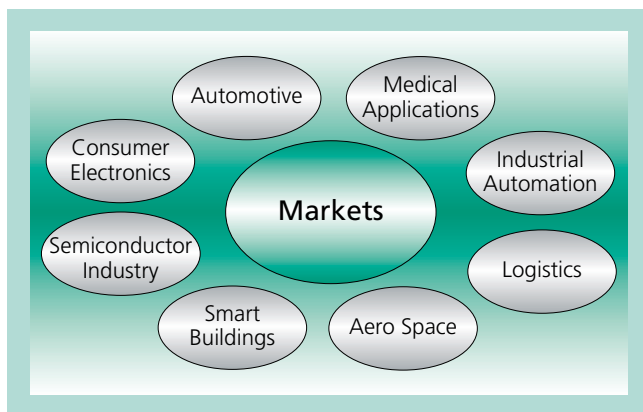
RESEARCH AND DEVELOPMENT AT THE FRAUNHOFER INSTITUTE FOR MICROELECTRONIC CIRCUITS AND SYSTEMS

The Fraunhofer IMS conducts research and development in many different application areas including

- Automotive
- Medical
- Consumer
- Smart Buildings
- Communication
- Aero Space
- Logistics
- Industrial Automation
- Semiconductor Industry

These applications are served by our business fields:

- CMOS processes
- ASIC design und development
- Sensors
 - Pressure Sensors
 - Image Sensors
 - Infrared Sensors
 - Bio Sensors
- Embedded systems hardware and software
- Wireless systems, ICs and transponders
- Smart Buildings



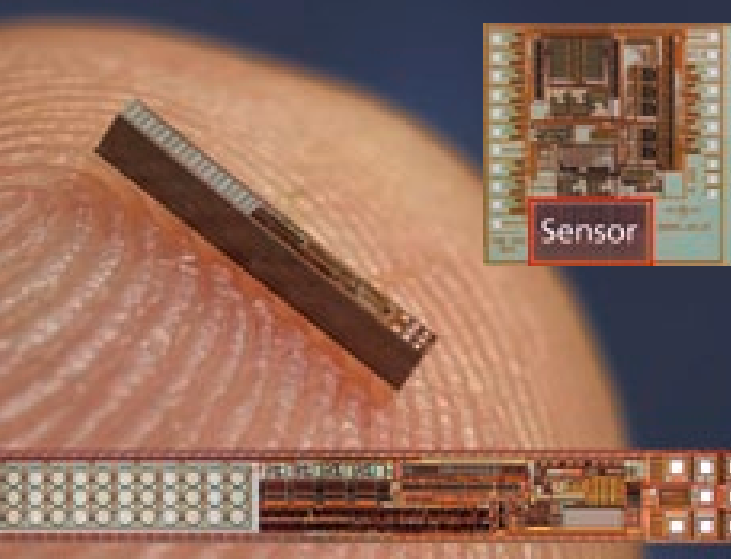
1. CMOS Process and Assembly

Based on standard CMOS process technology, IMS develops customer-specific processes and special options for standard processes (e.g. capacitors, polysilicon and thin-film resistors, high voltage transistors, EEPROM, OTP and several types of sensors).

Pressure Sensor Process

With a clear view on the needs of a rapidly growing sensor market, IMS leveraged its long experience in research and development of CMOS-compatible integrated sensors to establish micro-mechanical pressure sensors as one of its product lines.

At the heart of this product line is a pressure sensor that is integrated into standard CMOS technology. This micro-mechanical pressure sensor was designed for a large range of pressures, and can be monolithically integrated with many electronic devices, e.g. MOSFETs, capacitors, resistors or EEPROMs. The layout of the pressure sensor determines its pressure range, as the membrane's stiffness is directly related to its diameter.



High Temperature SOI Process

The high temperature SOI CMOS process uses SOI substrates for the production of ASICs that operate at temperatures of up to 250° C.

Only fully CMOS compatible process steps are used to manufacture not only standard CMOS circuit elements, including EEPROM, but also silicon based sensors, actuators and power devices.

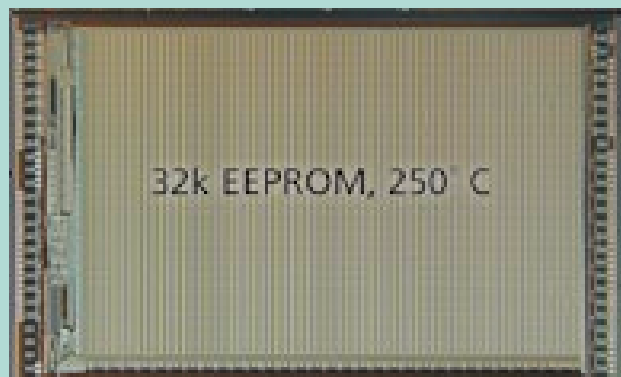
Power Devices

In close cooperation with industrial partners, Fraunhofer IMS provides a 600V-CMOS-process for half and full bridge driver chips for IGBTs.

CMOS Fabrication

Fraunhofer IMS provides numerous semiconductor production services in its 200 mm CMOS production line. The professionally managed class 10 clean room has more than 1300 m² floor space. The 24 hour, 7 days a week operation ensures the uniform quality of our products.

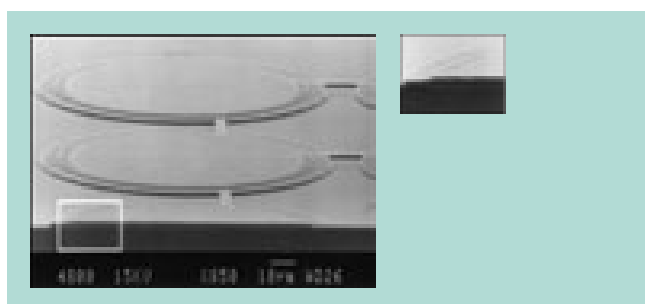
The Fraunhofer IMS production line especially caters to the production of smaller and medium quantities of ASICs. The production line operates under an ISO 9001:2000 and TS 16949 certified quality management system, assuring stability and reliability of products and production. Timely, reliable and customer-oriented production is our and our customers key to success.



2. Sensors

Pressure Sensors

The basic element of our pressure sensors is a surface micromechanical sensor that is fabricated using standard CMOS processing equipment. These sensors can be realized for a wide range of pressures, sharing a single chip with all electronic devices available in a CMOS process, e.g. MOSFETs, capacitors or EEPROMs. The sensors can be configured as absolute with capacitive readout. The necessary signal conversion, linearization and amplification circuits are realized on the same chip, effectively eliminating interference on sensor wiring that is a major issue for discrete solutions. We have already created a variety of innovative products using this monolithic integration of sensors and signal processing functions like programmable amplifiers, sensor linearization, temperature compensation or wireless interfaces.

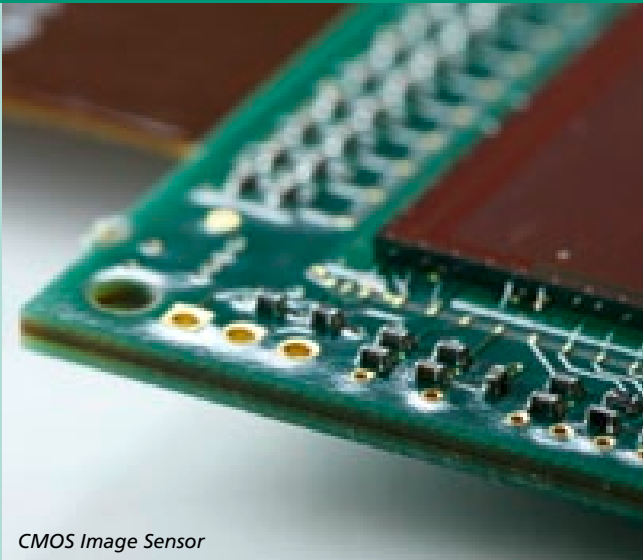


The layout of the sensor element determines its pressure range, which may be situated between 0.5 to 250 bar, as the sensor diameter controls the stiffness of the membrane: Smaller and stiffer membranes shift the pressure range to higher pressures. Thus the sensors are suitable for the measurement of pressures ranging from blood, air, and tire pressure all the way to hydraulic oil pressure. The small size of the sensor and its associated electronics enables innovative medical applications for the in vivo measurement of the pressures of blood, brain, eye or other body fluids.

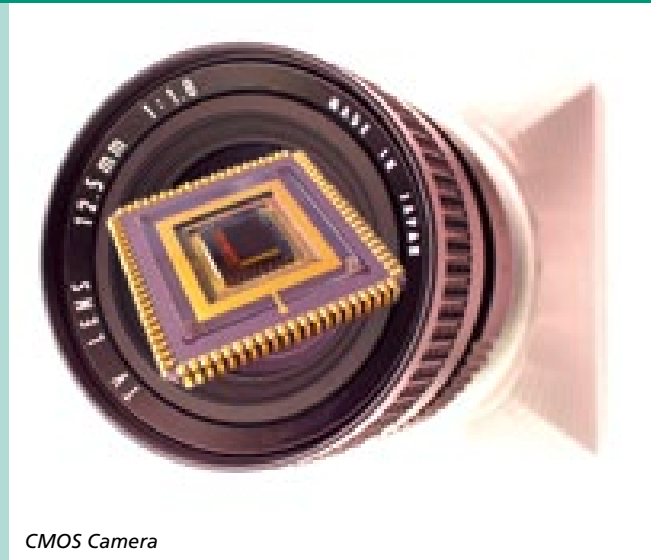
CMOS Image Sensors

Fraunhofer IMS image sensors are based on CMOS technology, which enables the monolithic integration of sensor and circuit elements on a single chip. This integration is used e.g. to control the sensitivity of each individual pixel to avoid blooming. Fraunhofer IMS has developed a dedicated 0,35 μm Opto CMOS process.

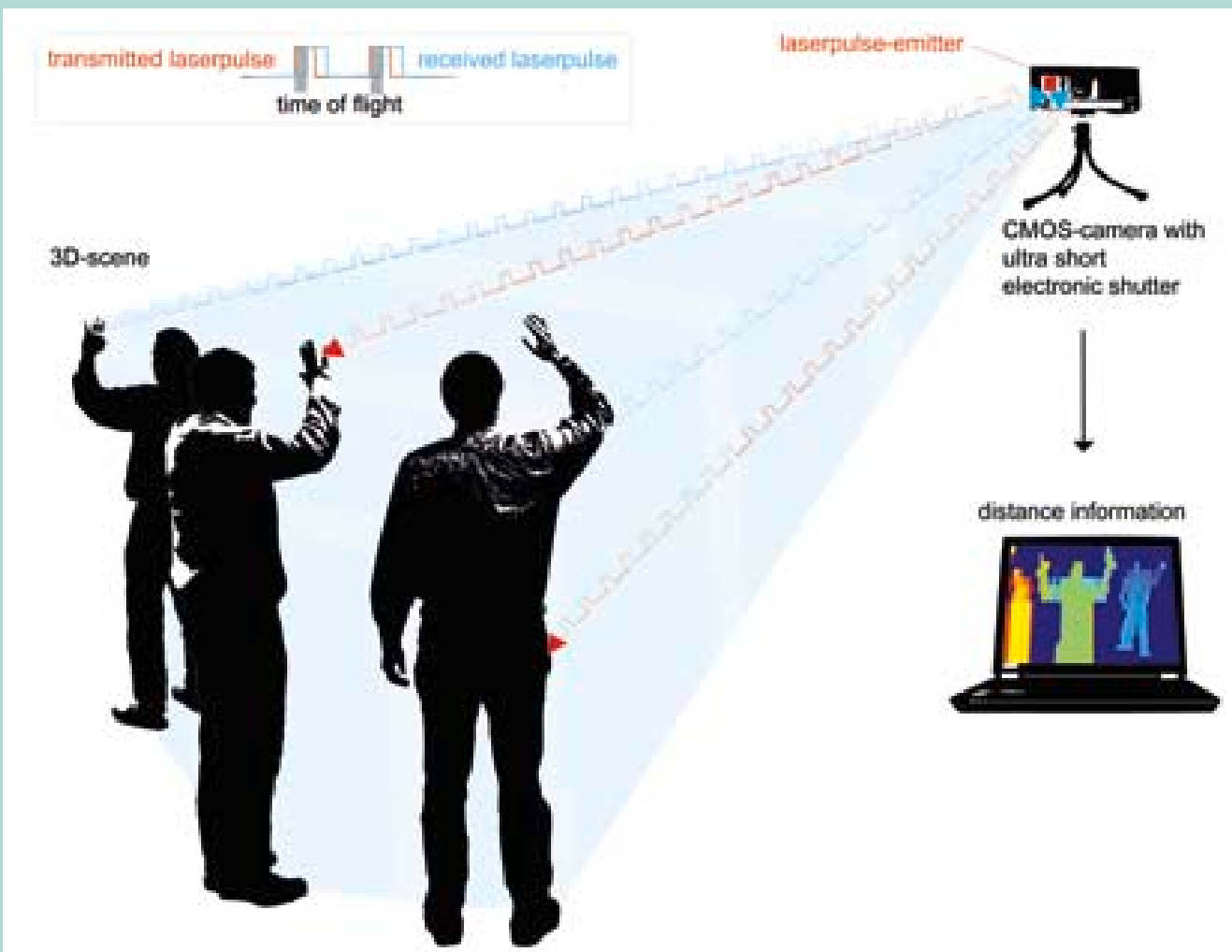
A wide range of CMOS image sensors has been developed for our customers and in research projects. The realized sensors include high dynamic range sensors, high speed sensors – which deliver 1000 high quality images per second – and high-resolution sensors with “region of interest” function for faster readout of subsections of the pixel array. The CMOS image sensors suppress smearing and blooming effects and always deliver sharp images. Electronic high-speed shutters enable the realization of 3D imagers base on laser pulsed based time-of-flight measurement.



CMOS Image Sensor



CMOS Camera



Infrared Sensor

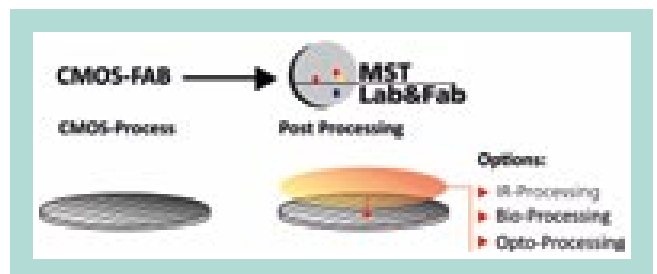
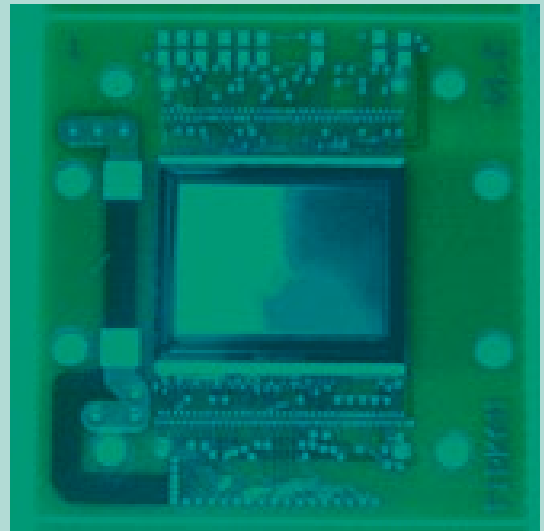
The demand for uncooled infrared focal plane arrays (IRFPA) for imaging applications is constantly increasing. Examples for the application of IRFPAs are thermography, pedestrian detection for automotive, firefighting and infrared spectroscopy.

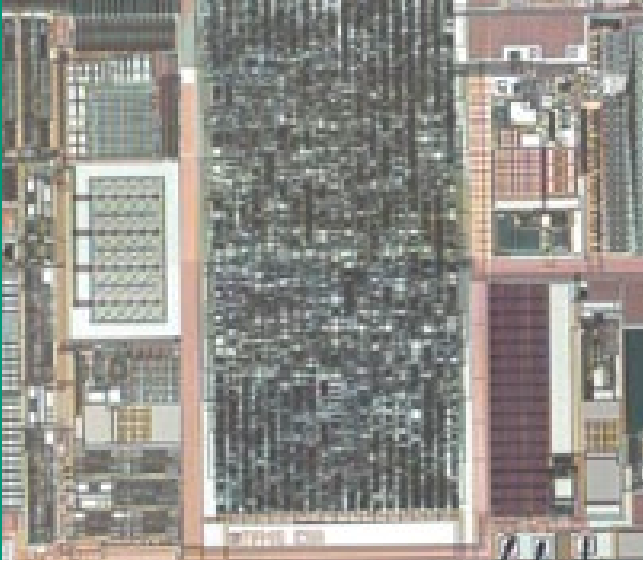
IRFPAs consist of an array of microbolometers located on top of a CMOS substrate which comprehends the readout circuit. Typical array sizes are for lowcost applications 160 x 120 or 320 x 240 pixels. State-of-the-art IRPGAs achieve VGA-resolution with 640 x 480 pixels.

The microbolometer is a special infrared sensor. The IR-sensitive sensorelement based on the principle for a microbolometer is fabricated by post-processing on CMOS wafers. The microbolometer converts the infrared radiation into heat energy and this induces a temperature rise resulting in a change of the electrical resistance. Typical microbolometers have pixel pitch values of 35 µm or 25 µm.

Biosensors

Biosensors for point-of-care and home diagnostics are increasingly asked for. Therefore Fraunhofer IMS advances in the development of a new generation of biosensors. These special sensors are developed in the Microsystems Technology Lab where standard CMOS circuits are prepared for or – in future – combined with bioactive layers. Typically, additional metals or oxides are added, as well as special surface treatment and activation or the dispersion of anchor chemistry for later analyte receptor immobilization. This new technology is called post-processing and it enables the production of different sensors for different applications by joining biosensitive layers with CMOS electronic readout circuitry. This “Bio to CMOS” processing leads to Biohybrid Systems.





3. ASIC Design

The development of analog, digital and mixed analog-digital integrated systems is a core competence of Fraunhofer IMS. Application specific integrated circuits (ASICs) enable our customers to provide cheaper and more powerful products. We offer the full spectrum from custom to IP-based ASIC solutions.

Full-custom ASICs are designed from scratch to accommodate the specific requirements of the customer, providing a highly optimized product. The IP-based ASIC is based on proven generic components, with lower design time and cost. Using a mix and match approach both design styles can be combined to leverage the benefits of both.

The close co-operation with our in house CMOS production line provides a seamless and efficient path from concept to series production. Our long experience in the development of integrated circuits, starting from concept through design, layout, and fabrication to testing ensures a short development time and a minimized design risk.

Our fields of design expertise are:

- Embedded microcontroller
- High-temperature ASICs
- Smart power integration
- Non-volatile memories
- Mixed-signal design
- Sensor transponder

Beside standard ASIC solutions for all kinds of applications, ASICs with sensors and sensor signal processing integrated on a single chip have been realized.

These ASICs often combine our core competences in ASIC design,

- System-on-Chip (SoC) solutions,
- Mixed-signal signal processing and
- Integration of RF building blocks for wireless energy and data transfer.

Our customers benefit from our research in these areas, which provides viable solutions for their applications – applications that demand miniaturization, energy efficiency, cost optimization and reliability.

4. Wireless Systems and Transponders

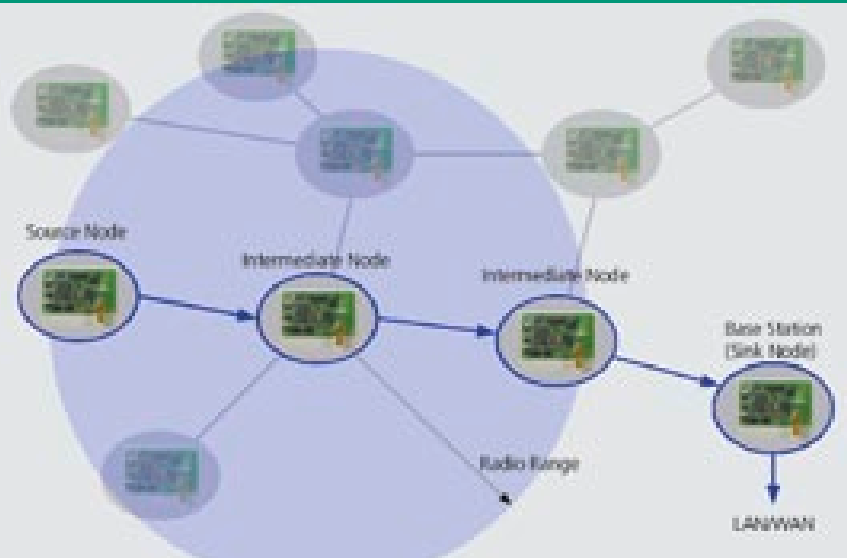
A core-competence of Fraunhofer IMS is the development and realization of wireless systems. Research and development focuses, among other things, on wireless sensor networks. These networks comprise autonomous sensor modules that are distributed over a large area or volume, and measure physical, chemical and other quantities. The measured values are transferred to a central agency, making use of intermediate nodes for data transfer, or they can be used by similarly distributed actor modules for decision-making and control processes. Development in this field includes new methods for communication (e.g. protocol stacks, localization) and the realization of cost-efficient, miniaturized components. The realization of new products in an efficient and timely manner is facilitated by the use of modular hardware and software components that allow a quick adaptation to application requirements.

Important applications of **wireless sensor networks** are in the field of:

- Industrial automation, e.g. logistics and inventory control.
- Agriculture e.g. monitoring of air and soil parameters.
- Facility management, e.g. remote monitoring of buildings and infrastructure elements.

Our customers face a number of challenges that are addressed by our R&D activities. One set these activities addresses tools for network development, deployment and maintenance. Others address the field of energy harvesting, the ability to extract module power from the environment and obviating the need for batteries or power cables.

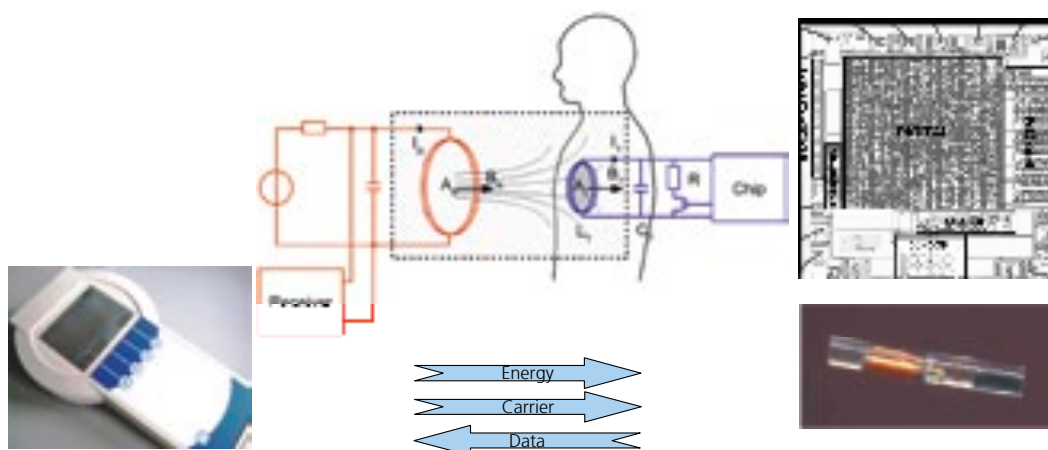
RESEARCH AND DEVELOPMENT AT THE
FRAUNHOFER INSTITUTE FOR MICRO-
ELECTRONIC CIRCUITS AND SYSTEMS



The **transponder systems** unit at the Fraunhofer IMS offers system solutions for the integration of novel portable or stationary transponder read-write devices and base stations into smart network-systems. It also provides base stations for transponder ASICs with integrated micro sensors developed at Fraunhofer IMS, thus

offering complete system solutions. These transponder systems are used in smart buildings and vehicles, industrial automation, medical devices and logistics.

Sensor-Transponder System for Medical Applications





5. Smart Room & Building-Solutions

At the **Fraunhofer-inHaus-Center**, Europe's leading innovation center for smart homes and buildings, IMS cooperates with six Fraunhofer-Institutes and nearly 100 industrial partners to develop, test and demonstrate innovative solutions of all kinds for different application fields in smart buildings. In detail IMS offers research, development and complete systems-solutions to component and systems manufacturers, builders and operators of homes and commercial buildings for new and added value functions on the basis of electronics and software.

At the **inHaus1-Facility (Smart Home-Lab)** new domotic techniques to control lighting, doors and windows as well as heating and ventilation for energy efficiency in homes are developed and tested. One focus lies on solutions for smart metering for more transparency in energy consumption. In the SmartHome-Segment we have also a lot of experience in the field of user interface solutions for easier control of technical equipment in homes. User acceptance tests in the smart home lab guarantee the new industrial products to have a better success chance on the market.

At the **inHaus2-Facility (Smart Building-Lab)** new technical solutions for commercial properties are being developed, e.g. for new benefits in facility management and building operation, in the operation process of nursery homes, hotels and offices.

One main IMS focus lies on the development of new concepts and electronic systems that provide unobtrusive assistance for elderly and handicapped people in order to maintain a self-determined life at nursery homes with commercial operation and to optimize the care service process. We concentrate especially on solutions like microelectronic sensor networks in rooms with software interpretation of data to get benefits like automatic detection of problems or emergency cases (ambient assisted living AAL).

Another main field of R&D in all inHaus-application segments is energy efficiency, like in the smart home field. In cooperation with component and systems manufacturers and also energy providers next-generation-metering and building automation technologies for energy efficiency are developed, tested and demonstrated.

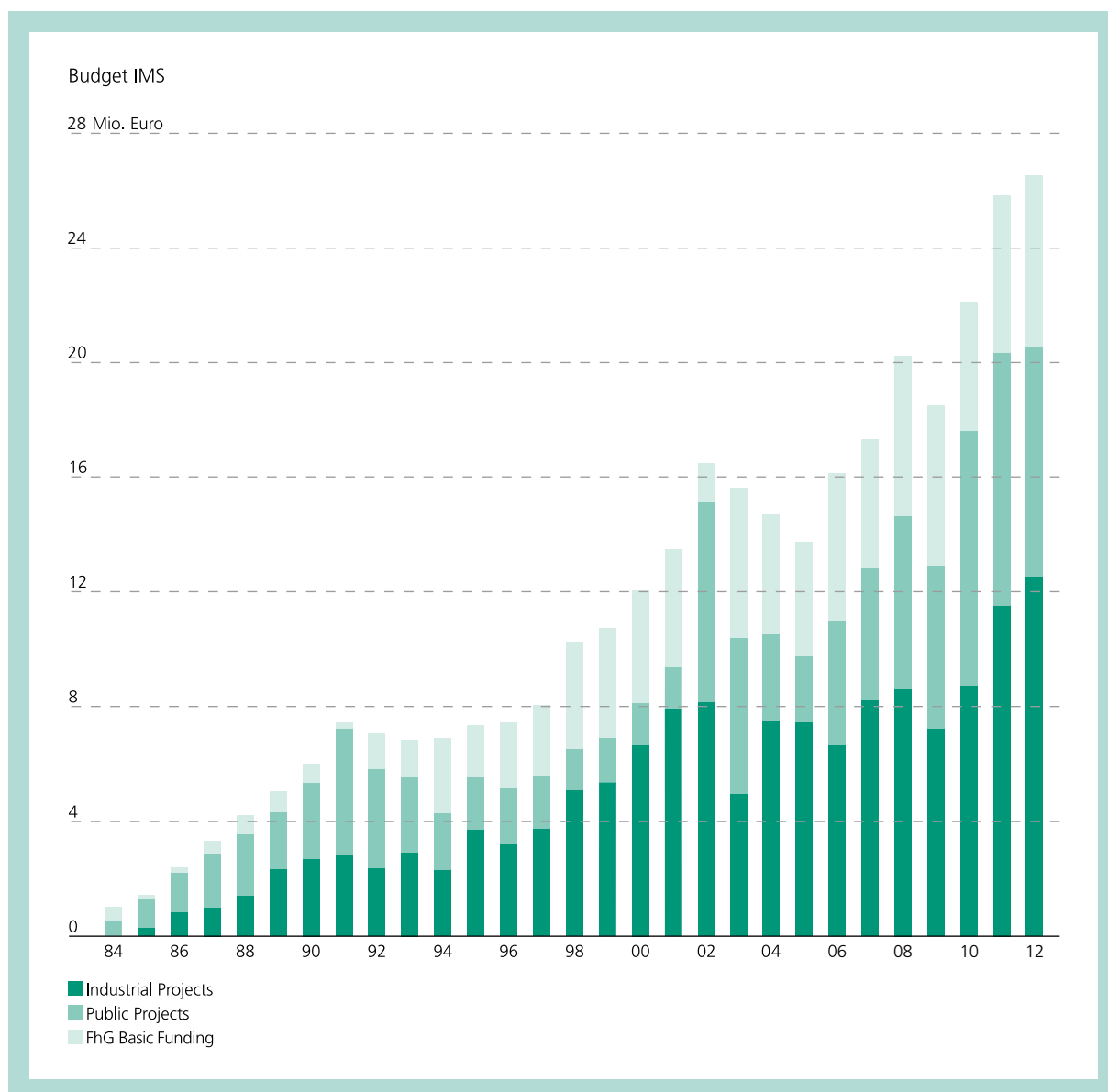
The inHaus Center offers R&D and complete systems-solutions to builders, modernizers or operators of homes and commercial buildings, to implement complete electronic and ITC systems for new and added value functions. This includes the following aspects:

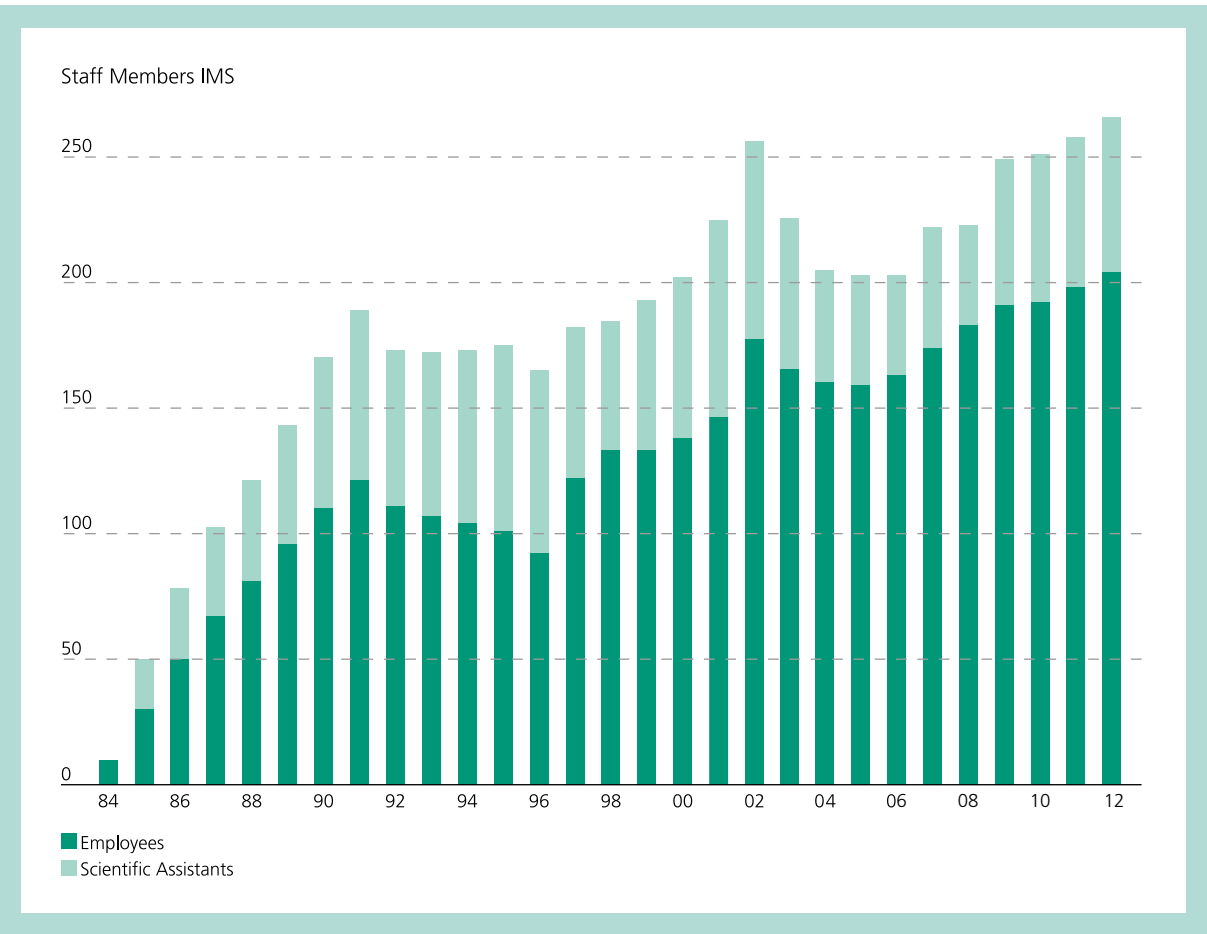
- Safety and security
- Multimedia
- Support for the elderly
- Energy saving
- Light management

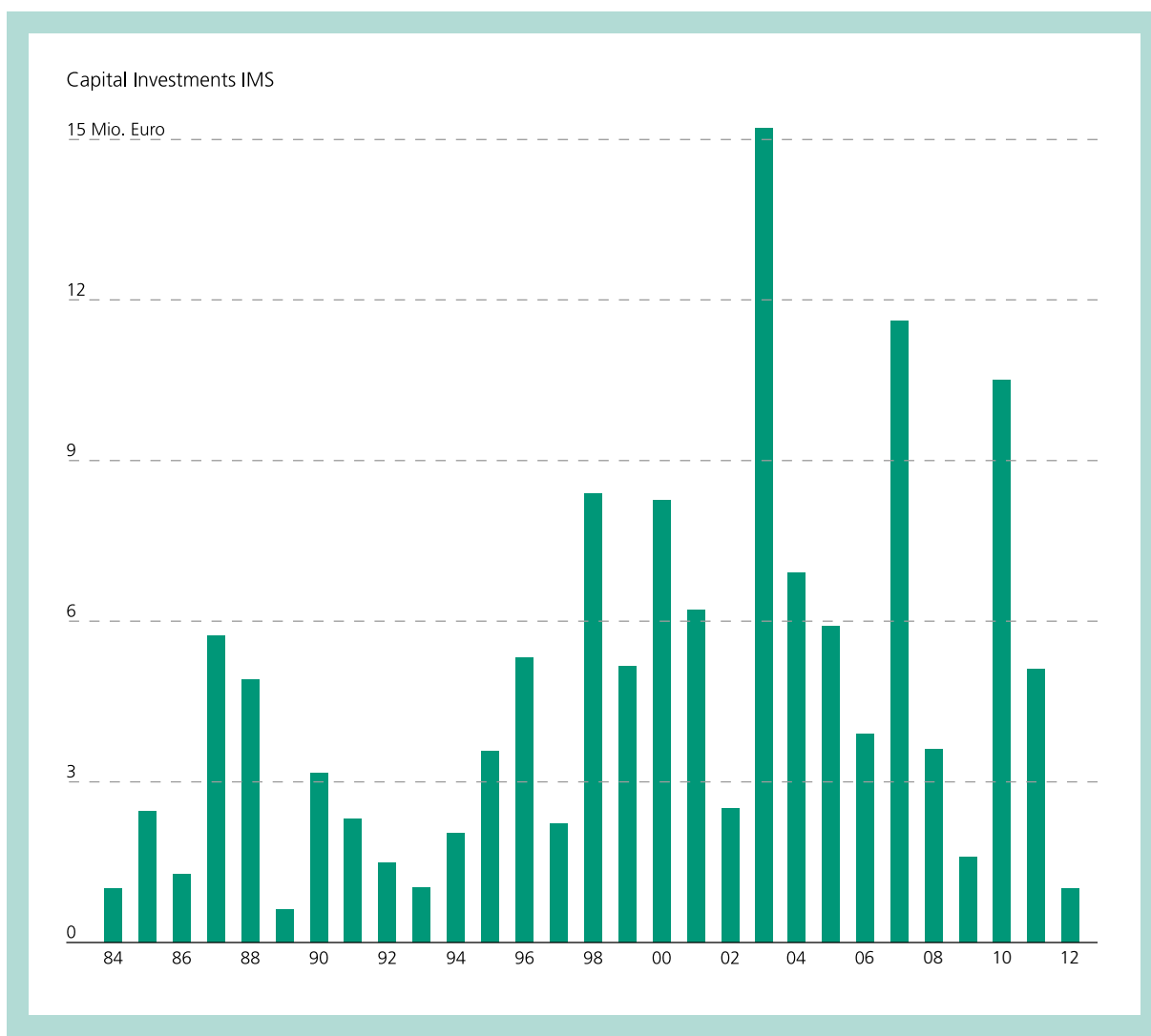


DEVELOPMENT OF THE IMS

Budget IMS	22
-----	-----
Capital Investment IMS	23
-----	-----
Staff Members IMS	24
-----	-----







SELECTED PROJECTS OF THE YEAR 2011

Selected Projects of the Year 2011

I	CMOS Devices and Technology	26
II	Silicon Sencors and Microsystems	36
III	CMOS Circuits	53
IV	Wireless Chips an Systems	61
V	Systems an Applications	81

REDUCING THE IMPACT OF PROCESS VARIATIONS ON THE SENSITIVITY OF CMOS PHOTODIODES

F. Hochschulz, S. Dreiner, H. Vogt, U. Paschen

When standard CMOS image sensors are employed in applications that require the detection of light with a very small spectral width, like 3D-time-of-flight imaging or other applications with laser light illumination, problems arise, that are negligible in standard imaging applications with broadband illumination. For a given wavelength a strong variation of the sensitivity upon small process related variations of the dielectric stack on top of the photodiodes leads to large die to die variations of the sensitivity.

Theoretical Background

Every digital imaging method is based on the absorption of the incident radiation by a substrate material. In case of CMOS image sensors this material is silicon. Upon absorption electron hole pairs are created, which are then separated by the built-in potential of the pn-junction of a photodiode. In the visible range of the spectrum one electron hole pair is created per absorbed photon. The amount of electrons that are detected per incident photon determines the sensitivity of a photodetector and is called quantum efficiency (QE). In CMOS image sensors the photodiodes are connected to the peripheral circuitry by metal interconnects, which are in turn isolated from each other by dielectric layers, commonly made of SiO₂. As CMOS processes include multiple metal layers, this SiO₂ layer is typically several microns thick. Additionally a coating made of approximately 750 nm silicon nitride is deposited on top of CMOS circuits, called passivation. This passivation acts as a diffusion barrier for ions and protects the surface from mechanical damage.

Currently two different ways to design CMOS image sensors are pursued. In front side illuminated (FSI) image sensors the light impinges from the same side as the metal interconnects while in back side illuminated (BSI) image sensors the light impinges from the back side of the silicon. Here, FSI image sensors are treated.

The radiant flux that passes through the layers on top of the photo active area is determined by interference effects of waves reflected at different material boundaries. This

effect modulates the QE periodically depending on two main parameters: the wavelength and the thickness of the dielectric layers that cover the silicon [1]. The amplitude of the modulation depends on the reflectivity of the material boundaries and thus on their refractive indices.

Motivation

Fig. 1 shows a simulation of the quantum efficiency for two different thicknesses of the dielectric stack. As can be seen there, the oscillations of the quantum efficiency as a function of wavelength are huge. The same is true for the quantum efficiency at a fixed wavelength and a variation of the SiO₂ thickness. The assumed thickness difference between the two curves in Fig. 1 of 0.13 μm is only ~2.6 % of the total SiO₂ thickness. Thickness variations of that magnitude can easily occur from process induced variations from wafer to wafer and on a single wafer from die to die. As image sensors tend to be large, a significant thickness difference can even occur on a single die, directly affecting the pixel response non-uniformity (PRNU). A measurement of the discussed photodiodes using a diffraction grating monochromator is shown in Fig. 2. In standard imaging applications, where the spectral width of the impinging radiation exceeds the period of the oscillations the QE oscillations are mitigated and the QE appears to be flat. For narrow spectral width applications the exact shape of the QE graph and the spectrum of the illumination contribute to the actual sensitivity of the system. Thus, for narrow linewidth applications measures are required to smoothen the dependency of the sensitivity on wavelength and/or thickness variations of the dielectric stack on the photodiodes.

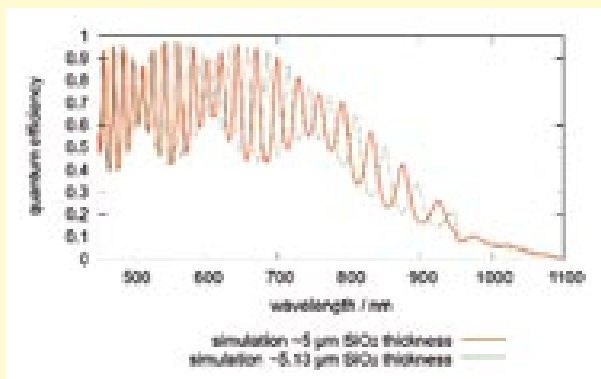


Figure 1: Simulation of the QE for two different SiO_2 thicknesses. The simulations were conducted using monochromatic light.

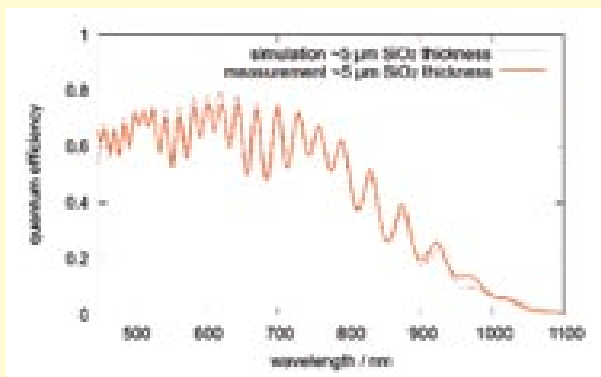


Figure 2: Comparison of measurements (solid lines) and simulations (dotted lines) of photodiodes featuring a SiO_2 thickness of approx. $5 \mu\text{m}$. The thicknesses of the different layers used in the simulations have been obtained from scanning electron microscopic cross sections. The spectrum of the measurement system was assumed to be Gaussian shaped. The spectral width of the measurement system is 0.8% and has been convoluted into the simulated QE.

Proposed Structure

When multiple optical path lengths are incorporated into a single photo active area the resulting sensitivity is a superposition of the sensitivity of the sub-areas. By exploiting the LOCOS (local oxidation of silicon) processing step, which is usually used for the isolation between devices, two different optical path lengths can be realized without any additional processing steps. A schematic drawing depicting photo diodes covered with either the thin gate oxide or the thick field oxide is shown in Fig. 3 together with the proposed structure, where both are combined on a photodiode. This proposed structure has been filed for patent.

Impact on wavelength dependent QE variations

The oscillations of the QE of the two regions in the photodiode with different thicknesses are out of phase and their superposition is smoother than the QE of each of the original areas. For a wavelength of 757 nm the oscillations are exactly out of phase. In this wavelength region the QE is especially smooth, as can be seen in Fig. 4 (blue solid line). A photodiode that has been produced using this method has been measured and is compared to a simulation in Fig. 5.



Figure 3: Schematic of the three investigated photo diodes. A photodiode under thin gate oxide (left), under thick field oxide (middle) and a photodiode according to the proposed structure with half of its area under thin and the other half under thick thermal oxide (right) is shown.

REDUCING THE IMPACT OF PROCESS VARIATIONS ON THE SENSITIVITY OF CMOS PHOTODIODES

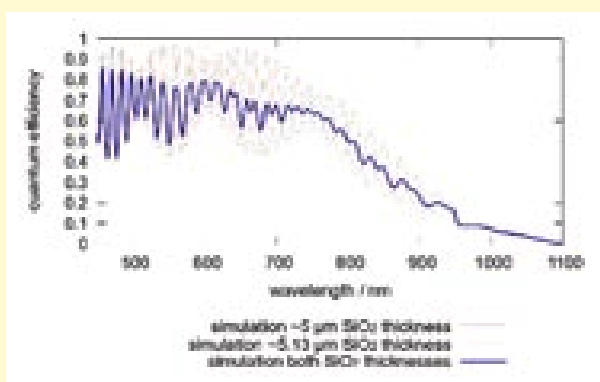


Figure 4: Simulation of the quantum efficiency of a photodiode according to the proposed structure (solid line) compared to photodiodes with a single SiO₂ thickness (dotted line). As can be seen the quantum efficiency as a function of wavelength is much smoother for the proposed structure, especially in a range around 757 nm.

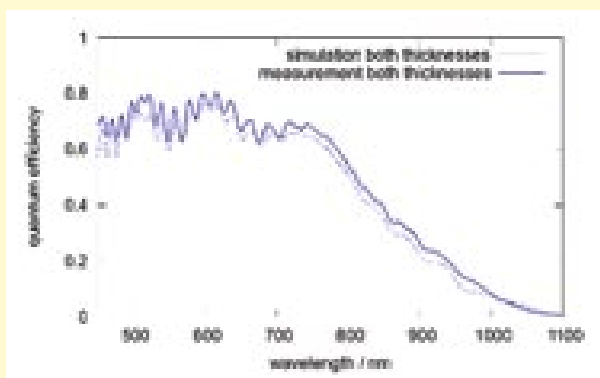


Figure 5: Comparison of measurements (solid lines) and simulations (dashed lines) of photodiodes produced according to the proposed structure with two different SiO₂ thicknesses. The thicknesses of the different layers used in the simulations have been obtained from scanning electron microscopic cross sections. The spectrum of the measurement system was assumed to be Gaussian shaped. The spectral width of the measurement system is 0.8% and has been convoluted into the simulated QE. These measurements confirm the smooth QE with respect to wavelength variations (see Figure 4).

Impact on process induced QE variations

Even more important than the reduction of the QE variations for different wavelengths is its reduction with respect to process induced thickness variations for a fixed wavelength. When assuming process variations for the SiO₂ thickness of $5 \pm 0.5 \mu\text{m}$ and for the SiN thickness of $750 \pm 100 \text{ nm}$ and simulating the QE for all thickness combinations, huge QE variations occur within this parameter range. These simulations are shown in Fig. 6 for a wavelength of 757 nm as an example. In this case the maximal QE of a photodiode with a single SiO₂ thickness is 0.81, the minimal QE is 0.37. For a photodiode according to the proposed solution the maximal QE is 0.64, the minimal is 0.51. Therefore these simulations yield a reduced impact of process induced thickness variations on the sensitivity of CMOS photodiodes. Further simulations over the visible wavelength range confirm this result over a broad wavelength range [2].

Conclusion

When standard CMOS image sensors are illuminated with a narrow spectral width light source strong modulations of the quantum efficiency dependent on the wavelength and on thickness variations of the layers that cover the silicon occur. By introducing multiple optical path lengths into a single pixel these quantum efficiency modulations can be significantly reduced. In this work the local oxidation of silicon processing step has been exploited to introduce a thickness difference into the SiO₂ layer that covers the photodiodes. Simulations and measurements confirm a significant reduction of the wavelength dependent quantum efficiency variations and of the process induced quantum efficiency variations over a broad wavelength range. In contrast to other options to reduce these modulations [3], here no additional processing effort is needed.

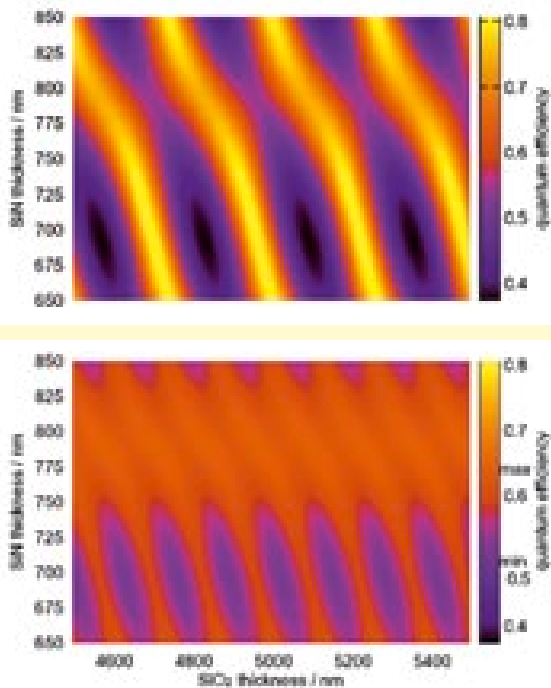


Figure 6: Color coded simulation of the quantum efficiency for different SiO₂ and SiN thicknesses for a photodiode with a single SiO₂ thickness (top) and for a photodiode with one half of its area under the given SiO₂ thickness and its other half under a 0.13 μm thicker SiO₂ layer (bottom). The simulations were conducted using a wavelength of 757 nm and monochromatic light. As can be seen the QE variations with respect to thickness variations of the dielectric stack that cover the silicon can be drastically reduced using the proposed solution.

References:

- [1] Magnan, P. "Detection of visible photons in CCD and CMOS: A comparative view" Nuclear Instruments and Methods in Physics Research Section A: Accelerators, Spectrometers, Detectors and Associated Equipment, 2003, 504, 199–212
- [2] Frank Hochschulz, Stefan Dreiner, Holger Vogt and Uwe Paschen, "CMOS photodiodes for narrow linewidth applications", IEEE Sensors 2011 Proceedings, 1600 – 1604, Limerick, Irland, Okt. 2011
- [3] Hochschulz, F.; Paschen, U. & Vogt, H. "CMOS process enhancement for high precision narrow linewidth applications" Solid-State Device Research Conference (ESSDERC), 2010 Proceedings of the European, 2010, 254–256

INTELLIGENT NANO-MODIFIED 3D-ELECTRODES

A. Jupe, A. Hoeren, A. Goehlich, H. Vogt

Introduction

Electrodes for the stimulation of neurons or for the recording of action potentials are well established in medical technology. They are used in cardiac pacemakers, cochlear implants as well as in deep brain stimulators. A miniaturization of these electrodes to micro-electrodes provides a basis for various new application areas, such as a usage for retina implants or brain computer interfaces. Micro-electrodes represent a significant advance forward in local resolution due to the fact that a higher number of electrodes with small diameters can be integrated on a smaller area. A miniaturization of the electrodes and the resulting increase in impedance implies that the electrode has to be driven by a CMOS integrated circuit.

An increase in the number of electrodes also means an increase in energy consumption and therefore an increase in temperature load which can lead to intolerable operation conditions, especially for implants. In addition to the optimization of the CMOS circuit with respect to energy consumption, the microelectrodes have to be optimized by improving the contact to the neurons. This can be achieved by a three-dimensional penetrating electrode. The charge transfer capacity can also be increased by coating the surface with a nano-porous material, for example iridium oxide or nanostruc-

tures like carbon nanotubes (CNTs). Microelectrodes, which are modified by CNTs show a promising potential due to the fact that neuronal cells can form connections with clusters of CNTs via axons or dendrites in a self-organized way [1].

As a part of the BMBF-funded project 'InMEAs' (integrated nano-modified multi-electrode-arrays) Fraunhofer IMS participates with the realization of a new generation of multi-electrode-arrays in collaboration with three other partners (RWTH Aachen – Institut für Werkstoffe der Elektrotechnik I, RWTH Aachen – Universitätsaugenklinik, Fraunhofer IKTS).

Development

Within this project Fraunhofer IMS will realize a CMOS-compatible structure ("Basis-CMOS-MEA"), which serves as a platform for the integration of 3d-gold-nano-needles and for the integration of aligned carbon nanotubes on planar electrodes.

Currently, CNTs can be synthesized at a process temperature of about 700 °C. A direct deposition of CNTs on standard CMOS wafers with an aluminium metallization is therefore impossible due to the CMOS temperature range of approximately 450 °C. With respect to the technical complexity an indirect transfer of CNTs (deposited on a separate sacrificial substrate) on a CMOS wafer e.g. by wafer bonding techniques appears to be very sophisticated. As part of this project, Fraunhofer IMS has evaluated CMOS-substrates with a high temperature tungsten metallization for direct POST-CMOS integration.

In the course of this study three types of wafers have been characterized by electrical measurements: a SOI-CMOS technology with tungsten metallization, a bulk-substrate wafer with hot aluminium copper metallization and a bulk substrate wafer with tungsten metallization.

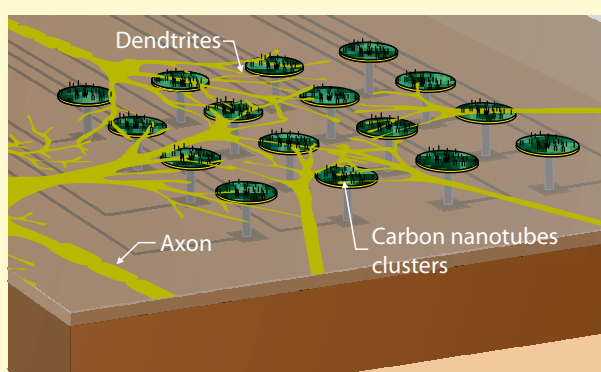


Figure 1: Schematic illustration of a neuronal network of dendrites and axons on planar electrodes modified by carbon nanotubes

Annealing studies

Thin film SOI wafer with tungsten metallization

In order to simulate the influence of the thermal budget of the CNT-deposition on the CMOS-readout-circuitry annealing studies have been conducted. At first annealing studies with pieces of a 120 nm thin film SOI-wafer (400 nm insulating layer) with CMOS test structures were performed in the interval of 500°C to 700°C in which the target temperature was constant for 30 minutes. The electrical input and output characteristics as well as the threshold voltage of MOSFETs with different width and length were measured. The threshold voltage is a significant parameter for the performance of a transistor. The threshold voltage of the SOI n-channel MOSFETs shows a comparatively low difference of about 200 mV after 700 °C annealing. In comparison, the p-channel SOI MOSFETs exhibits a much larger difference in threshold voltage of about 1,5 V after 650 °C annealing. The reason for this pronounced shift is currently under study.

The VIA-chains (VIA1 and VIA2), the contact chains (n+ silicon, p+ silicon, poly) as well as the Kelvin structures (metal-poly, metal n+, metal p+) were also characterized by resistance measurements. The single polysilicon contact shows a strong increase in resistance (in the mega ohm range) after 700 °C annealing due to a partial degradation of the contact. This is also observable for the VIA chain between metal 1 and tungsten plug. However, the VIA2 chain shows no visible damage of the contact after 700 °C annealing and the resistance is increased by only 35 Ω for the complete chain.

Bulk substrate wafer with hot aluminium metallization

As compared to the SOI technology, the semiconductor devices generated with the bulk substrate technology with a hot AlCu metallization show only small differences in threshold voltage shift (20mV – 50mV) of the n-channel and p-channel MOSFETs after 600 °C annealing. Kelvin structure, van-der-Pauw-structure, contact chains and VIA chains show a partial occurrence of aluminium spiking at higher temperatures (650 °C).

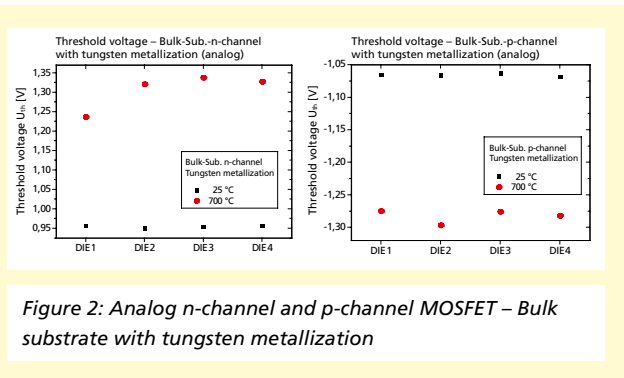


Figure 2: Analog n-channel and p-channel MOSFET – Bulk substrate with tungsten metallization

Bulk substrate wafer with tungsten metallization

As a consequence of the previous findings a combination of a bulk technology with a tungsten metallization has been fabricated in a test run. The electrical characterization was performed on n-channel and p-channel MOSFETs of different widths und lengths, as well as on contact chains after 700 °C annealing.

As depicted in figure 2, the analog n-channel MOSFETs (here: width 50 μm, length 5 μm) shows a threshold voltage shift of approximately 370 mV after 700 °C annealing. The analog p-channel MOSFET of the same ratio shows a comparatively small threshold voltage shift of approximately 225 mV.

The threshold voltage shift of the digital n-channel MOSFET (width: 20 μm, length: 0,8 μm) reaches a value of about 160 mV (fig. 3a) and the digital p-channel MOSFET of about

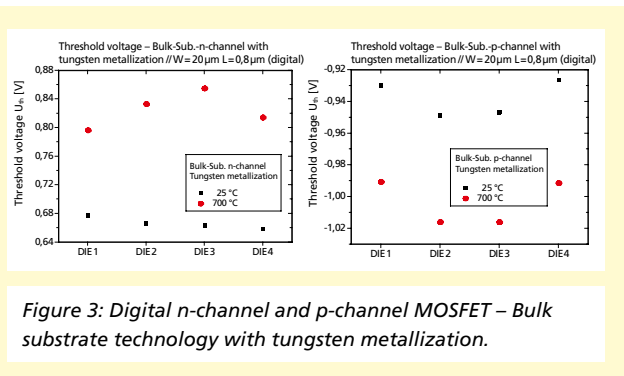


Figure 3: Digital n-channel and p-channel MOSFET – Bulk substrate technology with tungsten metallization.

70 mV (fig. 3b). So the evaluated transistors remain functional after this high temperature annealing step.

The investigated contact chains remain functional after 700 °C annealing. The ohmic resistance of the poly contact chain (49920 elements) increases by 250 kΩ after the high temperature step. This represents an increase of 30 percent for every single element, which seems to be acceptable for the intended application.

Summary

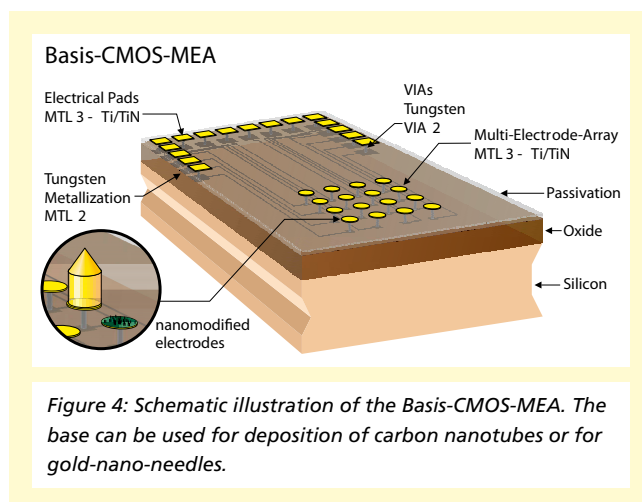
The conducted experiments have demonstrated that a CMOS bulk technology in combination with a tungsten metallization is quite promising for the direct POST-CMOS deposition of CNTs on a MEA-wafer. For this reason, a MEA-test structure with tungsten metallization has been designed. Figure 4 shows a schematic illustration of the MEA test structure.

The multi-electrode-arrays were created in different variants. Separate electrodes or electrode cluster (4x4) can be individually connected via 25 electrical pads. The individual variants differ in electrode diameter (10 μm – 80 μm) as well as in distance between electrodes (50 μm – 150 μm). In addition, some variants also comprise a counter and reference electrode.

The electrodes made of Ti/TiN layers are the basis for further nano modification with CNTs or with gold-nano-needles which will be developed in the next steps of this project.

References

- [1] Gabay, T., Ben-David, M., Kalifa, I., Sorkin, R. Abrams, Z.R., Ben-Jacob, E., Hanein, Y., „Engineered self-organization of neural networks using carbon nanotube clusters”, Physica A 350 (2005) 611 – 621



RADIATION-HARD CMOS IMAGE SENSOR PROCESS

J. Fink, F. Hochschulz

When designing ICs for medical imaging, satellite technology or safety and security applications, engineers and scientists are often confronted with radioactive environments, which influence the chip's performance or even its lifetime. As a whole the problem of radiation damage in CMOS electronics has been around for several decades and several successful methods in dealing with these effects have been developed. However, especially in versatile components like remotely operated wireless sensors, which have to cope with a multitude of physical surroundings, these additional design efforts are often omitted.

Hence knowing a technology's susceptibility to damage from high energetic radiation allows an evaluation of the operational limits of standard, cost-effective, multi-purpose designs as well as the development of custom, high performance ICs for harsh environments. In order to provide ASIC and system designers with this information Fraunhofer IMS has exposed individual transistors fabricated in the institute's main-line 0.35 μm CMOS process as well as a number of selected devices to ionizing radiation. During the tests with 1 MeV photons a maximum total dose of 10 kGy (1 Mrad) was applied over 24 hours.

1. Introduction

The irradiation tests with an 18.7TBq ^{60}Co source were performed at Fraunhofer INT in Euskirchen in November 2010. The radioactive isotope generated gamma-rays at energies of 1.17 MeV and 1.33 MeV. At these energies, the predominant effects of the impinging radiation on the ASICs are oxide charge build-up inside the gate and field oxides and charge generation at the Si-SiO₂ interfaces.

These additional charges can lead to a number of unwanted effects in a MOS transistor. If they are for example generated underneath the transistor gate, they can influence the current flow in the transistor channel, thus altering the transistor threshold voltage and the sub-threshold slope. Apart from that, charges, which are generated inside the field oxide insulation between adjacent transistors, can create parasitic current paths along the sides of the transistors. As a consequence, the leakage current of an NMOS transistor in the off-state (0 V gate-source voltage) increases. In turn this leads to an increase in the overall current consumption of an ASIC.

Finally, the gamma rays can theoretically also lead to Si bulk damage, knocking Si atoms off their original lattice positions. This effect can however be neglected due to its low probability at the energies provided by the ^{60}Co isotope.

2. Experimental procedure

The following list gives an overview of the structures, which were irradiated over a period of 24 h with doses ranging between 1 kGy and 10 kGy. All devices were designed and fabricated in-house at the Fraunhofer IMS in Duisburg.

- Linear transistors fabricated in a 0.35 μm CMOS technology (L035) with different W/L ratios.
- Enclosed-layout and ringed-source transistors fabricated in a 0.35 μm CMOS technology (L035).
- EEPROMs fabricated in a 1.0 μm silicon-on-insulator (SOI) technology (H10).
- Postprocessing coatings for color filters and microlenses.
- Fully operational 200 kPix visible light imager with on-chip ADCs fabricated in a 0.35 μm CMOS technology (L035).

Figure 1 gives an impression of the test facility at Fraunhofer INT. It shows some of the test structures placed underneath the radioactive source. During irradiation the source was positioned remotely at the end of the metal rod in the upper section of the image. All tests were performed under "worst-case" conditions, i.e. if possible the transistor gate potentials were connected to the positive supply voltage. This had the effect of maximizing the radiation damage by pushing the oxide charges as close to the transistor channel as possible.

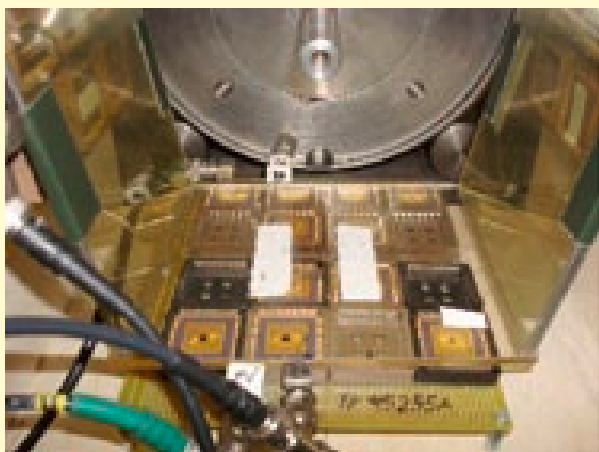


Figure 1: CMOS test circuits at the 18.7 TBq ^{60}Co irradiation facility at Fraunhofer INT.

The subsequent fully automated test of the irradiated devices started with a first measurement immediately after the irradiation. A second series of measurements covered ageing effects at room temperature over a period between one and eight months. Finally, a high temperature treatment at 250 °C for approximately 400 h concluded the scope of this analysis. Regarding the applied dose rates, it has to be noted that these were on the order of 10 rad/s. As a consequence any enhanced low dose rate effects (ELDRE) were neglected. Furthermore, the transistor dimensions were chosen such that the radiation-induced narrow channel effect (RINCE) was avoided in all but a few transistors with widths smaller than 1 μm .

3. Experimental results

The following sections summarize the most important results of the irradiation tests.

3.1. Linear transistors

Approximately 200 transistors with classical, straight, i.e. linear drain-gate-source topologies were evaluated. Immediately after exposure to the ^{60}Co source, the devices yielded thresh-

old voltage shifts of approximately -40 mV/kGy (NMOS) and 20 mV/kGy (PMOS). The leakage current at 0 V gate-source voltage remained constant for the PMOS transistors, while it increased by factors of 10^6 to 10^8 depending on the length of the NMOS transistors. Put into the broader context of comparable technologies, these results are on a par with the threshold voltage shifts reported in the literature. Despite their direct impact on the chip performance, the observed effects are not irreversible. More precisely the threshold voltage shift recovers partially during storage at room temperature. Measurements indicate a threshold voltage recovery of approximately 50 mV over eight months. This so-called annealing can be increased to the point of a full threshold voltage recovery if higher temperatures are applied. It was found that a high temperature treatment at 250 °C for about 400 h following the eight month room temperature annealing completely cancels the initial radiation effects.

3.2. Enclosed-layout transistors

An enclosed-layout transistor is a special type of transistor geometry, which aims to eliminate the parasitic current paths along the edges of conventional, linear transistors. Figure 2 shows a side-by-side view of the two layout approaches. As stated in the previous section the parasitic effects can lead

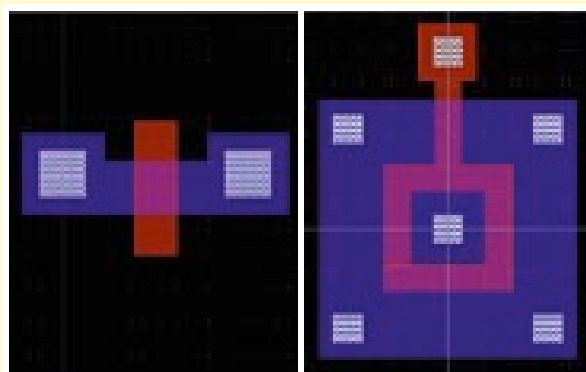


Figure 2: Layout screenshots of a conventional linear transistor (left) and an enclosed-layout transistor (right). The drain-source area is drawn in blue and the gate in red.

to a leakage current increase in the transistor off-state of a conventional NMOS transistor of up to a factor of 10^8 . In contrast to this, the leakage current of the tested enclosed-layout transistors increases only by a factor of 10^2 at the most, which proves the validity of this concept.

3.3. SOI EEPROMs

Electrically erasable memory cells (EEPROM) are often used to store system calibration data and are therefore a key component in many electronic devices. Within the scope of this test a number of EEPROMs designed at Fraunhofer IMS were tested. These memory cells are based on NMOS SOI transistors, which feature a floating gate structure. By changing the charge, which is stored on the floating gate, the threshold voltage of the whole transistor can be influenced, thus enabling a clear distinction between two logic states, i.e. a high and a low threshold voltage state.

The measurements show a direct impact of the cell's logic state prior to irradiation on the radiation induced threshold voltage shift. It was found that at approximately 5 kGy the distinction between the logic states vanishes, i.e. the cell loses the stored information as logic high and low states become indistinguishable, due to their different sensitivity to radiation. However, the cells can be reprogrammed. In that case all threshold voltages are shifted to lower values but the difference between high and low threshold voltage states, the so-called programming window, remains virtually unchanged. In a second test the degradation of the electrical difference between logic high and low states after 100,000 reprogramming cycles of irradiated and unirradiated cells was compared. These endurance tests showed no effect of the ionizing radiation.

3.4. Chip coatings

Fraunhofer IMS offers numerous post-processing options, which can be applied to standard CMOS wafers. Among these options are for example microlenses and color filters for visible light imagers.

In order to test their radiation hardness several of these coatings were applied to clean quartz wafers. These wafers were then characterized with respect to their transmission properties before and after irradiation. None of the applied substances showed a measurable change due to the gamma-radiation, i.e. the transmission characteristics remained unaltered.

3.5. Visible light imager

The impact of ionizing radiation on a more complex system was evaluated on a 200 kPix imager with on-chip ADCs, which was subjected to a total ionizing dose of approximately 3 kGy over 24 h. However, as the imager was not powered during the tests, the above mentioned worst case scenario for biased transistors was not used for this sensor. Although not specifically radiation hardened, the device showed no decrease in SNR or dynamic range during the electro-optical tests after the irradiation. In other words the system retained its full functionality.

4. Conclusion

A selection of transistors and devices fabricated by Fraunhofer IMS has been exposed to ionizing radiation. The study of the radiation effects on individual transistors yielded results, which are comparable to other $0.35\ \mu\text{m}$ technologies. Several ASICs such as EEPROMs and a visible light imager were exposed to doses of several kGy without a significant decrease in performance.

Currently Fraunhofer IMS is expanding its activities in the field of radiation hard design. These efforts will be supported by further radiation testing in the future.

TEST OF UNCOOLED PASSIVE IRFPAS IN BATCH-PRODUCTION

A. Utz, L. Gendrisch, S. Kolnsberg, F. Vogt

Introduction

Any object with a temperature above absolute zero emits electromagnetic radiation due to the movements of its atoms. In the range of room temperature at about 300K, the bulk of emitted radiant power is in the spectral range of about 8 to 14µm – which is the *far-infrared* (FIR) domain. Fraunhofer IMS develops and fabricates microbolometer based uncooled infrared focal plane arrays (IRFPAs) for that spectral range [1].

Along with the new challenges in the fabrication process, new demands on the test concept, test equipment and test execution arose. The test concept and its realization at Fraunhofer IMS are discussed in this article.

Test Concept

The microbolometers as FIR sensor elements are processed on a CMOS substrate which contains the readout IC (ROIC). This post processing step is done after the complete standard CMOS process is finished. After the processing of the microbolometers, the chips are equipped with an IR transparent

package, which encapsulates the sensors in a vacuum pressure atmosphere [3]. Fig. 1 shows the process flow including all test steps.

The first test is possible after the processing of the CMOS ROIC. This is a standard electrical test and can be executed fully automated using the existing test equipment. This test step is mandatory for the detection of electrically defect chips, failures in the process flow or changes of parameters.

Another test on wafer level can be done after the bolometers and packages are fabricated. At this point of the processing, it is already possible to fully electro-optically characterize the IRFPAs. The core parameter of an IRFPA is the noise equivalent temperature difference (NETD), which is defined as the ratio between pixel noise N and its sensitivity (so called signal transfer function, SiTF).

$$NETD = \frac{N}{SiTF}$$

To measure the SiTF, it is necessary to stimulate the IRFPA with radiation of two different intensities. Therefore, a controlled radiation source and well defined optical conditions are required for the test. The additional wafer-level test step forms a significant improvement of the process flow, as devices with defective bolometers or vacuum package can be identified before the dicing and packaging process. This allows to save a significant amount of time and money.

Finally, after dicing and assembly of the IRFPAs, a last test on component level is carried out. In this test step, the IRFPA's NETD can be tested using the original camera electronic. So this is the most accurate test.

The described three step test concept allows to detect electrically defect IRFPAs before they are equipped with the vacuum package and to detect IRFPAs with defect bolometers or packages before the assembly process. This is especially important for big chips (which IRFPAs typically are) with limited yield of

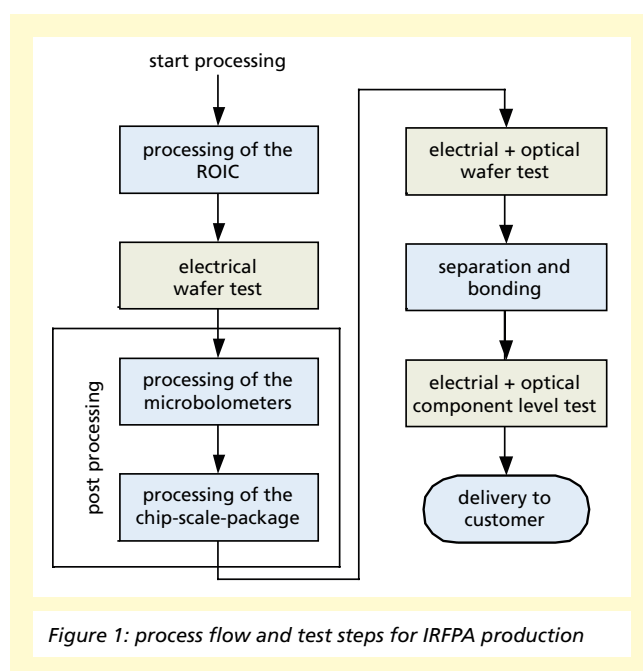


Figure 1: process flow and test steps for IRFPA production

the CMOS process as well as for products with high assembly costs which is also true in this case.

Realization

Besides its 0,35 μm CMOS technology, Fraunhofer IMS drives a fully equipped test floor in an additional clean room area. The test floor consists of multiple fully automated test cells combining IC test system, wafer prober and/or IC handler. The test cell which was chosen for the IRFPA test contains a test system of type Advantest M3670 and a wafer prober of type Accretech UF200a.

Optical Wafer Level Test: To allow wafer level NETD testing, the existing test cell had to be expanded by a number of

components. Fig. 2 shows a schematic representation of the resulting setup. The digital video data from the IRFPA is converted into the CameraLink format by a FPGA board and then transmitted to the framegrabber of an additional PC. The PC is responsible for image data acquisition and analysis. The communication between the single components is carried out via a GPIB bus, where the M3670 test system is the controller. I.e. the whole test execution is controlled by the test system.

A Black Body of type SBIR DB06 has been integrated into the wafer prober as radiation source. An optical baffle or IR optics ensures defined optical conditions, which means that the F-number ($F_{no.}$) of the setup is set to $F_{no.} = 1.0$

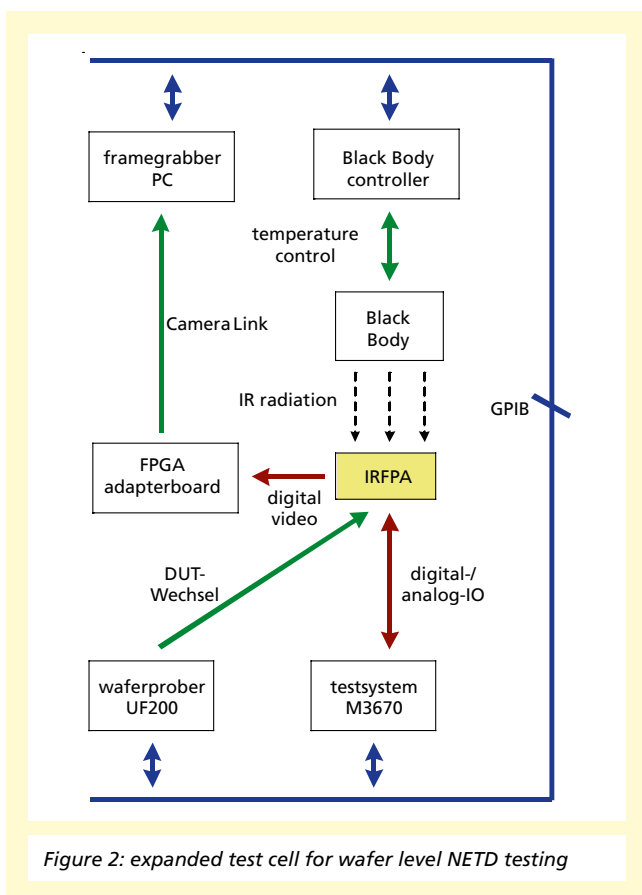


Figure 2: expanded test cell for wafer level NETD testing

Fig. 3 shows the resulting setup on top of the wafer prober. The test setup allows the fully automatic execution of electrical and optical tests on wafer level.

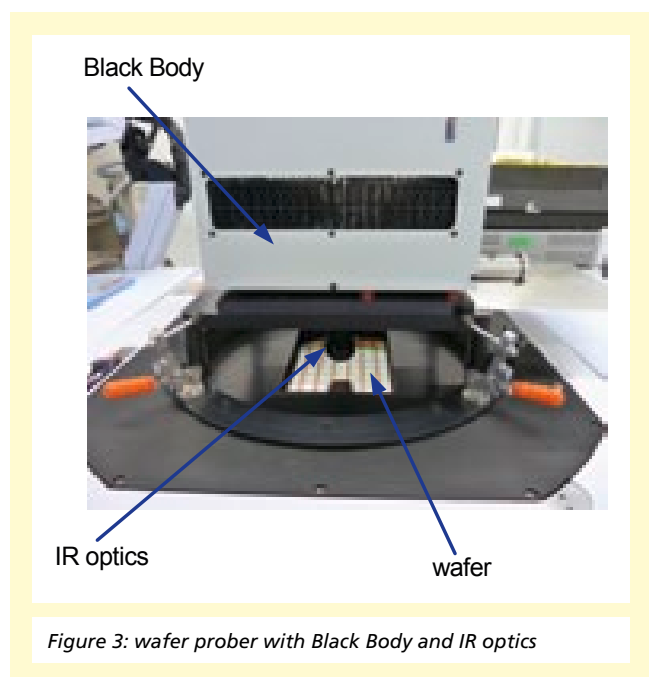


Figure 3: wafer prober with Black Body and IR optics

SILICON SENSORS AND MICROSYSTEMS
 TEST OF UNCOOLED PASSIVE IRFPAS
 IN BATCH-PRODUCTION

Final Component Level Test: A dedicated setup for the finally assembled IRFPA components has been developed for acceptance testing. The setup consists of two Black Body radiation sources, an optical baffle to ensure F/1.0 conditions and a contact unit for electrically and thermally contacting the device under test (DUT). Fig. 4 shows a schematic figure of this setup.

The Black Bodies consist of a thermoelectric cooler (TEC) and a Cu-block, which is coated with a high emissive painting. A negative temperature coefficient (NTC) thermistor is integrated into the Cu-block for maintaining the temperature of the radiation source. During test execution, one of the sources is set to $T_1 = 20^\circ\text{C}$ and the other one to $T_2 = 35^\circ\text{C}$. The Black Bodies can be moved under the DUT via a motor with linear

guiding. This concept allows the stimulation of the DUT with different IR intensities without moving the DUT and readout electronics or changing the temperature of the radiation source.

The electrical contact of the device is carried out via spring contacts. To ensure that the DUT reaches thermal equilibrium quickly after switching it on and that its temperature is stable to a very high level during test execution, the DUT is also thermally contacted via a Cu-block. As for the Black Bodies, the temperature is controlled by a TEC and maintained by a NTC type thermistor. Using this mechanism for temperature control, the DUT reaches thermal equilibrium within less than three minutes and its temperature uncertainty during test execution is only in the order of 5 mK.

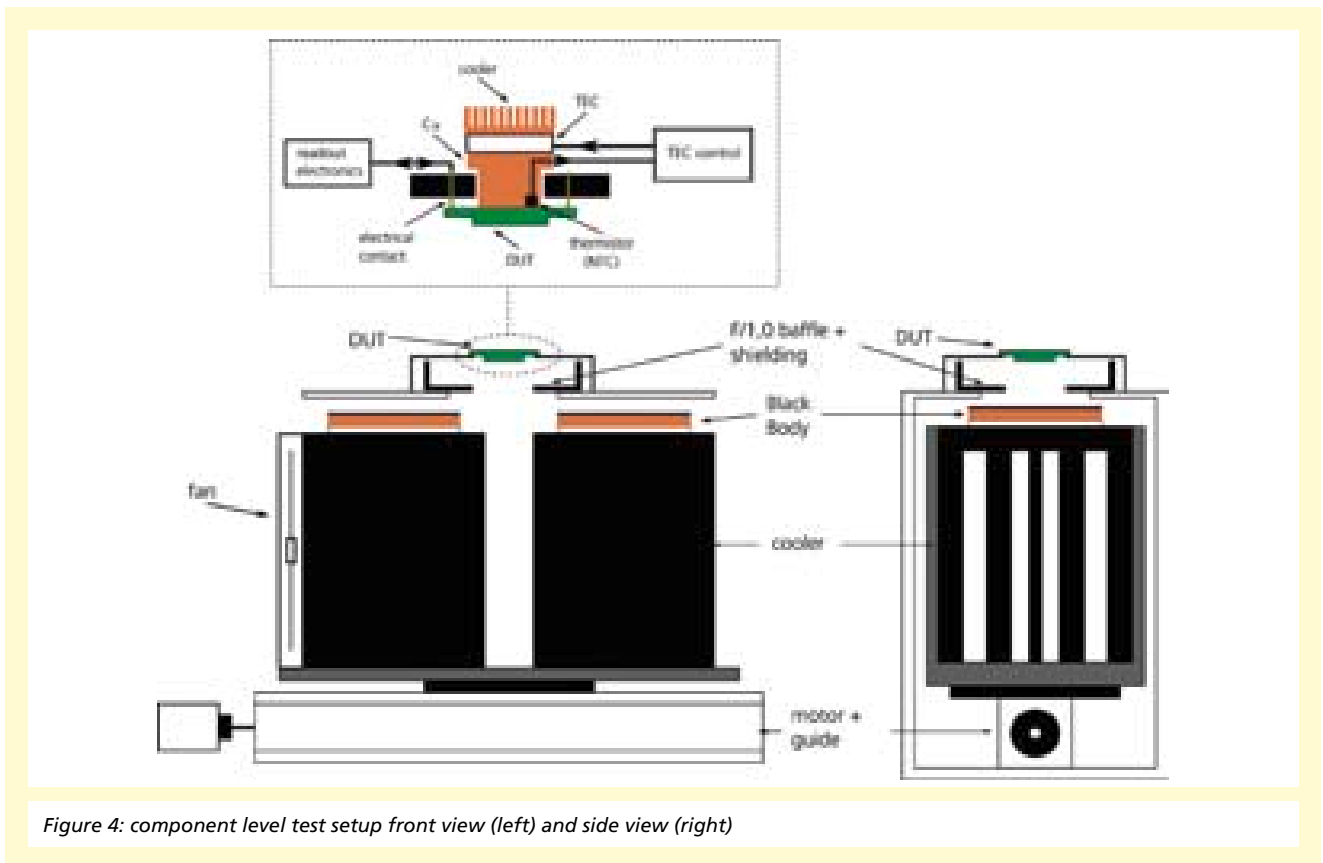


Figure 4: component level test setup front view (left) and side view (right)

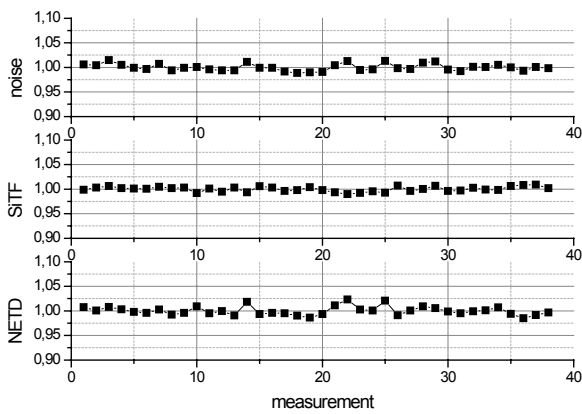


Figure 5: results of repetitive measurements on a single device

Evaluation

The measurement uncertainty of the wafer- and component-level test setups were calculated regarding thermal, mechanical and electrical sources of error. Hereby, the evaluation method proposed in [4] was followed. The precision of both setups was estimated by statistical means by measurements on a single device. Fig. 5 shows the results of such a measurement on the component level tester.

The resulting relative uncertainties and precisions for a confidence interval of 95 % are summarized in the following table.

	wafer-level	component-level
W_{NETD}	10.2 %	3.6 %
P_{NETD}	5.4 %	1.7 %

Conclusion

In this article, we discussed the test concept for IRFPA production and its realization at Fraunhofer IMS. The concept allows the electro optical characterization of the IRFPA on wafer- and component-level. Although the wafer-level test is not too accurate, it allows the detection of defective devices in an early state and so is a significant improvement of the production process.

References

- [1] D. Weiler; M. Russ; D. Würfel; R. Lerch; P. Yang; J. Bauer und H. Vogt: A digital 25 μ m pixel-pitch uncooled amorphous silicon TEC-less VGA IRFPA with massive parallel Sigma-Delta ADC readout. Proc. SPIE Vol. 7660, 2010
- [2] A. Utz, L. Gendrisch, D. Brögger, D. Weiler and H. Vogt: NETD Measurement of Far-Infrared Imagers on Wafer-Level under Ambient Pressure in Batch Production. Mikrosystemtechnik Kongress 2011, VDE, 2011
- [3] J. Bauer; D. Weiler; M. Russ; J. Hess; P. Yang; J. Voss; N. Arnold und H. Vogt: Fabrication Method for Chip-Scale-Packages based on a Chip-to-Wafer Process. Proc. SPIE Vol. 7834, 2010
- [4] BIPM: Evaluation of measurement data - Guide to the expression of uncertainty in measurement, JCGM, 2008

A FAR INFRARED UNCOOLED VGA-IRFPA FOR AUTOMOTIVE APPLICATIONS

D. Weiler

Abstract

The detection of pedestrian is a typical automotive application of uncooled IR-detectors (IRFPA = infrared focal plane array). An IRFPA detects the IR-radiation of pedestrians or animals directly without the need for an active illumination of the scene. An advanced digital IRFPA with an optical resolution 640 x 480 pixel (VGA) based on uncooled microbolometers with a pixel-pitch of 25 μm has been developed by Fraunhofer-IMS. The digital IRFPA is designed for thermal imaging applications with a full-frame frequency of 30 Hz and a high sensitivity with a NETD < 100 mK @ f/1. The IR sensor element is realized as a microbolometer based on amorphous silicon as the sensing layer. A novel readout architecture which utilizes massively parallel on-chip Sigma-Delta-ADCs located under the microbolometer array results in a high performance digital readout. Since packaging is a significant part of IRFPA's price Fraunhofer-IMS uses a chip-scaled package consisting of an IR-transparent window with antireflection coating and a soldering frame for maintaining the vacuum. The IRFPAs are completely fabricated at Fraunhofer-IMS on 8" CMOS wafers with an additional surface micromachining process.

Introduction

Warm bodies like humans or animals emit radiation in the long-wave infrared band (8 μm ... 14 μm) according to Planck's law. Due to this emitted radiation an uncooled IRFPA can detect hot spots passively without any active illumination. In contrast to uncooled IRFPAs near-infrared (NIR) detectors can only detect pedestrian with active illumination [1]. Uncooled IRFPAs operate at ambient temperature and benefit from the abdication of a Stirling cooler in terms of low-cost, low power dissipation, low weight, and reduced volume. Low-cost thermal imaging is dominated by uncooled infrared focal plane arrays (IRFPAs) using microbolometers based on vanadium oxide (VOx) or amorphous silicon (a-Si) as the sensing material. Typical applications for IRFPAs besides pedestrian detection for automotive driving-assistance systems are thermal imaging, fire fighting, biological imagery, or military applications like target recognition.

Digital VGA-IRFPA

Fraunhofer IMS has fabricated in 2009 the first uncooled infrared focal plane array (IRFPA) throughout Germany. The digital VGA-IRFPAs are completely fabricated at Fraunhofer-IMS on 8" CMOS wafers with an additional surface micromachining process [2]. The IR-sensitive element is realized as a microbolometer based on amorphous silicon as the sensing material. The microbolometer converts the infrared radiation absorbed by

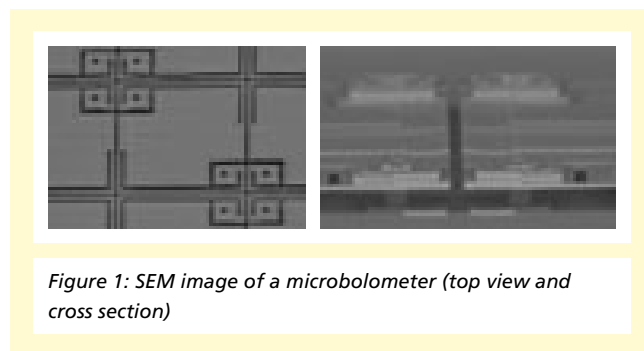


Figure 1: SEM image of a microbolometer (top view and cross section)

a membrane into heat energy and this induces a temperature rise resulting in a change of the electrical resistance. Two SEM images of a microbolometer are shown in Figure 1.

The microbolometers are fabricated in a 25 μm pixel pitch by post-processing CMOS wafers. The vertical and lateral pixel geometry was kept very simple and straightforward to ensure a solid baseline process with a high pixel operability [3]. Microbolometers have to operate in a vacuum-package to reduce thermal losses by gas convection. For reducing packaging costs Fraunhofer-IMS uses a chip-scaled package consisting of an IR-transparent window with an antireflection coating and a soldering frame for maintaining the vacuum [4]. The realization and principle of a chip-scale package is depicted in Figure 2.



Figure 2: Realization and principle of a chip scale package

The IR-transparent lid consists of silicon with a double-sided antireflection coating and is placed using a solder frame on top of the CMOS-substrate which includes the readout electronics and the microbolometers. The use of silicon as a transparent lid results in lower production costs compared to germanium and causes lower mechanical stress due to equal expansion coefficients between the lid and the substrate. The chip scale package is currently under development in terms of long-time vacuum stability. For automotive applications the chip scale package is mounted onto a detector-board as a chip-on-board solution, which is used in a IR-camera system. The block diagram of the developed digital VGA-IRFPA is shown in Figure 3.

The 640 x 480 microbolometer array is read out by using massively parallel Sigma-Delta-ADCs located under the array which results in a high performance digital readout. Blind

microbolometers with a reduced responsivity are located in a ring around the active microbolometer array. The blind microbolometers are read out identically to the active microbolometer. The $\Sigma\Delta$ -ADCs convert the scene dependent resistor change directly into 16 bit digital signals. These 16 bit image signals are fed into the digital video interface by a multiplexer. A sequencer controls the readout pattern by selecting each $\Sigma\Delta$ -ADC using a line and row control block. The configuration of the sequencer can be changed using an I²C-like interface. A built-in self-test supports the wafer test und reduces test time. The digital video interface provides three synchronization signals (horizontal, vertical and pixelclock) in addition to the image signals. A temperature sensor measures the temperature of the IRFPA. The temperature signal V_{temp} is an analog voltage proportional to the temperature of the IRFPA and can be used for TEC-less operation. The IRFPA needs one analog supply voltage of $V_{dda} = 3.3$ V and two digital supply voltages of $V_{dd1} = 3.3$ V and $V_{dd2} = 1.8$ V. Five different reference voltages are necessary for biasing the $\Sigma\Delta$ -ADC. Apart from a reset signal and the I²C configuration signals the IRFPA needs only one digital clock signal.

The technical data of the developed digital VGA-IRFPA are summarized in Table 1

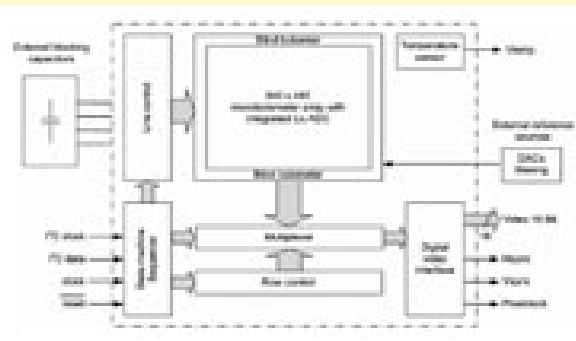


Figure 3: Block diagram of the developed digital VGA-IRFPA

Table 1: Parameter digital VGA-IRFPA

Parameter	Value
Image format	640 x 480 pixels
Frame frequency (progressive)	30 Hz
Output signal	16 bit (digital)
Temperature range	- 40 ... 80 °C
Power supply voltage	3.3 V and 1.8 V (digital) 3.3 V (analog)
NETD	<100 mK (design value)

A Far Infrared uncooled VGA-IRFPA for Automotive Applications

Electro-optical characterization

To characterize the developed digital VGA-IRFPA Fraunhofer IMS has designed a prototype IR-camera. This IR-camera consist of a IR-lens, a shutter, a reference voltage PCB, and a FPGA board. All IR-cameras have to correct the offset of the IRFPA periodically by closing a shutter. A reference voltage PCB generates from one main power supply voltage all required power supply and reference voltages.

An uncompensated IR image taken with the digital VGA-IRFPA is shown in Figure 4.



Figure 4: Uncompensated IR image

Apart from a simple offset correction the shown image is uncompensated, i.e. no gain, defect pixel, or noise correction has been done. High temperatures in the scene are displayed as dark gray, low temperatures as light gray. The IR-image has been taken at a warm summer day. Although the environment conditions are poor for IR-images due to high temperatures a good thermal contrast is visible. Humans can be distinguished excellent from the hot road surface.

Conclusion

A digital IRFPA with 640 x 480 pixel and a 16 bit output signal has been designed, fabricated and electro-optical tested. The microbolometers feature a pixel pitch of 25 μm and consists of amorphous silicon as the sensing layer. The digital readout of the microbolometer based on a massive parallel use of SD-modulators followed by sinc-filters. To complete an IRFPA a vacuum package is necessary which is realized as a "chip scale package". The developed digital VGA-IRFPA can be used for the detection of pedestrian as an automotive application with a for times higher optical resolution compared to conventional nigh vision systems.

References

- [1] D. Weiler, et al., "A far infrared VGA detector based on uncooled microbolometers for automotive applications", International Forum on Advanced Microsystems for Automotive Applications (AMAA '11) <15, 2011, Berlin>; pp. 327 – 334, 2011
- [2] D. Weiler, et al., "Improvements of a digital 25 μm pixel-pitch uncooled amorphous silicon TEC-less VGA IRFPA with massively parallel Sigma-Delta- ADC readout", SPIE Conf. on Infrared technology and Applications XXXVII, Orlando, Proc. of SPIE Vol. 8012, 80121F-1 - 80121F-7, 2011
- [3] M. Ruß, J. Bauer, and H. Vogt, "The geometric design of microbolometer elements for uncooled focal plane arrays", Proc. SPIE Conference Infrared Technology and Applications XXXIII, Volume 6542, 2007
- [4] J. Bauer, et al., "Fabrication method for chip-scale-vacuum-packages based on a Chip-to-Wafer-Process"; Conference on Electro-Optical and Infrared Systems: Technology and Applications VII; Toulouse; Proc. of SPIE Vol. 7834, 78340S-1 – 78340S-8, 2010

INTRAVASCULAR MONITORING SYSTEM FOR HYPERTENSION

M. Görtz, P. Fürst

Background

Caused by the higher average age approximately 10–30 % of the population in industrial nations comes down with hypertension (high blood pressure). About 10% of this group needs long term monitoring [1]. For these patients two systems exist at the moment:

- Catheter based measurement systems for short term blood pressure measurements in a clinical evaluation
- Extra corporal measurement systems for short or long term blood pressure measurements like blood pressure cuffs. These systems are inconvenient in handling and disturb the patients in daily life. A second disadvantage is that they do not allow continuous measurements.

The presented system is aimed to overcome these limitations by providing up to 36 blood pressure measurements per second with a fully telemetrically controlled implant that works without battery. Additionally highly precise information is gained on the transient heart rhythm and possible anomalies like syncopes.

Components of the measuring system

The implant which is shown in fig. 1 consists of two main parts. The first one is the pressure sensor which is inserted into the medical catheter and is designed as small as possible

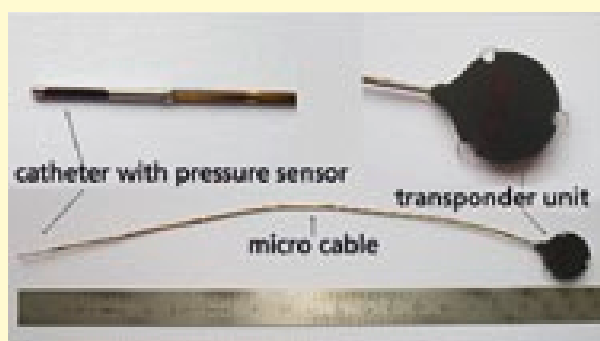


Figure 1: Implant with catheter, micro cable and transponder unit

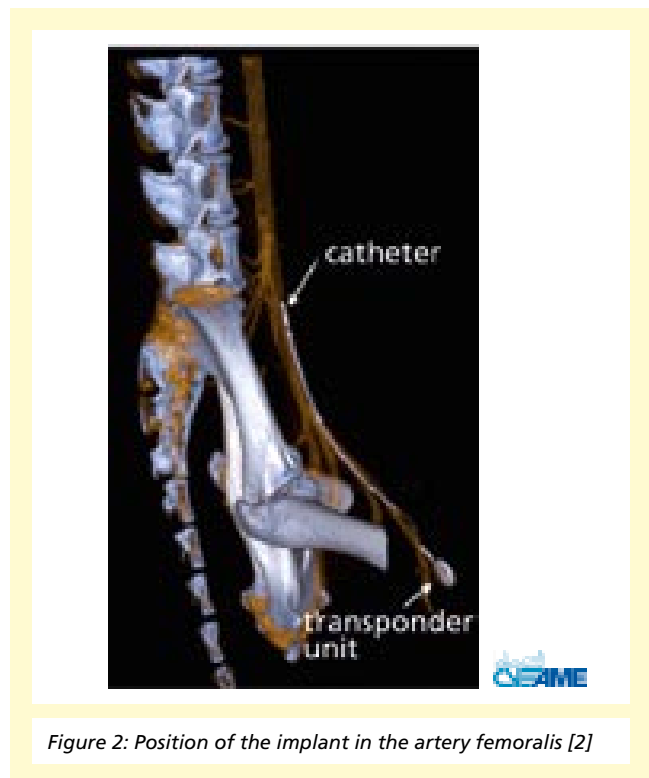


Figure 2: Position of the implant in the artery femoralis [2]

to avoid clotting and to minimize the flow resistance. The catheter is placed in the artery femoralis (fig. 2). The second main part is the transponder unit implanted just underneath the skin in order to guarantee optimal transmission parameters due to the transition through a minimum number of skin layers.

1. The pressure sensor chip

The pressure sensor chip (fig. 3) is integrated into the tip of a medical catheter and connected via a miniaturized cable to a telemetric unit. The size of the pressure sensor chip is 5.45 mm times 0.61 mm. Its thickness is 350 μm .



Figure 3: Pressure sensor chip

As shown in the schematic in fig. 4, the pressure sensor chip consists of a sensor part, an analog signal path and a digital state machine. The sensor part contains the capacitive micro-machined pressure sensor as well as a temperature sensor. The pressure sensor is fabricated along with the integrated signal conditioning circuitry. The pressure and the temperature sensor are readout by a capacitance/voltage (C/U) converter whose output is a differential voltage signal. The pressure sensor path is adjustable in offset and gain. The temperature sensor is realized by a parasitic bipolar transistor, which is biased by a reference current. The digital state machine controls the start- and measurement-phase, the adjustment of offset and gain as well as the clock-distribution and the sleep- and the rest-mode on the pressure sensor chip. A multiplexer, addressed by the state machine, optionally connects the analog output signal of the pressure sensor or temperature sensor to the data-pads (SD0, SD1). An offset and gain configuration is also transmitted by the data-pads. The bias block generates reference currents that are needed for the generation of the operating point of the C/U converter.

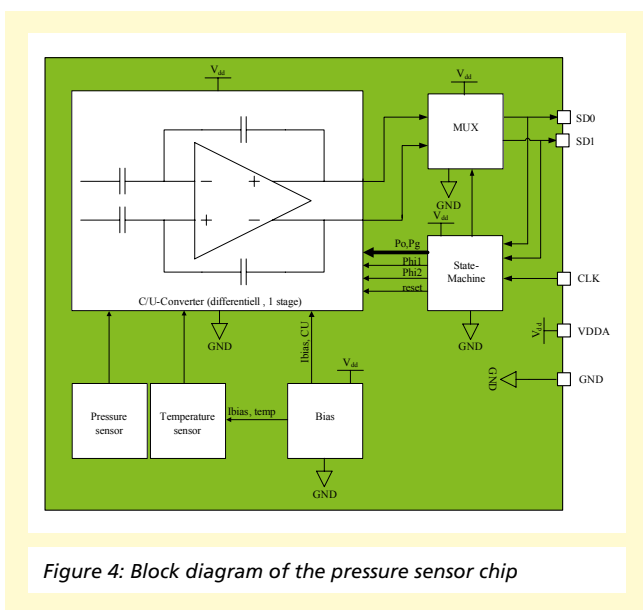


Figure 4: Block diagram of the pressure sensor chip

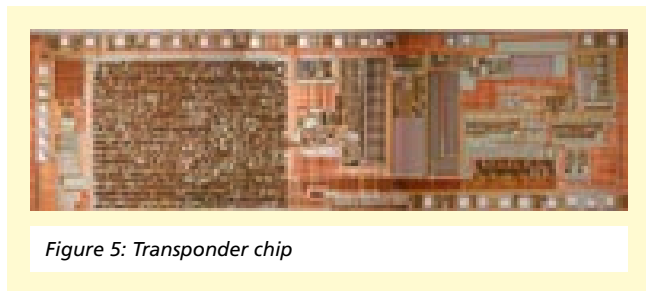


Figure 5: Transponder chip

2. The transponder chip

The passive transponder chip (fig. 5) receives energy by inductive coupling from an external reader station and controls and supplies the sensor chip. The analog pressure and temperature data from the sensor chip are converted by a 13 bit cyclic RSD ADC into digital values. Data transfer from the implant to the reader station is realized by amplitude modulation of the supplied energy carrier wave. The size of the transponder chip is 8 mm times 2.5 mm.

This transponder chip includes the following main blocks:

- HF-Front-End
- State machine (control unit)
- EEPROM
- Low-power sensor readout with a 12 bit cyclic redundant signed digit (RSD) ADC

The main features of the measurement system are:

- Battery-less operation
- Transmission: Digital with CRC to detect transmission errors
- A 256 x 1 bit organized EEPROM
- JTAG test access port (TAP) that implements the IEEE 1149.1 protocol.

The schematic of the transponder chip and its external components, necessary for telemetric mode, are presented in fig. 6. The schematic blocks for telemetry are allocated by the HF-front-end. The controlled supply voltage, required for sensor readout, is also generated by the HF-front-end. A state-machine (digital part of the chip) provides the protocol, which

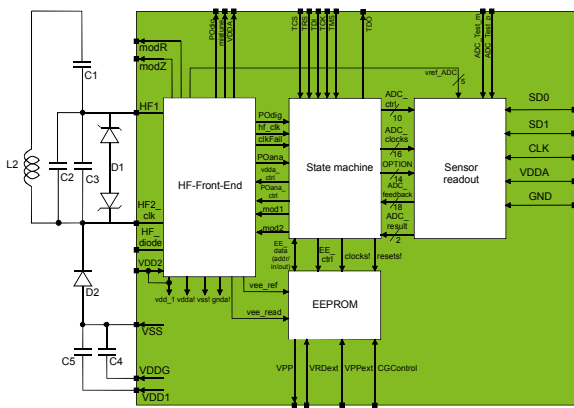


Figure 6: Block diagram of the transponder chip with external components

is necessary for data transmission of measured values. The internal EEPROM stores the ID and parts of the calibration coefficients. The setting data for offset and gain are transmitted by the bi-directional data-pads to the pressure sensor chip. After the measurement is finished the analogue output signals are transmitted, again by the data-pads, from the pressure sensor chip to the transponder chip, where they are digitalized by the sensor readout block. Next the digital data are sent by telemetry to the receiver coil of the external readout electronics.

Calibration

The calibration of the non linear and temperature dependent output of the pressure sensor chip is performed in a temperature controlled pressure chamber. A typical pressure characteristics and a typical calibration error better than 1.4 hPa is shown in fig. 7 and fig. 8.

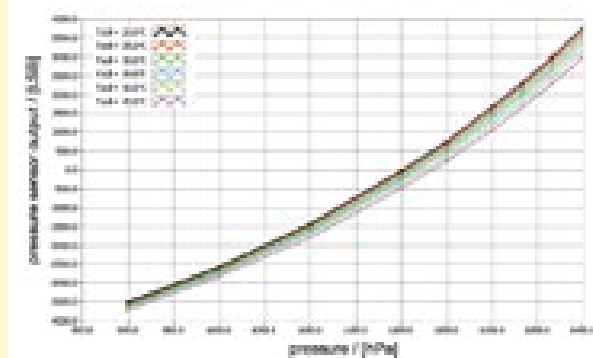


Figure 7: Typical pressure sensor chip characteristics

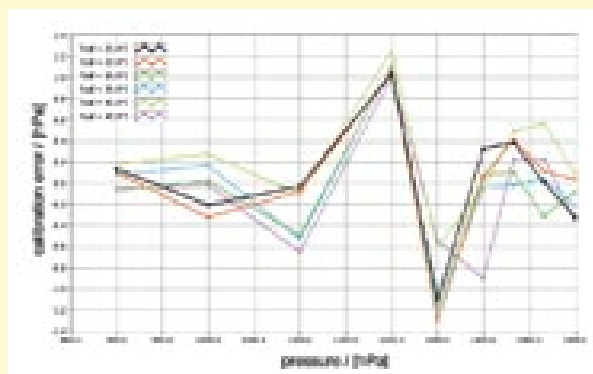
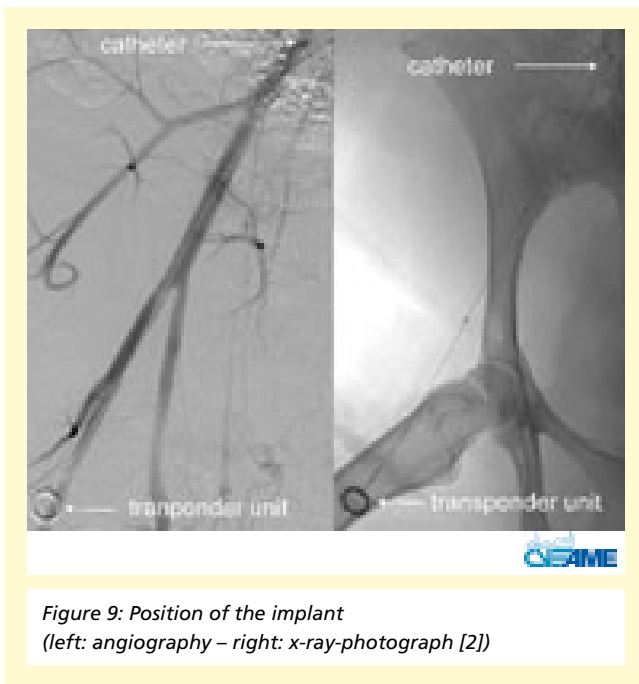


Figure 8: Typical calibration error example

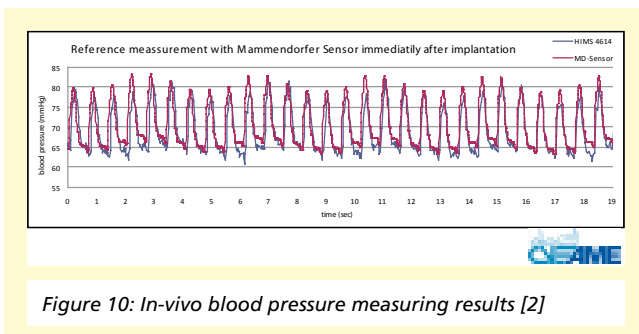
In vivo measurements

In vivo experiments with implants have been successfully completed. The implant was placed in the artery femoralis of a sheep. The position of the implant in the sheep is shown in fig. 9 on the left side as an angiography and on the right side as a x-ray photograph.

SILICON SENSORS AND MICROSYSTEMS
 INTRAVASCULAR MONITORING
 SYSTEM FOR HYPERTENSION



The wirelessly recorded data of the implant (blue signal in fig. 10) match the reference data of the Mammendorfer Sensor (red signal in fig. 10).



Implant specifications

The implant's specifications and geometry are shown in table 1:

Table 1: Implant specifications

Parameter	Value	Unit
pressure sensor signal rate	36	Hz
pressure sensor accuracy	±2	hPa
pressure range	900–1350	hPa
temperature sensor signal rate	18	Hz
temperature sensor accuracy	0.5	K
power consumption	300	µW
catheter length	12	mm
catheter diameter	1.05	mm
transponder unit diameter	17	mm
transponder unit height	3	mm
micro cable length	185	mm

The presented work is part of project "Intravasales Monitoring System für Hypertoniker - HYPER-IMS" funded by the German "Bundesministerium für Bildung und Forschung BMBF".



References

- [1] T. Götttsche, M. Gräfe, P. Osypka, M. Görtz, K. Trieu, H. Fassbender, W. Mokwa, U. Urban, T. Schmitz-Rode, B. Bender, R. Glocker, M. Fähnle; HYPER-IMS: A Fully Implantable Blood Pressure Sensor for Hypertonic Patients SENSOR+TEST Kongress 2009, Nürnberg
- [2] Nina Cleven, Anna Woitok, Michael Görtz, Thorsten Goettsche, Ulrich Steinseifer, Thomas Schmitz-Rode; Testing and Improvement of a long-term Monitoring System for Hypertension Patients, DGBMT Jahrestagung 2011

CMOS PIXELS FOR PULSED 3D TIME-OF-FLIGHT SENSORS

D. Durini, A. Spickermann

3D-Imaging based on the indirect time-of-flight (ToF) principle

Scannerless 3D scene reconstruction based on indirect time-of-flight (ToF) principle relies on measurements of the time elapsed between the moment in which a light signal, actively modulated and widened by a special diffusing lens to cover an entire scene, is sent by a light source and a moment at which, after being reflected by different objects in a scene, it impinges at the photosensor usually collocated aside this emitting light source [1]. The photosensor is here operated synchronously with the emission of the light pulse and enables the evaluation of the exact delay of the returned pulsed signal impinging on each individual pixel and the determination of the distance of different objects in the illuminated scene [2]. The indirect ToF measurement utilizes the integration of the photogenerated charge during a very short time window (in order of ns), synchronized with the emitted light signal (e.g. a laser-pulse). So short time scales require short transit time, low noise and the fast readout in each pixel [2, 4, 5, 6].

Development of the CMOS image sensor aimed at ToF based 3D imaging

The pixel of the sensor developed relies on a newly developed photodiode featuring lateral intrinsic drift field [4]. The photodiode is divided in two main parts: a pinned surface one and a part which resembles a buried CCD cell, as it can be observed in Fig. 1. The pixels and the entire sensor have been fabricated in the 2P4M automotive certified $0.35\ \mu\text{m}$ CMOS technology at the Fraunhofer IMS with the addition of an extra surface-pinned n -well yielding a non-uniform lateral doping profile [4], as shown in Fig. 1 (upper picture). The doping concentration gradient [4] of the extra n -well was chosen in such a way that it induces an intrinsic lateral drift field [2, 6] parallel to the Si-surface in the direction of the pixel readout node (x-axis in Fig. 1) as well as from the periphery of the n -well in the direction of the n -well centre (y-axis in Fig. 1) [4]. The potential distribution within this intrinsic lateral drift-field

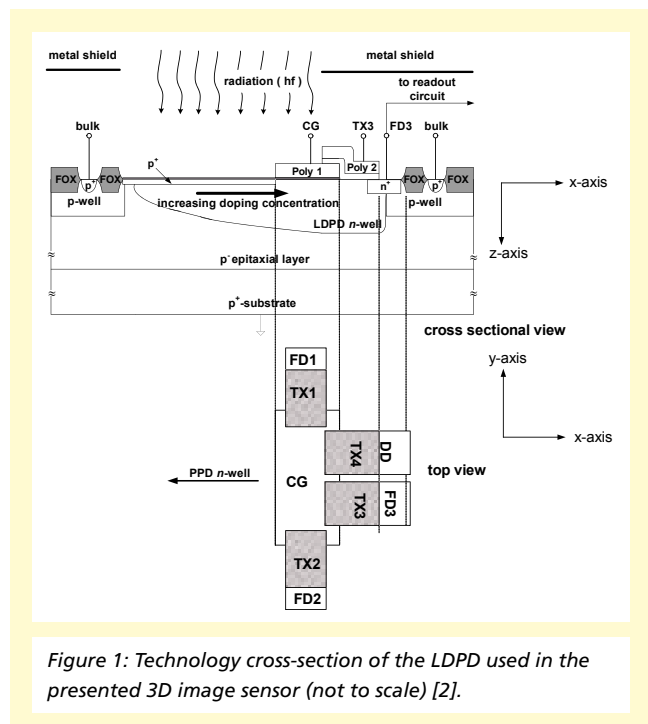


Figure 1: Technology cross-section of the LDPD used in the presented 3D image sensor (not to scale) [2].

photodiode (LDPD) n -well resembles a hopper [4] leading the photogenerated charge directly to the assigned readout nodes. It remains fully depleted during operation, sandwiched between the substrate and a grounded p^+ pinning layer on top of it (see Fig. 1). In this manner, the almost noiseless reset and readout operations of the photodetector are enabled. A buried collection-gate (CG) is fabricated at the one end of the n -well, which remains biased at a certain voltage V_{CG} . It induces an additional electrostatic potential maximum in the system and enables the proper and symmetrical distribution of the signal charge among the readout nodes. Each of the four transfer-gates (TX) plays two main roles: 1) it serves to create a potential barrier in the well to prevent the collected charge to be transferred into any of the three “floating” diffusions (FD) aimed at pixel readout or the so called “draining” diffusion (DD) permanently biased at a reset potential, or 2) to facilitate the transport of the photocharge into a desired FD or the DD.

SILICON SENSORS AND MICROSYSTEMS
 CMOS PIXELS FOR PULSED
 3D TIME-OF-FLIGHT SENSORS

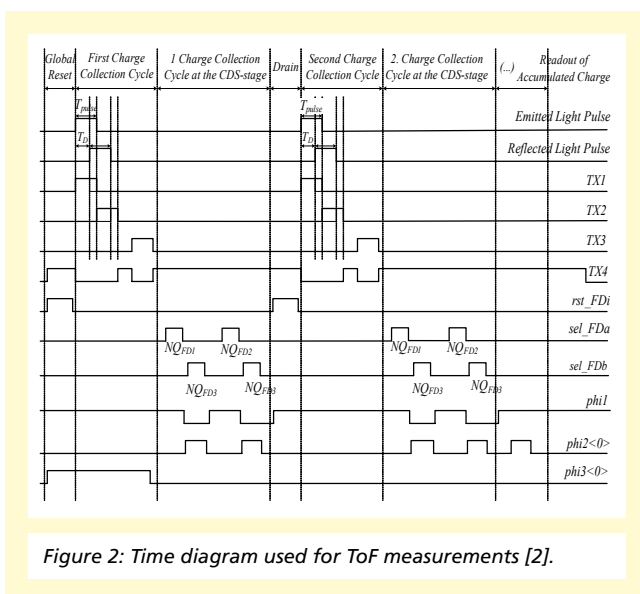


Figure 2: Time diagram used for ToF measurements [2].

A timing diagram proposed for ToF ranging application can be observed in Fig. 2 [2]. Here, the first shutter activation ($T_{TX1} = T_{pulse}$) begins synchronously with the emission of the laser pulse, followed by the second shutter activation ($T_{TX2} = T_{pulse}$) starting directly at the end of the TX1 pulse. If the time delay TD between the laser emission and the impinging light of the reflected laser pulse on the photodetector is equal to zero, the whole laser pulse is included in the first shutter period (TX1). Otherwise, the photogenerated charge is split into two parts and the charge ratio transferred to FD1 and FD2 contains the information about the time delay. After the end of the TX2 pulse, a short cycle of charge draining follows (TX4 is ON, whilst TX1, TX2 and TX3 remain OFF) to clear the LDPD by using the DD connected to the reset voltage. Following, an additional measurement using FD3 is performed for the same integration time ($T_{TX3} = T_{pulse}$), only without emitting the laser pulse, to determine the amount of charge generated by the ambient light. The electronic background illumination suppression is performed in this way. Here, the first charge collection cycle is over and a second one begins without reset-

ting the FDs. Between the cycles, TX4 remains ON to drain the unwanted charge carriers from the LDPD and CG regions. The cycles depicted in Fig. 2 [2] repeat themselves until short before reaching the FD's full-well capacity. Note, that the use of the LDPD allows a photocharge accumulation at each FD ("in-pixel" accumulation) over several (N) shutter periods. Moreover, using non-destructive readout after different shutter periods allows further extension of the dynamic range (DR).

The high-voltage option of the 0.35 μm CMOS process used features lowly doped wells and enables power supply voltage operation of analog circuits from 5V up to 8V, while the digital circuits are operated at 3.3V. For the generation of the doping concentration gradient, appropriately sized windows have been designed in the extra mask mentioned above (see [4]). The chip area is 6.45 mm \times 9.10 mm and it contains 128 \times 96 active pixels (as shown in Fig. 6) [2]. The pixel size is 40 μm square with 38 % fill factor [2].

The sensor was characterized using a special measurement setup using a 905 nm wavelength pulsed laser active radiation with $T_{pulse} = 30\text{ ns}$. For the measurements, the sensor was operated at a master clock frequency of 33MHz allowing for integration time of 30 ns [2]. The responsivity of the LDPD at the mentioned wavelength is of 230 $\mu\text{V}/\text{W}/\text{m}^2$ [2], whilst the



Figure 3: A 3D image obtained using the ToF camera system [2].

full well capacity of each of the three FDs is 78 ke^- [2]. The measurements with in-pixel accumulation have shown that each FD can accumulate photocharge resulting from over 2000 laser pulses with excellent linearity [2]. The dynamic range achieved is about 60dB and indirect charge transfer measurements confirmed that it was well below the minimum required 30ns. NEP was 0.31 W/m^2 [2] per pulse, downscaled using a measurement with 512 pulses.

Conclusion

A ToF based 3D camera system with the incorporated pulsed laser source was implemented based on the intrinsic LDPD image sensor. First distance measurements deliver an acceptable accuracy, an example of which can be observed in Fig. 3, where a human hand can be clearly observed providing 3D information.

References

- [1] O. Elkhaili, et al., "A 4x64 pixel CMOS image sensor for 3D measurement applications", *IEEE J. of Solid-State Circuits*, vol. 39, no. 7, pp. 1208–1212, July 2004.
- [2] A. Spickermann, D. Durini, A. Süß, W. Ulfig, W. Brockherde, B. J. Hosticka, S. Schwöpe, A. Grabmaier, "CMOS 3D Image Sensor Based on Pulse Modulated Time-of-Flight Principle and Intrinsic Lateral Drift-Field Photodiode Pixels", *Proc. 37th European Solid-State Circuit Conference (ESSCIRC)*, Helsinki, Finland, 12–16 Sept. 2011, pp. 111–114
- [3] R. Lange, et al., "Solid-state time-of-flight range camera", *IEEE J. of Quant. Electr.*, vol. 37, no. 3, pp. 390–397, March 2001.
- [4] D. Durini, et al., "Lateral drift-field photodiode for low-noise, high-speed, large photoactive-area CMOS imaging applications", *Nuclear Instruments and Methods in Physics Research A* 624, pp. 470–475, 2010.
- [5] B. Büttgen et al., "Robust Optical Time-of-Flight Range Imaging Based on Smart Pixel Structures", *IEEE, Trans. On Circ. And Syst. I*, Vol. 55, No. 6, pp. 1512–1525, Juli 2008.
- [6] C. Tubert, et al., "High speed dual port pinned-photodiode for time-of-flight imaging", *Proc. IISW* 2009.

CMOS HIGH-FRAME-RATE HDTV SENSOR

G. Varga, D. Durini

Motivation

Limitations in quality control performance represent an obstacle in evolution of the marble and stone processing industry. A way to automated surface analysis is pivotal in realising improved product quality and greater operational efficiency thus reducing the environmental impact of stone processing and reducing the product's time to market. Such improvements are considered to be of major significance to secure existing markets and to develop new opportunities. This issue has been addressed in the EC funded project PROVIPS, developed by the Fraunhofer IMS in close cooperation with partners from Italy, Portugal, Finland and Germany.

PROVIPS project dealt with the design and development of a high-speed automatic system used for ornamental stone classification. In order to reach this goal, the PROVIPS consortium developed a flexible and versatile classification tool able to perform customer defined custom classification of marble slabs and tiles according to the requirements of the end-user.

The task for Fraunhofer IMS was to design and develop a CMOS image sensor (CIS) for a spectral camera to be used in the automatic vision system able to acquire images at high frame-rates with high resolution.

The produced spectral camera based on the CIS is used for the surface colour analysis of the marble slabs and piles. For this purpose, the properly washed and dried marble stones moving on a specially designed conveyor will be illuminated by white light which will be partially absorbed and partially reflected from the stone surfaces, depending on their particular characteristics. The partially reflected radiation will be then separated in basic spectral colours using special prism optics for this endeavour, impinging afterwards on the CIS designed for this purpose.

The CIS represents the core of the spectral camera and its characteristics determine the entire systems performance. The sensor is responsible for the spatial resolution (in terms of

TABLE I – Main technical specifications of the sensor:

Process:	2P4M 0.35 μm (Opto) CMOS + UV-transparent passivation
Format:	1280 x 960 active pixels
Shutter mode:	Global
Power supply voltage:	3.3 V
Pixel pitch:	12 μm x 12 μm
Optical fill factor:	50 %
Full well capacity:	190,000 e^-
Readout (random) noise:	94 e^-
Dark current:	2650 e^-/s
Dynamic Range:	66 dB
Quantum Efficiency:	@ 250 nm: 18 % @ 400 nm: 60 % @ 700 nm: 70 % @ 1000 nm: 10 %
Frame rate Full frame:	40 – 200 fps with 2, 4 or 8 channels
Output analogue channels:	8
Row-readout-cycle-time:	5 μs
ROI frame (1280 x 180):	1000 fps
Max. line frequency:	192 kHz (active pixels)
Max. pixel rate:	245.76 MHz
ROI Random line access:	yes

number of pixels per image) and also for the data resolution (in terms of information quantization, etc.).

Following the defined specifications expressed in Table I, the CIS was designed and fabricated by Fraunhofer IMS.

Development of the CIS

Although the CIS was designed to specifically meet the spectrographic specifications required for the task described, it can be also successfully applied in high speed (up to 200 fps) HDTV cameras.

The high speed and large full-well capacity HDTV image sensor for spectrographic applications was designed and fabricated in the 2P4M automotive 0.35 μm CMOS process available at the Fraunhofer IMS, using its enhanced version for optoelectronic applications (Opto-process).

Silicon sensors usually lack sensitivity in the UV range under 400 nm because of the nitride passivation layer on top of the photoactive area which absorbs the major part of the UV radiation. In case of spectrographic measurements, where the energy distribution of the radiation over the spectrum is desired, this blind spot in the UV causes great information losses. In special cases, where the UV-range contains most of the spectral information, common silicon sensors cannot be used. The opto-process at the Fraunhofer IMS is featuring a new UV-sensitivity enhanced passivation layer. This special passivation layer is responsible for quantum efficiencies of at least 12 % even at a wavelength of 250 nm, allowing the sensor to be used in cases where especially a UV-sensitivity is needed.

As specified by the PROVIPS partners, the pixel pitch of the PROVIPS sensor is 12 μm , and is based on an n^+ photo-diode (n^+ PD).

The 1280 \times 960 pixels high speed and large full-well capacity HDTV image sensor comprises additional series of barrier pixels, followed by illuminated dummy pixels, dark pixels, and finally test pixels. The final pixel matrix consists thus of 996 rows and 1312 columns altogether. Each pixel is read out in a double sampling modus using for this purpose correlated double sampling (CDS) stages arranged in parallel, one per column, at the bottom and top of the pixel matrix. The CDS output signals are then transmitted to the alternating sample and hold (S&H) stage, after which they will be transferred through a multiplexer to the output channels. The two-stage multiplexer contains a pre-charge stage and a final, output stage. This architecture, properly controlled, makes a faster readout of the signals possible, which was necessary to meet

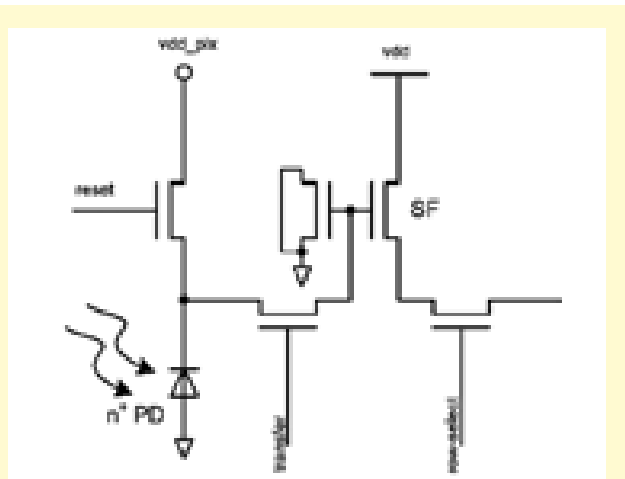


Figure 1: Schematic presentation of the 12 μm (square) pixel.



Figure 2: Micro-photograph of the 19.8 mm \times 18.7 mm fabricated high frame-rate HDTV sensor.

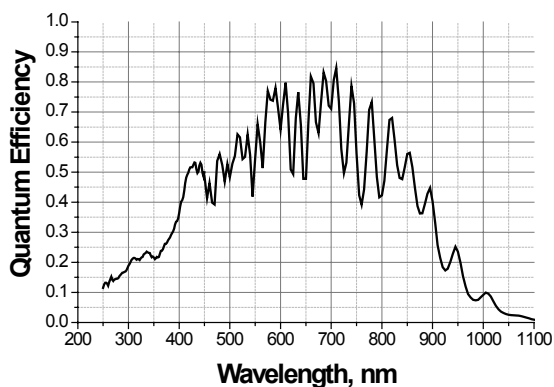


Figure 3: Wavelength dependent quantum efficiency curve of the n^+ PD used in the $12\ \mu\text{m}$ (square) pixels of the fabricated high frame-rate HDTV CIS.

Conclusion

Within the project, we built a high full-well-capacity, HDTV CMOS-sensor with a global shutter, and flexible region-of-interest selection, which can acquire full-frame images at a high frame-rate of 200 fps. This makes the sensor predestined for spectroscopy, machine vision or similar high-performance applications, where high readout speeds in connection with a high spatial or high spectral resolution are required.

Furthermore, the special UV-passivation layer makes the sensor able to acquire and offer more information and energy out of the available radiation. This great UV-sensitivity makes the image sensor open up new perspectives, especially in spectrographic or similar applications.

the requirement of 200 frames per second readout speed. Furthermore, the multiplexer also determines the destination channel of a pixel value, depending on the channel readout-mode.

Finally, the values are being read out using 2, 4 or 8 output channels provided with one output buffer per channel, depending on the frame rate operation modus elected. The image sensor outputs are fully differential and were designed to meet the requirements of the 14-bit analogue-to-digital converter (ADC) existent in the camera module.

INTERFACE FOR OLEDs ON CMOS CIRCUITS

S. Weyers

Introduction

Organic **L**ight **E**mitting **D**iodes have shown their versatility in applications from mobile phone displays to advertising signs to room and road lighting. This technology is used for brilliant high resolution displays as well as large area light sources. Exciting new application fields are made possible by the fact that OLEDs can also be used to compensate one drawback of silicon based technologies. Due to the silicon bandstructure it is not possible to realize efficient light sources in CMOS circuits. By combining OLEDs and CMOS circuits this drawback can be compensated to realize completely integrated opto-electronic applications based on silicon technologies. In cooperation with the Fraunhofer IPMS in Dresden an interface between CMOS and OLEDs was developed. This interface allows the deposition of OLEDs directly on top of CMOS circuits and it also provides electrical connectivity to drive the OLEDs.

Applications

With the combination of OLEDs on CMOS integrated microdisplays can be built that contain all necessary logic and driver electronic located in the CMOS part underneath the OLEDs. This monolithic approach reduces the weight, size and cost of systems making it especially suitable for mobile projection, near-to-eye applications like electronic camera viewfinders or head-mounted displays.

By including photodiodes in the circuit it is even possible to combine light emission and detection in one chip. This combination opens up a broad range of new applications:

- Single chip reflection light barriers
- Optical sensors that require embedded illumination:
Slope sensors, wave front sensors
- Lab-on-chip modules with embedded microfluidics, excitation and sensors
- Optical fingerprint sensors
- Microdisplays with eye tracking ability for head-mounted-displays
- Chip-to-Chip communications

OLED on CMOS Interface

The CMOS circuit is fabricated in a standard 0.35 μm technology at the IMS. Up to and including the top metal layer no modifications to the standard process flow are required. Starting with the passivation layers the process is adapted to the requirements of the CMOS to OLED interface. In a standard process the main purpose of the passivation layers is the mechanical and chemical protection of the chips. For the interface between CMOS and OLEDs the passivation also has to provide a structural as well as an electrical interface. The structural interface for the deposition of the OLED layer on top of the CMOS circuit requires a smooth and planar surface. Any steep edge can cause a discontinuity of the OLED film after deposition which results in defective display pixels. To achieve the required surface quality the passivation stack has to be planarized to compensate the topography of the top metal layer. While this fulfills the requirements for global planarity the surface roughness of its top layer was found to be too high for a high quality of the OLED layer. Therefore, an additional dielectric layer is deposited on top of the passivation and polished by chemical-mechanical planarization. In this way a surface roughness well below 1 nm (RMS) is achieved. For the electrical connection of the OLEDs to the CMOS circuitry Tungsten filled vertical interconnects are processed through the passivation to the top metal layer of the standard

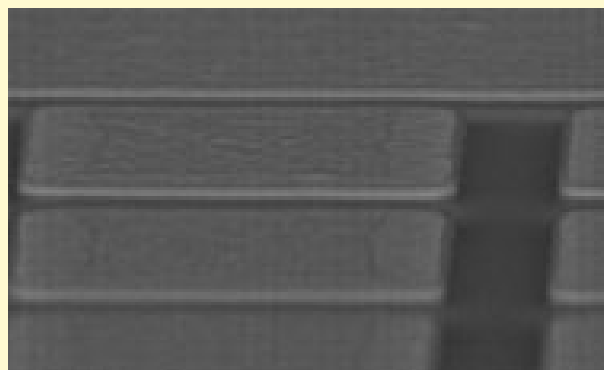
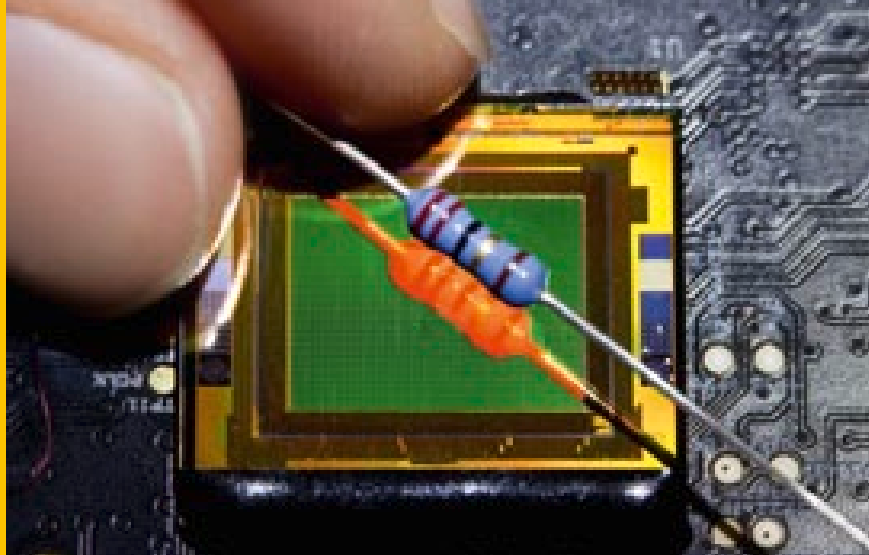


Figure 1: Metal electrodes of the OLED on CMOS interface

CMOS CIRCUITS INTERFACE FOR OLEDs ON CMOS CIRCUITS

Figure 3: Bidirectional OLED microdisplay in feedback mode
[Source: Fraunhofer IPMS]



process. Subsequently a thin metal layer is deposited on top and structured to act as the bottom electrode for each pixel of the OLED display [Figure 1]. For these electrodes it is important to use a thin metal layer to achieve small step heights at their edges to avoid any discontinuity of the OLED layer, but it also has to be a continuous metal film to achieve a sufficient conductivity. Also, in order to avoid any short circuits through the thin OLED layer to the top electrode the surface roughness of this metal layer has to be below a few nanometers. By optimizing the process parameters for deposition and structuring of this metal film all of these requirements were achieved using standard CMOS equipment. As a result the electrodes contain of a continuous film with a surface roughness of 1 nm (RMS). Besides its electrical function the metal layer also serves as a reflector for the emitted light to increase the luminance of the OLEDs.

After processing the OLED on CMOS interface the bond pads are opened as final step of the CMOS process flow.

Then the wafers are transferred to the Fraunhofer IPMS for OLED processing. The OLED layer is deposited through a shadow mask as one continuous film covering the whole display area. The single display pixels are defined by the shape of the metal electrodes of the interface. Finally, a thin film encapsulation is applied to protect the OLEDs from the environment [Figure 2].

Results

In cooperation with the IPMS, which designed the chip and deposited the OLEDs, a bidirectional OLED microdisplay has been realized using this interface [1]. It has a monochrome

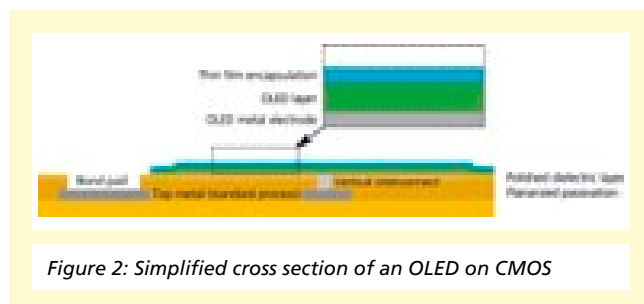


Figure 2: Simplified cross section of an OLED on CMOS

320 × 240 pixels display (QVGA) with a pitch of 36 μm and a 160 × 120 pixels image sensor with a pitch of 72 μm. Since the chip is designed as a prototype for a wide range of applications the peak luminance can be varied from 100 to 24000 Cd/m² with a contrast ratio of 3000:1 at 1000 Cd/m² (characterizations have been done with a green OLED deposited).

Except for the video readout ADC all necessary drive, control, and configuration circuitry were integrated into the chip. For demonstration it can be operated in a feedback mode where the display directly shows the picture acquired by the image sensor [Figure 3].

A head-mounted display has been realized acting as a see-through device. In this application the microdisplay is used to project additional information while the image sensor is used for basic eye tracking.

Conclusions

The developed interface for OLEDs on CMOS has enabled the monolithically integration of light emitting devices in silicon based technology.

We were able to achieve all required physical and electrical properties for the interface to provide a high quality basis for microdisplay. This was verified by the fabricated prototype. This prototype can be used to evaluate and demonstrate the applications that can be addressed by combining a microdisplay and an image sensor in one chip, and will be used as a basis for further designs.

References

- [1] Richter, B., et al. "Bidirectional OLED microdisplay: Combining display and image sensor functionality into a monolithic CMOS chip", IEEE International Solid-State Circuits Conference Digest of Technical Papers, pp. 314–316, 2011

HIGH TEMPERATURE EMBEDDED MICROCONTROLLER FOR HARSH ENVIRONMENTS

H. Kappert

Fraunhofer IMS has a long time history in the field of embedded microcontrollers. Based on in-house developed cores compatible to established industry standard microcontrollers as well as application specific cores, we have realized various customer specific embedded microcontrollers with dedicated peripherals and extensions. From the very first implementation our major design goals have been the availability of a rapid prototyping capability and an advanced test and debug support including fabrication test as well as hardware/software debugging of the final Integrated Circuit (IC).

Today we have realized a complex mixed signal chip including an embedded microcontroller for use in an extended temperature range up to 250 °C based on our high temperature SOI CMOS process. This chip has been defined and realized for the validation of the process design kit (PDK) as well as for evaluation and demonstration of the existing SOI CMOS process.

Technology

One of the various processes available in the Fraunhofer IMS in-house CMOS fabrication line is a high temperature capable silicon on insulator (SOI) CMOS process. This special process provides fully isolated CMOS devices implemented in a thin silicon film without well region. It eliminates the p-n junction between source / drain and bulk, which results in dramatically reduced leakage currents. This process also features a tungsten metallization to eliminate the effect of electro migration. This effect results in a dramatic reduction of reliability of standard aluminum metallization at high temperature. In addition to standard CMOS transistors and passive devices like resistors, capacitors and diodes, the process provides non-volatile memory based on EEPROM. Today a 1.0 µm SOI CMOS process is available; a 0.35 µm process allowing higher integrated circuitry and reduced die size will be available in 2012. Based on our SOI technology we are able to design and fabricate mixed signal ASICs for use in harsh environments with operating temperatures up to 250 °C. A full featured process design kit (PDK) is available for Cadence design tools. It includes all supported devices as well as digital standard cells and IO cells. Memory generators for RAM and

ROM are also available. Automated tools for circuit and layout synthesis are supported as well as extraction and back annotation of parasitic resistors and capacitors for accurate circuit simulation.

System overview

Based on the Fraunhofer IMS 1.0 µm SOI CMOS process, we have implemented an embedded microcontroller IC. It is based on the IMS3311 controller core which is opcode compatible to a Freescale 68HC11 microcontroller.

The embedded microcontroller features standard peripherals like:

- Parallel Input/Output (I/O) Ports
- Timer with capture compare unit
- Synchronous Peripheral Interface (SPI)
- Serial Communication Interface (SCI)

In addition it is equipped with on chip memories like:

- RAM (256x8 Bits)
- ROM (2048x8 Bits)
- EEPROM (128x8 Bits)

Besides these digital components, the IC includes a 10 Bit Analog/Digital Converter (ADC) and an on chip voltage reference.

The overall chip is a complex mixed signal IC featuring all of the devices provided by the SOI CMOS process and requiring all features of the PDK during the design phase. The design

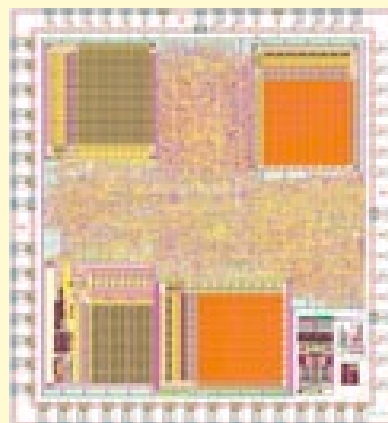


Figure 1: Layout of Embedded Microcontroller IC

CMOS CIRCUITS

HIGH TEMPERATURE EMBEDDED MICROCONTROLLER FOR HARSH ENVIRONMENTS



has been chosen to validate the PDK and for evaluation and demonstration of the process capabilities. A layout plot is shown in figure 1. The design phase has been successfully finished and the device is currently in production.

Evaluation Chips

In preparation of the microcontroller IC several critical design blocks, were realized as evaluation chips. Especially the ADC and the EEPROM have been fabricated for early evaluation. Chip photos of the evaluation chips are shown in figures 2 and 3. Measurements have been successfully finished and show the expected performance and proper operation of the designs for the extended temperature range up to 250 °C.

Test and Debug

As stated above a comprehensive test and debug capability is a major design goal. Therefore this mixed signal design was implemented using a full scan approach. Based on the full scan implementation and a dedicated test controller, hardware and software debugging is enabled within the final IC, supporting single step software execution as well as hardware break points. The realization of the high temperature embedded microcontroller and its design environment also required an upgrade of the existing ScanDebugger, our software tool providing high level access to the scan chains and a graphical user interface for interactive debugging. This led to the reimplementation of the ScanDebugger in Tcl/TK, a powerful programming language and graphical user interface toolkit commonly used by CAD vendors.

Rapid prototyping

During the implementation of the hardware and the final on chip application code a standard FPGA evaluation board has been used for rapid prototyping. This allowed software development and verification of the whole digital system before the final IC was available.

Conclusion

We have implemented an embedded microcontroller for high temperature operation up to 250°C. It is designed based on

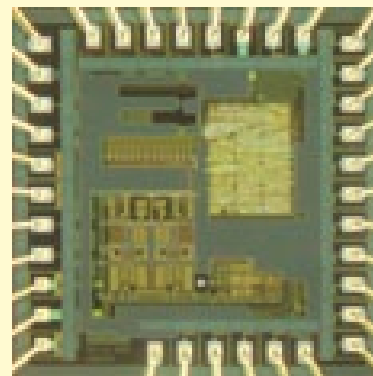


Figure 2: Chip photo of ADC evaluation chip

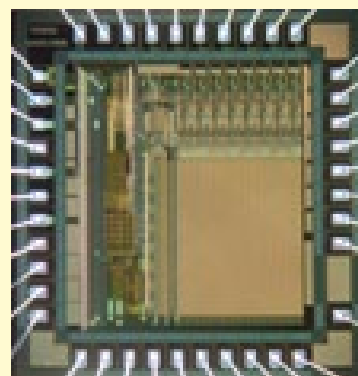


Figure 3: Chip photo of EEPROM evaluation chip

the Fraunhofer IMS 1.0 μm SOI CMOS. The implementation of this complex mixed signal IC was used for a comprehensive validation of the PDK. First evaluation chips have been realized successfully. Currently the described chip is in fabrication and is expected for evaluation at early 2012.

Within the next generation this IC will be extended by additional functions and increased memory size. Realized in the new 0.35 μm SOI CMOS process currently under development the IC will provide more functionality on a drastically reduced silicon area.

The presented chip shows one possible realization of a high temperature mixed signal integrated circuit including an embedded microcontroller. Customer specific ICs can be derived easily from the presented design with customer/application specific analog and digital circuit modules.

MIXED-SIGNAL/ANALOG SIGNAL CONDITIONING CIRCUITRY FOR WIDE TEMPERATURE RANGE APPLICATIONS

A. Schmidt

Data acquisition and signal processing at elevated temperatures are facing various problems due to a wide temperature range operation, affecting the accuracy of the circuits' references and elementary building blocks. As the most commonly used analog building block, the operational amplifier (op-amp) with its various limitations has to be enhanced for wide temperature range operation. The proposed high gain operational amplifier features a folded-cascode and gain-boosted input stage and is fabricated in the Fraunhofer IMS High Temperature 1.0 μm SOI CMOS process. The op-amp was designed for an operating temperature range of -40 to 300 $^{\circ}\text{C}$. Major effort was put into a robust design approach with reduced sensitivity to temperature variations, targeting customer specific high precision applications in a high temperature environment.

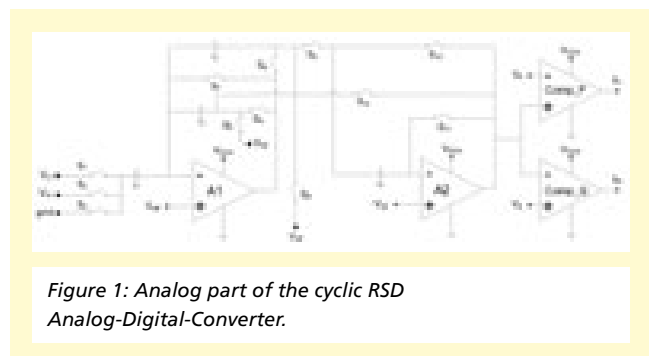
Introduction

SOI CMOS is the most commonly used technology for integrated circuits suitable for high temperatures and harsh environmental conditions. With a wide temperature range reaching from -40°C to 300°C SOI circuits have to meet requirements like high accuracy and fast operating speeds. As the basic analog building block the op-amp and its performance determines the overall performance of e.g. analog-digital-converters, switched capacitor filters, voltage regulators and reference circuits. Therefore one major concern is to optimize the op-amp's performance for a wide temperature range operation. Key parameters are thereby the signal gain and bandwidth over the overall temperature range, which typically have to be maximized.

Basic transistor and passives parameters will remain a function of temperature and process-variation. As future process-technology developments cannot eliminate these sources of error, the compensation of the effects has to be considered in the design. An increasing impact on analog circuit design is expected over the next years, making it even more challenging to design high speed and also precise integrated circuits. Any contribution addressing this major problem will therefore have a lasting impact on circuit design.

Application and Requirements

The proposed high gain operational amplifier is one basic building block for use in analog signal processing and is especially designed for a cyclic RSD analog-digital-converter



with a desired resolution of 13 bit which is shown in figure 1. The input signal range reaches from 0 V (gnda) to 5 V (vdda). The analog-digital-converter has to operate properly in a temperature range of -40°C up to 300°C . It is realized using switched capacitors technique. Therefore the load capacitance of the amplifiers varies between 2 pF and 50 pF.

The moderate sample rate of 1400 samples per second gave us the ability of lowering the power consumption of the amplifier. Due to RSD code usage, the analog-digital-converter is able to correct earlier false decisions and to convert an analog input signal within 12 cycles into a 13 bit digital result.

For the sample and hold functionality as well as for the basic operations like voltage addition, subtraction and multiplication by two, two precise operational amplifiers A1 and A2 are used. In order to keep the amplification error within the range of ± 1 LSB/2, the op-amps require a minimum DC gain of approximately 85 dB over the entire temperature range. To ensure

MIXED-SIGNAL/ANALOG SIGNAL
CONDITIONING CIRCUITRY FOR WIDE
TEMPERATURE RANGE APPLICATIONS

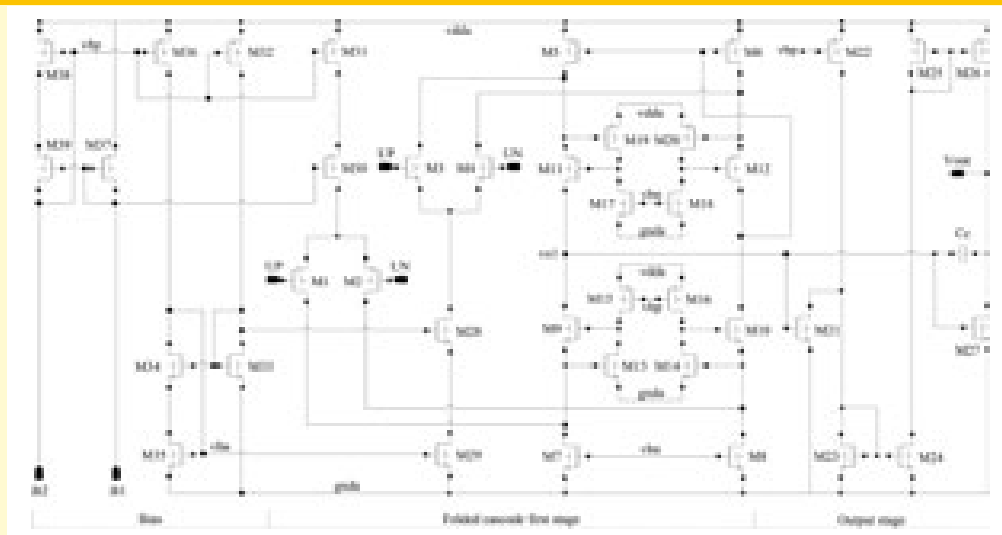


Figure 2: Complete circuit implementation of the proposed amplifier including a folded cascode differential gain stage, the biasing circuit and second gain stage.

a precise operation with even higher resolution, a minimum DC gain of 100 dB is desired. Since the offset of both op-amps is eliminated during the mathematical operations within each conversion cycle, there is no need to cancel the offset of the amplifier itself. For other applications, of course, detailed offset analysis and cancellation techniques are required.

Circuit Description

The circuit has been fabricated in the Fraunhofer IMS High Temperature 1.0 μm SOI CMOS process. In order to meet the requirements of high DC gain even at elevated temperatures as the primary design goal, a folded cascode differential stage amplifier with additional gain enhancement techniques has been realized. Figure 2 shows the circuit implementation of the op-amp [1].

Rail to rail input operation is supported by using PMOS and NMOS differential input stages consisting of the transistors M1, M2 and M3, M4, respectively. Using rail to rail input also achieves higher gain in the input common mode range (ICMR) where both input pairs are active.

The folded cascode structure consists of the transistors M9-M12. The gain boosting technique, firstly introduced in [2], has been utilized here. As shown in [2] this technique is suitable to maximize the gain at lower frequencies while not affecting the

bandwidth of the amplifier [5–7]. Negative feedback is applied through transistors M13 and M14 for the NMOS cascode transistors M9 and M10. Transistors M19 and M20 form a negative feedback path for the PMOS cascodes M11 and M12. By using this technique, the output resistance at node vo1 is drastically enhanced resulting in a significantly larger DC gain within the first stage. The resulting gain on a logarithmic scale is the sum of the gain of the cascode structures and the feedback amplifiers [6].

Several different approaches for high temperature operational amplifiers have been reported [3] [4] [8]. Even though using the gain boosting technique sufficient gain at high temperature operation was not achieved. Therefore a second stage is necessary. It is formed by the transistors M21-M27. Although losing the benefits of a single stage amplifier, e.g. wide bandwidth operation and no need for frequency compensation, the additional second stage shows important improvements for the target application. First of all the additional gain pushes the overall DC gain to 108 dB, even at 300°C. Better rail to rail output operation is achieved due to the push-pull output stage. The current in the output path, formed by M26 and M27, can be dynamically adjusted by M21 supporting the driving capability of the output stage in case of positive displacement of the differential input pairs.

Using a second gain stage requires frequency compensation using a miller capacitor C_c . The size of the capacitor is adjusted properly to find a resulting minimum unity gain frequency of 1 MHz and a minimum phase margin of about 55° , also in case of high capacitive load. The whole op-amp is biased by enhanced wide swing current mirrors formed by transistors M28 – M39.

Simulation and measurement results

Figure 3 shows the simulated input common mode range (ICMR) of the amplifier at -40°C and 300°C . The op-amp was configured as a unity gain buffer. The difference of the output voltage to the input voltage due to amplification error stays below 0.5 mV over the overall input signal range up to 250°C . At 300°C the upper level is limited to 4.87 V with the current design.

Figure 4 shows the simulated Bode plot of the described op-amp for different temperatures. It can be seen that the DC gain at -40°C is approximately 125 dB with a unity gain frequency of 3 MHz. At a temperature of 300°C the amplifier has a DC gain of approximately 108 dB and a unity gain frequency of 1.02 MHz. The phase margin varies between 55° ... 70° degrees.

With the present chips, the simulation results have been proven by measurements of the stand-alone amplifier as well as within the application. Table I summarizes all important specifications of the operational amplifier. Figure 5 shows a chip photo of the op-amp.

Conclusion

An operational amplifier targeting high temperature range applications up to 300°C has been successfully realized in a $1.0\ \mu\text{m}$ SOI CMOS process. As a primary design goal high gain and significantly high bandwidth at extended temperatures have been reached. The op-amp is well suited for use in precision high temperature application i.e. analog-digital-converters or signal processing.

Further activities in the field of precision mixed-signal circuitry are the implementation of on-chip voltage- and current

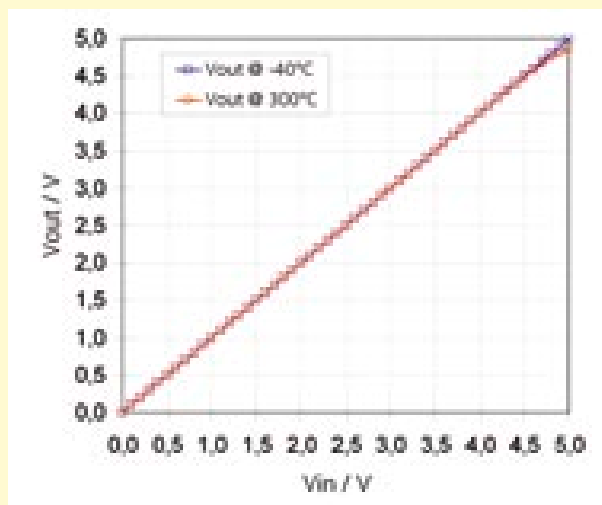


Figure 3: Simulated input common mode range (ICMR) of the op-amp.

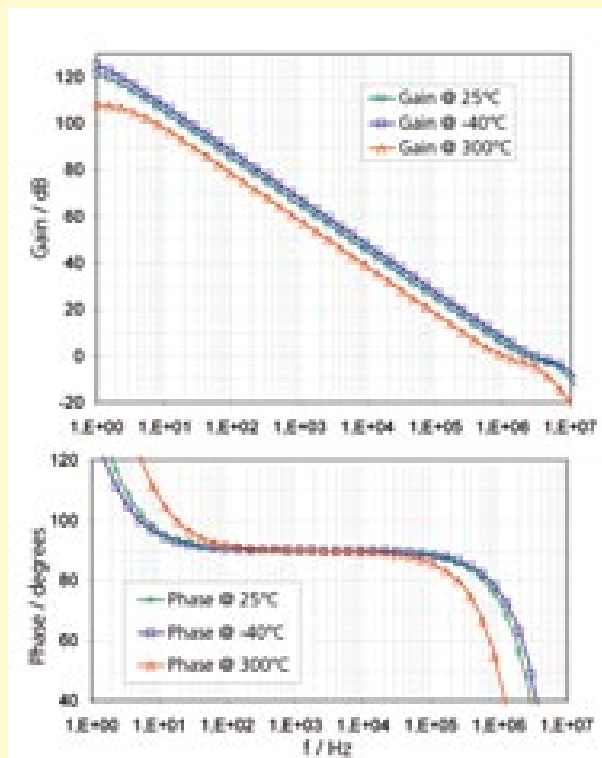


Figure 4: Simulated gain and phase of the proposed op-amp.

MIXED-SIGNAL/ANALOG SIGNAL
CONDITIONING CIRCUITRY FOR WIDE
TEMPERATURE RANGE APPLICATIONS

Table 1: Op-amp specifications summary.

Parameter	Value Min / Max
Temperature range	-40°C/300°C
Voltage supply	5 V
Supply current	143 µA/210 µA
Power consumption	0.71 mW/1.05 mW
Input common mode range (ICMR)	0 V/4.9995 V @ 25°C 0 V/4.87 V @ 300°C
Open loop DC gain	125 dB @ -40°C 120 dB @ 25°C 108 dB @ 300°C
Phase margin	55°/70°
Slew rate	0.7 V/µs / 0.8 V/µs
Power supply rejection ration (PSRR+)	75 dB/90 dB @ 1 kHz 53 dB @ 100 kHz

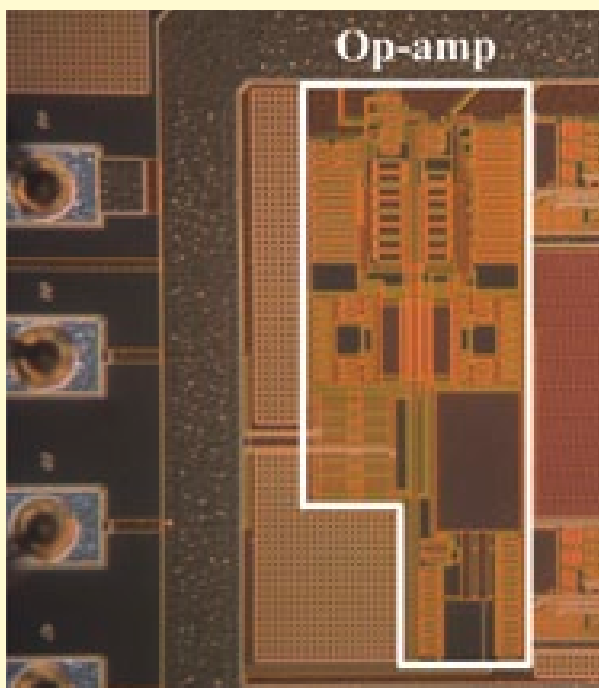


Figure 5: Chip photo of the op-amp.

references as well as leakage compensated switches for use in switched capacitor circuits.

These basic analog building blocks enable precise data acquisition and signal processing circuitry for a wide temperature range from -40°C to 300°C and can be integrated within customer specific integrated circuits.

References

[1] Schmidt, A.; Marzouk, A. M.; Kappert, H.; Kokozinski, R.; "A Robust SOI Gain-Boosted Operational Amplifier Targeting High Temperature Precision Applications up to 300°C", International Conference on High Temperature Electronics (HiTEN), Oxford, July 2011.

[2] Hosticka, B.J.; "Improvement of the gain of MOS amplifiers", IEEE Journal of Solid-State Circuits Issue 6 page 1111, Dec. 1979.

[3] Eggermont, J.P.; Gentinne, B.; Flandre, D.; Jepsers, P.; Colinge, J.P.; "SOI CMOS Operational Amplifiers for Applications Up To 300°C", Proceedings 2nd International High Temperature Electronics Conference (HiTEC), Volume II, pp. 21–26. 1994.

[4] Finvers, I.; Haslett, J.; "A High Temperature Precision Amplifier", IEEE Journal of Solid State Circuits, Vol 30, No. 2, Feb. 1995.

[5] Amourah, M.M.; Geiger, R.L.; „Gain and bandwidth boosting techniques for high-speed operational amplifiers”, ISCAS 2001. The 2001 IEEE International Symposium on Circuits and Systems Issue 1, page 232, May 2001.

[6] Musa, R.; et al.; "Design of Single-Stage Folded-Cascode Gain Boost Amplifier for 100mW 10-bit 50MS/s Pipelined Analog-to-Digital Converter", ICSE '06. IEEE International Conference on Semiconductor Electronics, Dec. 2006.

[7] Gentinne, B.; Colinge, J.P.; Jaspers, P.G.A.; Eggermont, J.P.; "Improvement of the performances of SOI CMOS operational amplifiers by means of a gain-boosting stage", IEEE International SOI Conference Proceedings, Oct. 1993.

[8] Ohme, B.; Larson, M.R.; Erickson, S. R.; "High Temperature Precision Amplifier", International Conference on High Temperature Electronics (HiTEN), Sept. 2005.

DIGITAL RADIO RECEIVER FOR AN UHF RFID SYSTEM WITH AN UNDERSAMPLING DIGITALIZATION SCHEME

S. Grey, G. vom Bögel

Abstract

This paper describes a digital radio receiver for UHF-RFID systems based on an undersampling scheme for the signal digitalization. The original UHF signal is transferred into a digital intermediate frequency by means of undersampling, the signal is decimated with a CIC filter and demodulated using a digital coherent demodulator, delivering the base band signal after low-pass filtering. The details of the system are presented as well as some measurements.

I. INTRODUCTION

A. UHF in RFID

The use of Ultra High Frequencies (UHF) for RFID Systems has grown considerably in the last years. The implementation of the radio identification in the logistic and commerce fields, as well as the standardization by the EPCglobal [1], have open the doors for a wide range of practical applications of the RFID technology. The channel characteristics, the frequency tolerances in the Tags, and the possibility of multifunctionality for other frequencies/standards, increase the challenges for the RFID-Readers. The idea of a reconfigurable and adaptable RFID-Reader emerges with the intention of creating an "universal" reader. These challenges have been explored by [2] and presented a solution in [3]. Many of the presented solutions are based in the idea of making the signal processing in the digital domain, directing the approach to the Software Defined Radio.

B. Software Defined Radio

The concept of Software Defined Radio, for now on referred as SDR, describes a system where the processing of the RF signal takes place in the digital domain. Ideally an ADC (Analog Digital Converter) is connected directly after the antenna. The digital signal processing and protocol implementation are defined in software, enabling the possibility for configuration and optimization without the need of changing any hardware components. The SDR approach is already present in many of the actual communications systems, and is becoming strong as a solution for future telecommunication implementations [4].

An SDR solution brings some advantages to a system, it makes it reconfigurable and reprogrammable; An SDR-based

system can be updated to new standards by just changing the software. However, a fully SDR system requires a high performance level on the Analog digital converter and the signal processor. A possible sampling scheme for SDR-based UHF-RFID systems was presented in [6], this scheme is used as base for the digital radio receiver described in this paper.

C. Standard UHF-RFID Readers

The standard UHF-RFID readers use a direct down conversion architecture; basically the RF signal is filtered, amplified and then coherently demodulated using the same local oscillator used for the field generation [5]. The signal is then low-pass filtered to eliminate the 2nd harmonic of the carrier produced after the demodulator. As digitalization scheme a sigma delta ADC is used to digitalize the baseband signal and then passed to the baseband processor. The figure 1 shows the general architecture of the UHF-RFID readers.

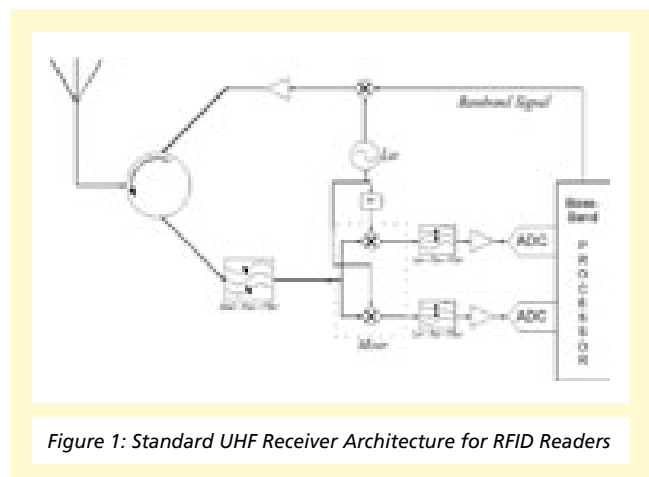


Figure 1: Standard UHF Receiver Architecture for RFID Readers

WIRELESS CHIPS AND SYSTEMS
**DIGITAL RADIO RECEIVER FOR
 AN UHF RFID SYSTEM WITH AN
 UNDERSAMPLING DIGITALIZATION
 SCHEME**

This structure is a well known receiver architecture and presents some problems we will discuss shortly:

- Self mixing: The local oscillator signal couples into the input of the mixer creating a time variable DC offset that increases the noise level of the signal [5]
- 1/f noise: The noise increasing due to the self mixing factor is indirectly proportional to the frequency.
- Inter-modulation products: The nonlinearities of the mixer generate other signals that can appear as in-band distortions after the mixer.

D. Undersampling in UHF-RFID Systems

The use of undersampling or bandpass sampling for direct digitalization of high frequency signals has been explored widely in [6], [7], [8], [9], [10], [11] and others, the problems arise when considering the SNR deterioration due to noise overlapping. The possibilities of implementing the undersampling scheme in UHF-RFID Systems have been explored in recent work [6]. In this paper practical results are shown of the in [6] presented concept, the undersampled signal is used as input signal of a digital coherent demodulator which delivers the base band signal after low-pass filtering.

1) Advantages of Undersampling: The advantages and characteristics of the undersampling have been well studied and explored in [12] [13] [14]. The most important is that the

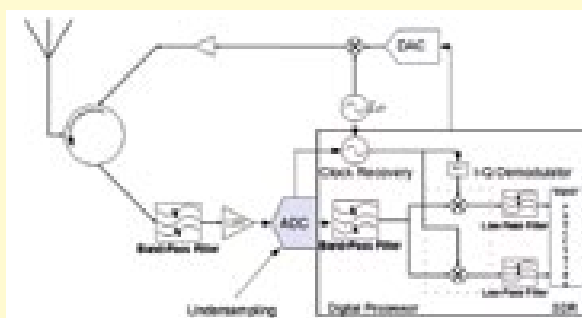


Figure 2: Receiver Architecture using Undersampling for Frequency Translation

signal digitalization and frequency translation take place in a single process. By using an undersampling scheme the system could be reduced by eliminating the mixer, thus allowing to realize the signal processing in the digital domain in an earlier stage. See figure 2.

II. SYSTEM OVERVIEW

The signal after the carrier-suppressing circuit is amplified by a low-noise-amplifier (LNA), bandpass filtered to limit the bandwidth of the signal and digitalized by a high-speed analog-digital-converter (ADC). The -3 dB bandwidth of the bandpass filter is used to calculate the sampling frequency of the ADC, see [15] for more details. A schematic diagram of the system is presented in figure 3.

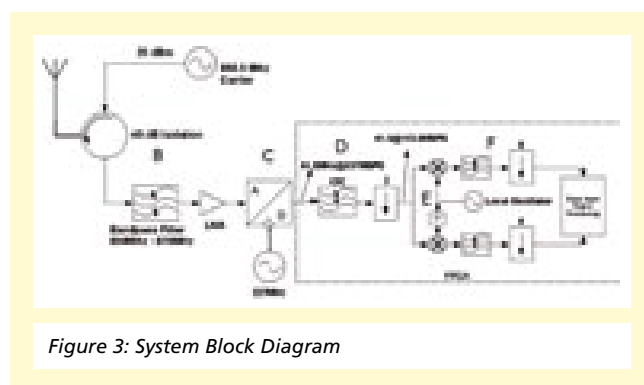


Figure 3: System Block Diagram

A. Test Transponder

A test-transponder was used to create the backscatter signal. The test-transponder sends a test signal to the reader using the backscatter modulation techniques. This test-transponder consists of a dipole antenna and microcontroller that creates a FMO encoded signal, this one is used to switch the antenna impedance to create the backscatter signal.

B. Analog Front-End

The carrier frequency is selected to be 866.5MHz and is generated by a signal generator, the carrier is supplied to a carrier-suppressing circuit which isolates the carrier from the

received signal with approx. 40 dB [16], facilitating the digitalization of the signal. Due to the limited dynamic range of the ADC a high isolation factor is necessary in order to be able to digitalize signals of small power, in other words to increment the reading range.

The carrier suppression circuit separates the TX signal from the RX signal. The TX is sent to the transponder using a patch antenna and the RX signal is supplied to the ADC after a bandpass filter and an LNA.

C. Sampling

The sampling is performed by high speed 12 bits ADC, the sampling frequency is chosen according to the bandpass sampling theorem, which basically states that a band-limited signal can be sampled and reconstructed if it is sampled at least twice its bandwidth. This theorem has been well documented in [13] [15] [14], showing that there are frequency spans where the signal can be sampled without destructive aliasing, these conditions can be described by equations 1 and 2. The reader is directed to [15] for further details on bandpass sampling.

$$\frac{2 \cdot f_{max}}{n+1} \leq f_s \leq \frac{2 \cdot f_{min}}{n} \quad (\text{equation 1})$$

Where

$$n \leq \text{round}\left(\frac{f_{min}}{f_{max} - f_{min}}\right) \quad (\text{equation 2})$$

n is the number of replicas between 0 and the lower frequency limit of the baseband signal. The signal frequencies after the undersampling can be determined by:

$$f'_x = \begin{cases} f_x - \frac{n}{2} \cdot f_s, & \text{for } n \text{ par} \\ -(f_x - \frac{n+1}{2} \cdot f_s), & \text{for } n \text{ odd} \end{cases} \quad (\text{equation 3})$$

Where f_x is the original frequency of a determined signal, f_s is the sampling frequency, the value of n corresponds to the one used to calculate f_s and f_o is the frequency of the signal after the undersampling.

In order to reduce the SNR deterioration due to noise overlapping, the sampling frequency is calculated with a small value of n , refer to 1 for details. Measurements have shown that frequencies over 200 MHz give good results (approx. one fourth the carrier frequency), sampling signals over 300 MHz (approx. one third the carrier frequency) have given even better results. For purposes of implementation a sampling frequency of 227 MHz is chosen. Sampling the 866.5 MHz signal at this rate creates a digital intermediate frequency, further referred as IF, of approx. 41.5 MHz. Figure 4 shows the signal's spectrum after undersampling.

D. Decimation

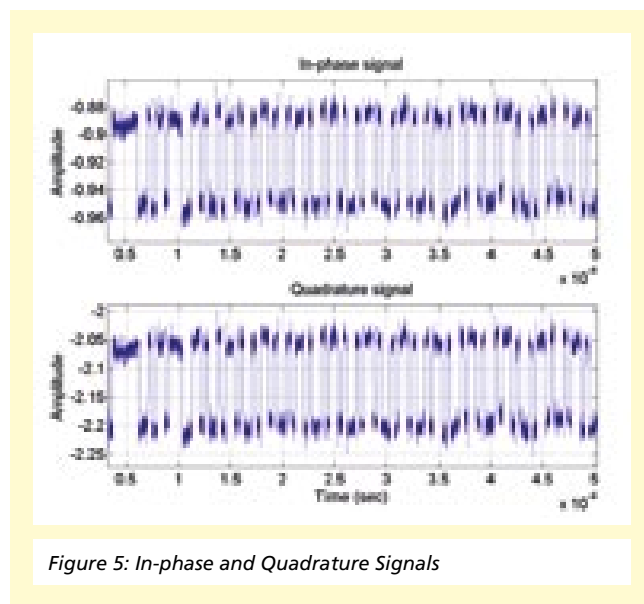
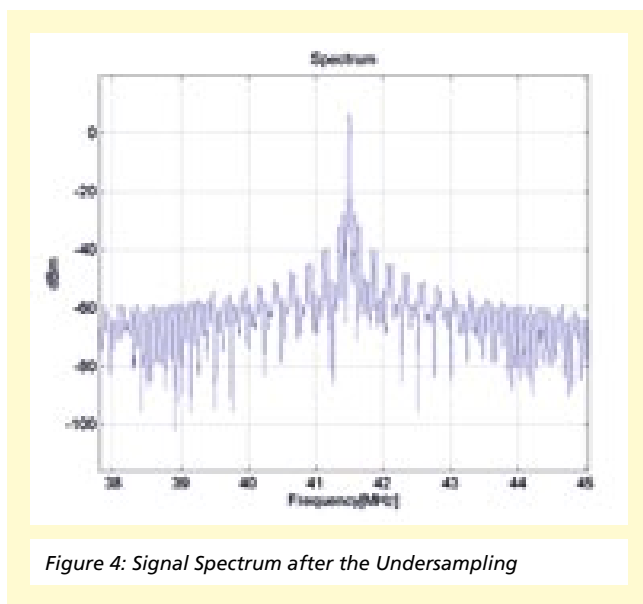
The decimation block is a 3rd order CIC filter that decimates the signal by 2 resulting in a sampling frequency of 113.5 MHz which complies with the Nyquist sampling criteria. Please refer to [17] for more information on the CIC filter.

E. Demodulation

For the digital local oscillator a Digital Direct Synthesizer, further referred as DDS, is used. This one delivers a sine and cosine signals which frequency can be controller in a numeric way. These two signals together with two multipliers are used to construct an IQ demodulator, see Figure 3. The frequency of the DDS is fixed to the IF frequency in order to shift the IF signal to base band, where the carrier is converted to DC.

F. Filter and Decimation

The low pass filter is configured as an FIR decimation filter which filters and decimates the signal by 8, reducing the sampling frequency of the signal to approx. 14,18 MHz, resulting in a 7.09 MHz bandwidth. The low-pass filter eliminates the 2nd harmonic of the IF carrier produced as a result of the multiplication with the local oscillator. The filter delivers the recovered baseband signal for further signal processing.



III. MEASUREMENTS AND ANALYSIS

The measurements and tests were made using a signal generator for the carrier, a carrier suppressing block and patch antenna, see section II. The distance between the test transponder and the antenna is 1m. The received signal is filtered, amplified and supplied to the ADC. The last samples the analog signal and delivers the digitalized one to an FPGA for the signal processing. The signal processing blocks described in section II are implemented in the FPGA, the resulting signals after the processing blocks are transferred to a PC using a serial interface. The results are analyzed using Matlab [18].

A. Signal after ADC

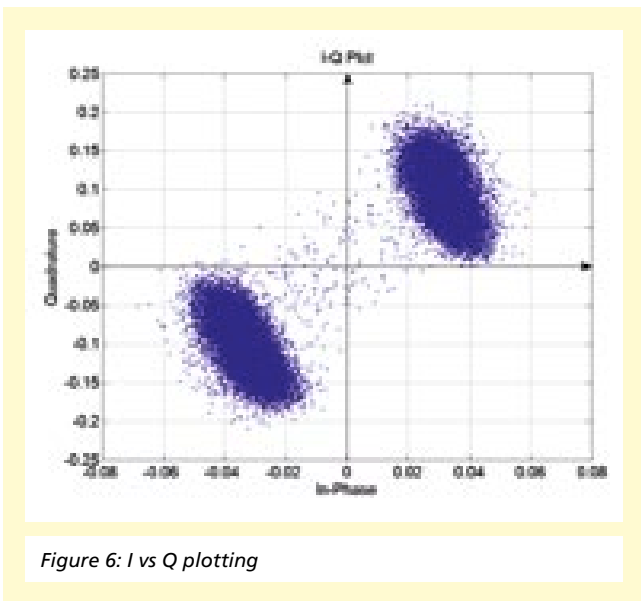
Figure 4 shows the signal after sampling, the plot shows the shifted frequency spectrum after the undersampling. The RF signal is sampled directly after the bandpass-filter and the LNA, the sampling frequency is 227 MHz and shifts the signal in frequency to an IF of 41.5 MHz.

The spectrum is calculated using the FFT algorithm, it shows the carrier as the main signal centered at 41.5 MHz, the information signal is seen as side lobes around the carrier.

B. Signal after Demodulator and Low-pass Filter (Base band signal)

The signal is demodulated and low-pass filtered, figure 5 shows the two resulting signals after the IQ demodulator: On the top plot is the In-phase signal and on the bottom the Quadrature signal. It can be seen that the information is contained in both of the signals, due to a phase difference between the carrier and the local oscillator.

The time signal shows a typical EPCglobal [1] communication frame, with the start of frame at the beginning and some information following it. The measurement was realized at a short distance which explains the high Signal to Noise Ratio (SNR), these circumstances help on the visualization and recognizing of the signals' form. C. I-Q Complex Plane The transmitted symbols can be better recognized by plotting the signal in the complex plane, i.e. I vs Q plot. Figure 6 shows the resulting complex plot of the two signals, two main value zones can be well recognized. Each zone represents one of the two symbols sent, with an approx. 45 degrees phase offset from the ideal 0 degrees of an ideal coherent demodulator. In order to plot the signal around the origin, the DC offset



produced by the remaining carrier and the demodulation is removed by a high-pass filter.

The figure 6 shows that the information is not lost and can be extracted from the signal.

IV. CONCLUSIONS AND OUTLINE

This paper presents a practical digital receiver using undersampling techniques for the digitalization, it shows how it is possible to use this sampling technique to sample the UHF signal directly, shift the signal in frequency and substitute the analog mixer. The signal is digitally demodulated to obtain the baseband signal proving its feasibility. It remains the implementation of the baseband processing as future scope of the system; The goal is to develop an SDR based UHF RFID reader and prove its advantages vs. traditional readers. The overall system performance will be tested once all the reader functionalities have been implemented, thereafter a comparison with the traditional systems could take place.

REFERENCES

- [1] EPCGlobal: EPC Radio-Frequency Identity Protocols Class-1 Generation-2 UHF RFID;
- [2] C. Angerer, B. Knerr, M. Holzer, A. Adalan, and M. Rupp: Flexible Simulation and Prototyping for RFID Designs; proceedings of the first international EURASIP Workshop on RFID Technology, Sept. 2007
- [3] C. Angerer: A Digital Receiver Architecture for RFID Readers; International Symposium on Industrial Embedded Systems, 2008. SIES 2008.
- [4] W. Tuttlebee: software Defined Radio: Origins, Drivers and International Perspectives; John Wiley Sons, LTD, 2002
- [5] Daniel M. Dobkin: The RF in RFID: Passive UHF RFID in Practice
- [6] S. Grey, G. von Bögel, A. Hennig, F. Meyer: Direct Digitalization and Frequency Translation using an Under-sampling Scheme for Software-Defined-Radio based RFID UHF-Systems; RFID SysTech, European Workshop on Smart Objects: Systems, Technologies and Applications
- [7] Paul McCormack: Effects and Benefits of Undersampling in High-Speed ADC Applications; White paper: National Semiconductor Corporation
- [8] Dennis M. Akos: A Software Radio Approach to Global Navigation Satellite System Receiver Design; Ohio University, August, 1997
- [9] Xiangyang Wang, Shuyang Yu: A Feasible RF Bandpass Sampling Architecture of Single-Channel Software-Defined-Radio Receiver; International Conference on Communications and Mobile Computing

**DIGITAL RADIO RECEIVER FOR
AN UHF RFID SYSTEM WITH AN
UNDERSAMPLING DIGITALIZATION
SCHEME**

- [10] Andr Bourdoux, Jan Cranickx, Antoine Dejonghe, Liesbet Van der Perre: Receiver Architecture for Software-Defined-Radio in Mobile Terminals: the Path to Cognitive Radios; Radio and Wireless Symposium, 2007 IEEE
- [11] Yoshio Kunisawa: Study on a Multiple Signal Receiver using Undersampling Scheme;
- [12] Hill, G: The Benefits of Undersampling; Electronic Design, July 11, 1994.
- [13] Richard G. Lyons: Understanding Digital Signal Processing, Second Edition; Prentice Hall PTR, March 2004.
- [14] Karl-Dirk Kammeyer, Kristian Kroschel: Digitale Signalverarbeitung; B.G. Teubner Verlag Wiesbaden 2006.
- [15] Vaughan, R., Scott, N. and White, D: The Theory of Bandpass Sampling; IEEE Trans. on Signal Processing, Vol. 39, No. 9, September 1991, pp. 1973–1984.
- [16] Jae Ho Jung Joon Hyung Kim Sung Min Kim Kwang Chun Lee New circulator structure with high isolation for time division duplexing radio systems; Vehicular Technology Conference, 2005. VTC-2005-Fall. 2005 IEEE 62nd
- [17] Eugene B. Hogenauer: An Economical Class of Digital Filters For Decimation and Interpolation; IEEE Transactions on Acoustics, Speech and Signal Processing, Vol. ASSP-29, No. 2, April 1981
- [18] www.mathworks.com

RADIO FREQUENCY POWERING OF MICROELECTRONIC SENSOR MODULES

G. vom Bögel, F. Meyer, M. Kemmerling,

Abstract

In RFID applications the use of the electromagnetic field for the power supply of transponders is state-of-the-art. In the context of this presentation the use of the electromagnetic field for the supply of sensor modules will be discussed. Based on the question, if the omnipresent radiation from the power supply network and from radio transmitters and mobile phone base stations is useable (Energy Harvesting), the feasibility for the operation of self-sufficient sensor modules is explained. Additional conditions of typical applications (operating range, measured variable) and technology (antennas, frequencies) are considered.

1 Introduction and objective

The RFID technology shows that for the purpose of identifying objects, RFID transponders can be read from more than five metres away. The RFID transponder consists of only the microchip and an antenna. The microchip draws the energy to transfer data, such as serial number or expiration date, solely from its antenna and the thus received radio interrogation field of the RFID reader. Today, the microchip requires less than one microwatt of electric power for this quite simple function. In many areas efforts are being made to transfer the potential of this technology to other applications by equipping the microchip not only with data storage, but also with sensors and / or actuators. This allows acquisition of physical values, like temperature, pressure and humidity, at locations that are difficult to access. Application examples can be found in many areas:

- a) Early detection of moisture damage in e.g. public buildings to prevent accidents, as for instance the collapse of the skating arena in Bad Reichenhall in 2006;
- b) Measurement of forces in wind turbine gearboxes for performance-optimised rotor settings.
- c) Wireless acquisition of glass breakage, window and door position, and much more.

Unlike simple RFID transponders, sensor transponders have a significantly increased energy requirement which is higher by a factor of ten to hundred. Thus, the achievable read distance drops to just a few decimetres. Today, this can already be used for applications such as blood pressure measurement in the human body. However, the majority of read distance applications is considerable greater than one meter.

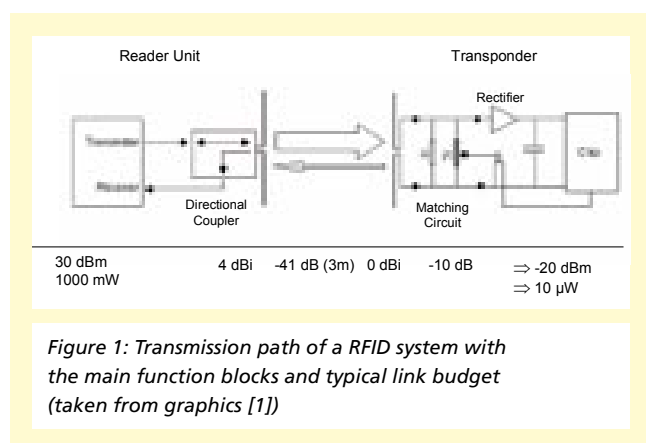
The challenge now lies in the development and optimisation of suitable components and processes. Technologies in the

field of energy harvesting are obvious. Here we will look at the use of radio signals for the supply of sensor transponders.

2 Power consumption in microelectronic systems

2.1 Power in RFID transmission paths

The first things shown on a typical RFID transmission path are the levels of electric power at the main components in the system and the utilisation options for sensor modules. Figure 1 shows the components that determine the energy transfer within a transmission system on the example of RFID and indicates typical performance levels occurring at, or being consumed by the components (link budget). According to European standard, the radiation from a half-wave dipole is not to exceed two watts for the operation of UHF RFID systems. This is usually only utilised by stationary readers which, for instance, are used for gateways. The maximum radiated power in mobile reader units is usually below 500 mW. The



WIRELESS CHIPS AND SYSTEMS

RADIO FREQUENCY POWERING OF MICROELECTRONIC SENSOR MODULES

calculation example in figure 1 assumes an amplification of 1000 mW for a stationary reader. Losses in the directional coupler and use of a directional antenna with 4 dBi gain results in a radiated power of about 1250 mW.

The main components in the receiving system are the antenna and the rectification. The design of these assemblies determines how much of the available alternating electromagnetic field in "direct current power" can be used for the operation of a circuit. Typical performance values are in the range of just a few microwatts. Due to parasitic effects of the components, the rectification alone consumes 50 to 90 % of the power. Figure 2 uses the parameters from the calculation example in figure 1 to show the performance range in dependence on the distance between reader and transponder.

To utilise the small AC voltage applied to the antenna, rectifiers with voltage multipliers are used, e.g. the voltage multiplier according to "Villard". In implementations on transponder ICs, three to six stages are connected in series. New transponder ICs achieve sensitivities of -18 dBm (corresponds

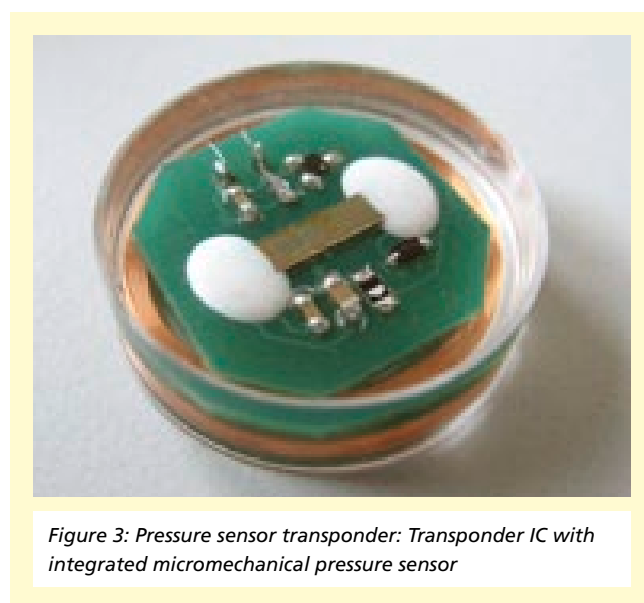
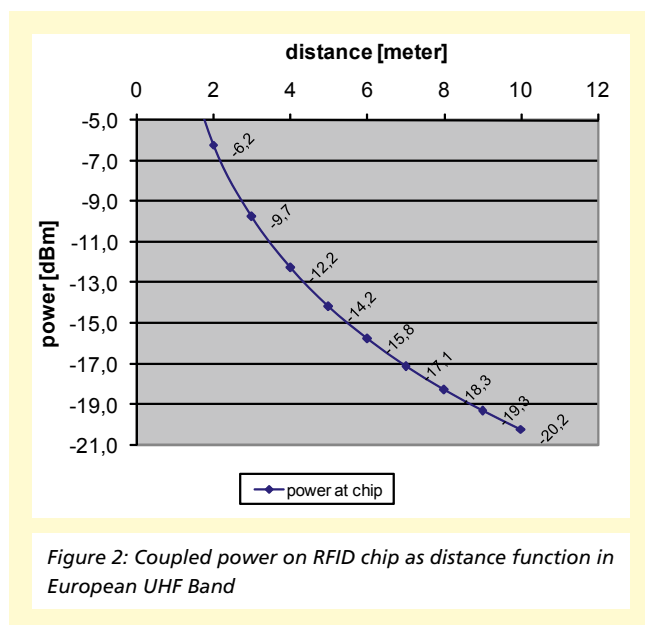
to an input power of 16 μ W [2], i.e. more than eight meters read distance can be reached with simple dipole antennas as considered in the calculation example.

2.2 Energy consumption and power input in sensor modules

The energy consumption and power input of sensor modules depend largely on the application and the sensor used. The spectrum starts with simple switch contacts for the acquisition of binary states. Not taking into account energy conversion losses (see chap. 2.1 RFID), the power input of a detection circuit is a few microwatts.

Even modules used for temperature measurement require only about 20 μ W with suitable low-power design. Assuming that the temperature is a slowly changing variable, a very low pulse-pause ratio can be selected. The energy input at a sampling rate of, for instance, one minute, an operating voltage of 2 V and a measurement duration of 10 ms is about 0.2 μ Ws per minute.

More complex sensor modules are equipped with pressure or humidity sensors, for example. They offer capacitive evaluation, thus allowing energy-efficient circuit technology. Here,



typical values for power input are 200 μW (equals -7 dBm) [3]. Especially the pressure can quickly change, depending on application. This results in a significantly higher sampling; in extreme cases the pause will be set to zero. Figure 3 shows the assembly of a sensor transponder with integrated pressure sensor that acquires approx. 40 pressure measurements per second and transmits them wirelessly. In this case, the energy input is 18 mWs per minute, thus significantly higher than on the temperature sensor. A battery with a capacity of 1000 mAh would have a life of about one year, without consideration of voltage conversion losses and expenditures for data transfer.

Consideration must also be given to the transfer of measurement data to a processing site. Here we look only at wireless transfer processes.

The most energy-efficient method is the principle applied to RFID, where the sensor module does not actively send but rather carries out an impedance change [1]. In this case no additional energy consumption must be considered for the total energy balance. The relatively short range of several meters (see chap. 2.1) is a drawback.

Another common method is the use of low power transmission modules. They allow a data transfer of typically 100 m outdoors at a power input of about 60 mW. In the example of the temperature sensor, this results in an additional energy requirement of 0.3 mWs per minute for the transfer of measured values. Thus, the energy requirement for data transfer is significantly higher (by a factor of approx. 1000) than pure sensor data acquisition.

The use of standardised transfer processes such as Bluetooth, ZigBee, WLAN etc. leads to significantly higher energy consumption since the protocols and connection mechanisms are more elaborate and complex [6]. The selection of the transfer process plays therefore a major factor in the overall energy requirement of the sensor module.

3 Energy supply via radio

3.1 Use of radio and mobile radio

Our living environment is nearly completely irradiated by electromagnetic radiation due to TV, radio and mobile radio transmitters. Since, for instance, the programs emitted by radio transmitters sometimes use a power in excess of 100 kW, distances of several to tens of kilometres to these transmitters are realistic, given the density of the broadcasting towers existing in Germany. Here the use of electromagnetic radiation for energy supply makes sense. First examples for the use of wireless radio and short-range radio for energy harvesting application are mentioned under [4] and [5]. However, for the evaluation of these methods certain parameters and conditions must be considered:

Frequency: Suitable are TV, radio and mobile radio frequencies since they provide comprehensive emission at significant power. Satellite radio is not an option due to the large distance to the transmitter (satellite). The 50/60 Hz mains frequency in buildings is also not recommended since – according to the induction principle – the low frequency generates only a very low voltage or requires extremely large antenna coils.

Distance: The electromagnetic field strength falls off somewhat with the square of the distance.

Bandwidth: The bandwidth of an antenna defines the frequency range in which the properties of an antenna meet specified standards. A distinction is made between the bandwidth of the antenna radiation characteristics and the bandwidth of antenna matching. Both factors are linked and cannot be viewed separately [8, 9]. In principle, broadband antennas can receive radiated signals from several transmitters to be used as energy source. Typical bandwidths have values between 1% and 10% of centre frequency. Special broadband antennas have a ratio of 10 between upper and lower cut-off frequency.

Under optimal conditions, the following basic values can be achieved for the use of TV, radio and mobile radio frequencies. The indicated power available is determined by the field strength calculated on site, by subtracting the free space loss

from the transmitting power. For television and radio, an omnidirectional transmitter is assumed, for mobile radio a transmitter with directional antenna.

- **TV (analogue):**

- Frequency: 500 to 750 MHz
- Transmitting power: 100 kW (80 dBm)
- Free space loss at 1.5 km distance: 89 dB
- Power at 1.5 km distance: 250 μ W (- 9 dBm)
- Free space loss at 10 km distance: 106 dB
- Available power at 10 km distance: 2.5 μ W (-26 dBm)
- Antenna size (dipole) ca. 40 cm

- **Radio (analogue):**

- Frequency: 88 to 108 MHz
- Transmitting power: 100 kW (80 dBm)
- Free space loss at 1.5 km distance: 75 dB
- Available power at 1.5 km distance: 3 mW (+ 5 dBm)
- Free space loss at 10 km distance: 91 dB
- Available power at 10 km distance: 79 μ W (-11 dBm)
- Antenna size (dipole) ca. 75 cm

- **Mobile radio (GSM, D-net):**

- Frequency: 880 to 920 MHz
- Transmitting power: 25 W (44 dBm)
- Free space loss at 100 m distance: 71 dB
- Available power at 100 m distance: 2 μ W (27 dBm)
- Antenna size: 17 cm (like UHF-RFID)

The free space loss considers only the visual contact between transmitter and receiver, thus representing the most favourable transmission path. If the receiver is located inside buildings, transmission losses or diffraction effects must be considered. Per transmission through a wall, additional attenuations of 10 to 30 dB occur (depending on material parameters).

At this point, digital methods for broadcast transmitters (DVB-T, DAB) are not taken into account because they work with significantly lower transmitting power; the same applies to UMTS. A comparison of these frequencies shows that VHF radio band

has respectable performances available which would be useful for the supply of radio modules. The radio bands MW, SW, LW not considered here would also be useful, however, they require even larger antenna structures.

At this point it should be noted that use of the electromagnetic field of the above listed transmitters for energy supply of all types of devices is not permitted according to the Regulatory Authority RegTP. The reason for this is a possible partial weakening of the field and a resulting loss of reception. The power required for the operation of individual microelectronic sensor modules is probably below the detection limit, especially when considering that the operation is in the far field of the transmitter.

3.2 Use of short range radio

Inside buildings, short-range radio solutions can also be considered for energy supply. Examples are KNX for building automation, WLAN for data transfer between computers and RFID reader gates to track objects and people. In general, a distinction can be made between existing and extended infrastructure.

As widely spreading standard in existing infrastructures, WLAN networks according to ISO 802.11 are an option. Basic values:

- Frequency: 2.4 to 2.5 GHz
 - Transmitting power: 100 mW (20 dBm)
 - Free space loss at 5 m distance: 54 dB
 - Available power at 5 m distance: 0.4 μ W (34 dBm)
 - Antenna size (dipole) ca. 6 cm

This is based on a room-by-room illumination via access points; thus, a typical distance of five metres can be assumed for the estimation. The power available in this distance is only 4 μ W and – under practical aspects – lies already below the limits for use. The use of existing WLAN infrastructures is therefore not feasible.

Other available radio systems are not considered due to insufficient transmitting power or insufficient dispersion.

The expanded infrastructure includes transmitters specifically

installed for the supply of the sensor modules. Such a method is known, for instance, from localisation systems [7]. Here, the density of the WLAN access points is increased according to accuracy requirements of the object localisation. In this case the transponders to be localised (attached to the objects) are battery operated.

If the expanded infrastructure is acceptable for the application, often the use of RFID transmitters is suitable. The calculation example in chapter 2.1. shows that even moderate transmitting powers can provide sufficient power for distances up to about 8 m. Another advantage is the data transfer, which allows extremely energy-efficient operation on the side of sensor modules.

3.3 Voltage conversion and energy storage

Chapter 2.1 already shows the voltage conversion, which converts the antenna output signal to a supply voltage by means of rectification and multiplication. This allows the use of relatively low power for operation [10]. Additional approaches can be found in [11, 12]. [12] shows a step-up converter that can convert voltages starting at 30 mV into operating voltage. Now the expansion of the application area of the "simple" RFID concept from chap. 2.1 takes place by collecting energy in electronic circuits before actual use, thus realising sensor modules as described in chap. 2.2. Figure 4 shows the archi-

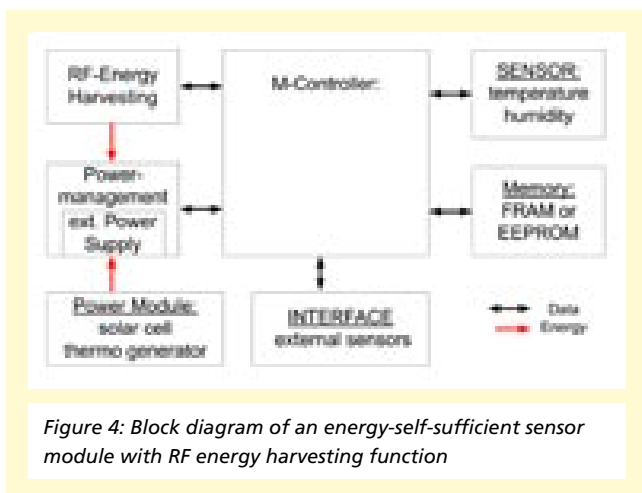


Figure 4: Block diagram of an energy-self-sufficient sensor module with RF energy harvesting function

ture of such a sensor module as block diagram. A capacitor that meets specific requirements, such as large capacity and low leakage current, is sufficient as buffer. In addition to gold caps, polymer film caps can be used.

When applying this principle, large ranges are procured through reaction times or low sampling rates. When read distances reach for instance ten metres, the buffer must be loaded for a few seconds.

Figure 5 shows the photo of a folded dipole antenna that has been matched to the chip impedance of the energy harvesting chip.

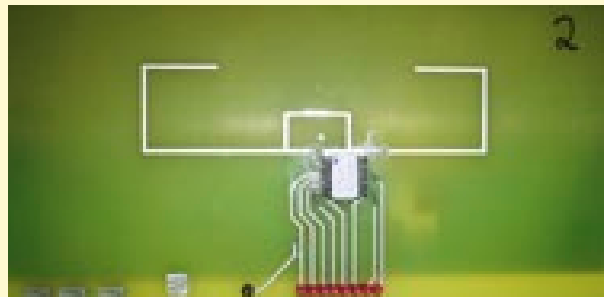


Figure 5: Antenna with radio energy harvesting chip from Fraunhofer IMS

4 Applications

4.1 Building automation

Technical equipment for buildings includes numerous sensors that are integrated in the building automation. Examples are window contacts, glass breakage detectors, smoke detectors, switches, light sensors for shading control and room sensors with temperature and gas sensors for climate control, like shown in a simplified scenario in figure 6. Since wiring is very costly, the application is still very limited. An improvement can be achieved with the concept illustrated above (chapters 3.2 to 3.4). In this case, a "room controller" that is connected to the 230 V network can be installed in each room (e.g. under



Figure 6: Building automation scenario as example for radio frequency powering of sensor modules.

the ceiling or in a light fixture). It illuminates the room with a carrier field similar to a RFID reader. Thus, sensor modules as described above as well as RFID sensors and regular RFID transponders, for instance used for object and people tracking, can be interrogated. This way expensive wiring and maintenance (battery change) can be avoided.

4.2 Machine monitoring

Manufacturing and processing machines provide only good results if they are optimally adjusted, have low wear and a long service life. This requires the availability of sufficient measurement data that can be used to optimise device settings, determine maintenance requirement, control production steps and create quality records. In this connection, wireless energy-self-sufficient sensors are a practical solution for the acquisition of measurement data from rotating or moving parts, where a wired solution would only be possible at considerable constructional and financial expenditure or where a large risk exists for errors or failures, for instance due to wear-related cable breaks.

5 Summary

The sensors to be used and the required data transfer ranges with their corresponding energy consumption are important influencing factors for the application of sensor modules with energy harvesting functions.

Looking at radio frequencies as energy source shows that the VHF radio band has usable field strengths available. With broadband antennas, more transmitters could represent a reliable supply of sensor modules. However, the disadvantages are the size of the antenna and illegality of operation.

In buildings, an expanded infrastructure with RFID transmitters creates a solid base for the operation of sensor modules. It was shown that even moderate transmitting powers can provide sufficient power for distances up to 8 m and that the extremely energy-efficient RFID technology on sensor module side can be used for data transfer.

6 Literature

- [1] Finkenzeller Klaus: RFID Handbook. 4. edition., Munich: 2008
- [2] Whytock, Paul: NXP commits to SIGE Roadmap, *Microwaves&RF*, June 2010
- [3] Andreas Hennig, Gerd vom Bögel, Anton Grabmaier: A Data Transmission Technique for Passive Sensor-Transponders in Medicine, 2010 IEEE International Conference on RFID, Orlando, USA
- [4] Energy Harvesting Forum, <http://www.energyharvesting.net/>
- [5] Energy Harvesting Journal, by IDTechEx <http://www.energyharvestingjournal.com/>
- [6] Jackson, Robert: Wireless-Sensornetzwerke und Technologien zur Energiespeicherung, National Instruments Germany GmbH - Monatliche Veröffentlichungen 2010, ftp://ftp.ni.com/pub/branches/germany/artikel/.../06_ni_vfi.pdf
- [7] Ekahau Real-Time Location System (RTLS), <http://www.ekahau.com/>
- [8] IEEE Std 145-1983; The Institut of Electrical and Electronical Engineers, June 1983
- [9] Balanis, Constantine A; *Antenna Theory - Analysis and Design*; 2nd ed; John Wiley & Sons; USA, 1997
- [10] Feldengut, Tobias: Voltage Rectification: The Energy-Bottleneck for Passive RFID Systems, RFID-Systech 2009 Bremen
- [11] Powerharvester Receiver. <http://www.powercastco.com/products/powerharvester-receivers/>
- [12] Linear Technology: Auto-Polarity, Ultralow Voltage Step-Up Converter and Power Manager: <http://www.linear.com/pc/viewCategory.jsp?navId=H0,C1,C1003,C1799>
- [13] Berg, Markus: Integration des IMS eigenen Transponderfrontends in ein mikrocontrollerbasiertes Transponder-system für den UHF ISM Frequenzbereich (Integration of IMS Transponder Frontend into a Microcontroller-based Transponder System for UHF ISM Frequency Range; Thesis for Masters Degree; Fraunhofer IMS & FH Dortmund; October 2010; Duisburg

WIRELESS INTEGRATED PRESSURE SENSOR FOR QUALITY CONTROL OF VACUUM INSULATION PANEL

G. vom Boegel, M. Goertz, M. Kemmerling

1 Abstract

The pressure inside a vacuum insulation panel (VIP) is an important indicator for thermal insulation properties. The sensor transponder described in this paper fulfills the function of contact less measurement of pressure and temperature through covering layers and presents the best opportunity of quality assurance. The sensor transponder is placed inside the VIP and consists of a fully integrated microelectronic circuit and an antenna, both mounted on a printed circuit board. Measurements are taken with a mobile reader unit.

2 Introduction

For the purpose of thermal insulation of e.g. building, container or cooling devices vacuum insulation panels are a good choice in comparison to cut-to-fit materials such as polystyrene with respect to the thickness of the panel and insulation effect. A typical panel consists of an almost gas-tight enclosure and a rigid core with submicron pore size from which the air has been evacuated [1]. However, the insulation quality of the panel depends strongly on the quality of the vacuum and as the thin enclosure is prone to mechanical damage a quality control during production of the panel as well as before and after installation is crucial. An analysis of pilot projects in application of VIPs in construction over the last five years shows that nearly all appearing damages of VIPs can be traced back to uncaredful treatment in transportation and installation of VIPs [2]. So it is strongly recommended to have a test procedure at the end of the installation. An exchange of a panel before applying the covering layer is much less expensive and much more efficient than afterwards. Thermal measurement principles like heat-flow measurement or infrared pictures are not appropriate due to practical aspects. Furthermore a long term monitoring of the intra-panel gas pressure as an indicator for the insulation effect is also desirable. The following chapters describe the development and application of a miniaturized integrated pressure sensor operating as a transponder for wireless measurement of the intra-panel pressure as a solution for the above mentioned necessary improvements [1].

3 System Components

3.1 Transponder System

The combination of sensors and transponders – the so called sensor transponders – finds more and more interest in many applications [3,4] like automotive (tire pressure monitoring), logistics (cool chain monitoring) and newly in construction industry [6]. The transponder system for the monitoring of vacuum insulation panels consists of a mobile reader unit and the VIP-built-in sensor transponders. Figure 1 shows the handling while taking current pressure and temperature values. A measurement is initiated by the reader unit, while the RF field of the reader activates the sensor. The sensor electronics takes the measurement from the integrated sensors and transmits a data packet to the reader unit. The reader displays the sensor values and additional information like the unique identification



Figure 1: Readout of the inside pressure and temperature of a VIP

WIRELESS INTEGRATED PRESSURE SENSOR FOR QUALITY CONTROL OF VACUUM INSULATION PANEL

number of the sensor transponder and a time stamp. For later documentation and analysis all data is stored on a memory card.

The activation of the sensor transponder takes place by inductive coupling. As a built-in device the sensor transponder consists of an integrated capacitive pressure sensor chip and an antenna coil including some discrete electronic components for the transmission of power and data. The on-chip electronics contains an RF interface for the wireless communication. A magnetic field with a frequency of 133 kHz is generated by an external antenna coil that is connected to a handheld reader. The radiated field transfers power to the second antenna coil of the sensor transponder located inside the VIP by inductive coupling. The induced voltage is rectified and is used to supply the microelectronic circuit. Apart from the power, the transponder extracts its clock from the frequency of the magnetic field. The digitized sensor values are coded together with the identification number, status information of the sensor transponder and check sum to a data packet to be transmitted. For this transmission the method of absorption modulation is used, which is frequently used in transponder systems [4]. The field damping of absorption modulation is evaluated by the reader. If the check sum of the transferred data is valid, pressure value processing will be continued.

3.2 Embedding of Sensor Transponders in VIP

For the direct measurement of pressure and temperature inside the panel the sensor has to be placed inside the enclosure. The actual size of the sensor transponder is about four millimeters in thickness and about 25 millimeters in diameter. So it is advised to form a cavity of this size into the VIPs core board and to insert the sensor transponder in this place. This establishes a fixed mounting position and avoids shifting during handling and evacuation process.

Figure 2 shows the principle of embedding the sensor transponder inside the panel: The left photograph shows a cutted

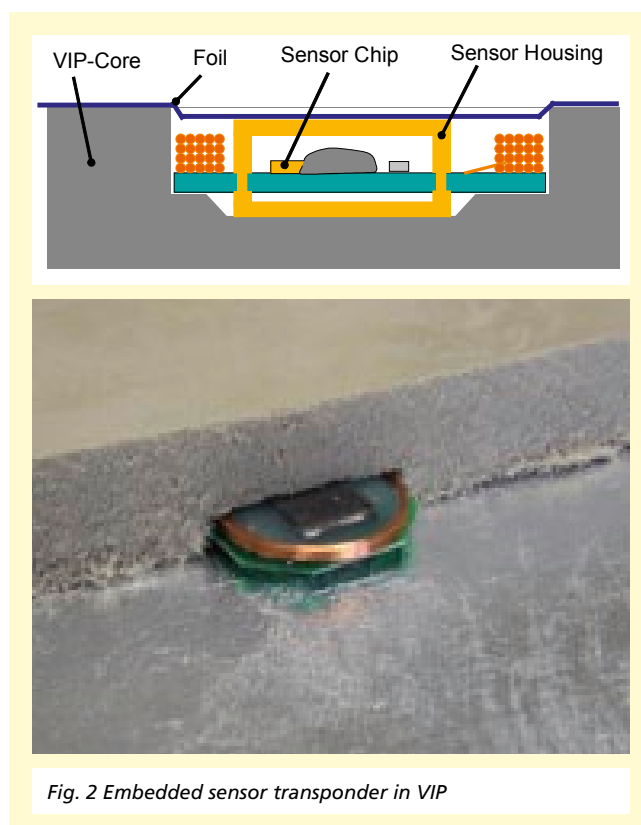


Fig. 2 Embedded sensor transponder in VIP

core board with an inserted transponder, while on the middle photograph the surface of an evacuated panel is seen. In this configuration a reading range of up to 50 centimeters is possible, depending on reader parameters. The drawing on the right side of figure 2 shows a cross section of an embedded sensor transponder. For reliable behaviour the sensor chip is encapsulated in a stable housing. This keeps mechanical stress away from the encapsulation such as forces from foil and core as well as bending effects. In future versions the thickness of the sensor transponder will be reduced to about two millimeters.

The transmission of energy and data has to take place through the layers of the enclosure foil. This foil typically consists of several layers with one or more aluminum layers for a better impermeability. Usually the thickness of the aluminum layer is

far below one micrometer and therefore it has a low impact of transmission properties. Using foils with relatively thick aluminum layers of several micrometers shows an attenuation of the electromagnetic field and a mistuning of antennas. The result is a limited reading range or even impossible readout.

3.3 Microelectronic Circuit with Surface Micromachined Pressure Sensor

Micromachined capacitive pressure sensor is a mature technology that is well-known [5]. Thin diaphragms which deflect under pressure are appropriate basic structures for the detection hereof. A deflected plate shows specific stress and strain states proportional to the deflection and hence proportional to the pressure. For strain based sensors the distance change between the deflected plate and another fixed plate can be used to detect a change in the capacitance, provided both plates are conducting. Known for its ideal elastic behavior silicon is an excellent material for the creation of a diaphragm.

The pressure range is design controlled by adjusting the diameter of the sensor diaphragm, keeping the thickness to be fixed. This allows the fabrication of various sensors for low (0.01 bar to 0.5 bar e.g. for VIPs with pyrogenic silica) up to high (350 bar max.) pressure ranges on a same wafer or even on a same device. For low and atmospheric pressure the diaphragm diameter is about 100 μm . A close up view of a sensor cell reveals the extreme aspect ratio of the diaphragm diameter and the cavity height considering that the diameter is in the range of some tens up to a hundred micrometer. The small cavity height ($< 1 \mu\text{m}$) limits the deflection of the diaphragm automatically, once the top plate touches the bulky bottom substrate.

In order to readout the small capacitance of the pressure sensor cell only very small current is needed to charge or discharge the capacitor. Combining this with CMOS circuits allows the realization of low power consuming systems.

Since the surface micromachining technique is a planar technology similar to a CMOS process the pressure sensor process module can be integrated. A co-integration of pressure sensor and CMOS process has been implemented. A high voltage option and EEPROMs are also available.

3.4 Calibration

From the production process the sensors have a spreading in raw values as well as a non-linear behaviour in pressure and temperature. However, a precise measurement is possible using an appropriate calibration and correction algorithm. After readout of the sensors specific equations have to be computed in the reader using the raw values and additional calibration coefficients to get the real values. For the calculation of pressure a 2nd order polynomial and for temperature a 1st order polynomial have to be computed. The coefficients for the polynomials are generated in the calibration process and stored in the memory of the sensor transponder.

The calibration process is performed after the assembly of the sensor transponders and before the insertion into VIPs. The sensor transponders are placed inside a vacuum chamber where temperature and pressure can be applied controlled by a computer, and the raw data of the sensors is taken for further calculation steps. The calibration process is executed in the following steps:

1. Setting temperature and pressure, wait settling time,
2. Gathering raw data from sensors by wired interface,
3. Repeat step one and two for two temperature points and three pressure points,
4. Calculate calibration coefficients for each sensor according to the "best fit" algorithm,
5. Store calibration coefficients in memory of each sensor and
6. Final inspection of each sensor.

WIRELESS INTEGRATED PRESSURE
SENSOR FOR QUALITY CONTROL OF
VACUUM INSULATION PANEL

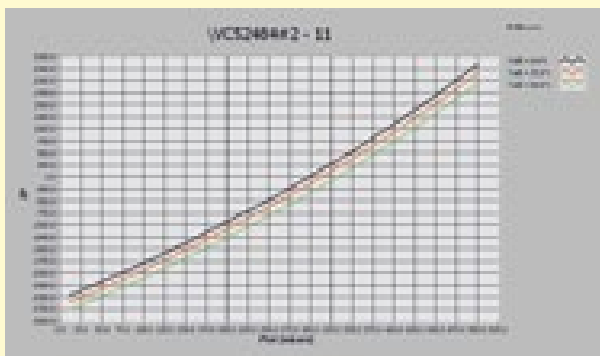


Figure 3: Typical pressure characteristics (Pist: applied pressure, ZP: raw values)

4 Experimental Results

The first step of characterization of the sensor transponders was the measurement of the pressure gradient over the pressure range from near vacuum up to ambient pressure. Figure 3 shows typical curves from the measured „raw” data ZP of the sensor transponders up to 500 mbar. The applied temperature was set to 0 °C, 25 °C and 50 °C. The pressure resolution is 0.1 mbar at a fix temperature which is a very acceptable value. The pressure shift due to temperature variation results in about 1.0 mbar per Kelvin without compensation. The calibration procedure comprises also the temperature compensation so that the expected overall pressure shift due to temperature variation results in about 1.0 mbar per 50 Kelvin. The overall accuracy can be estimated with +/- 2.0 mbar within the temperature range of 0 °C to 50 °C.

A subsequent test took place using sensor transponders embedded in VIPs. During manufacturing several transponders were assembled in panels with different “starting” pressures. The panels under test were stored in a climatic chamber at 50 °C and 60 % humidity. In irregular intervals the panels were temporarily removed and measurements were taken. The results compared to ambient pressure are shown in figure 4.

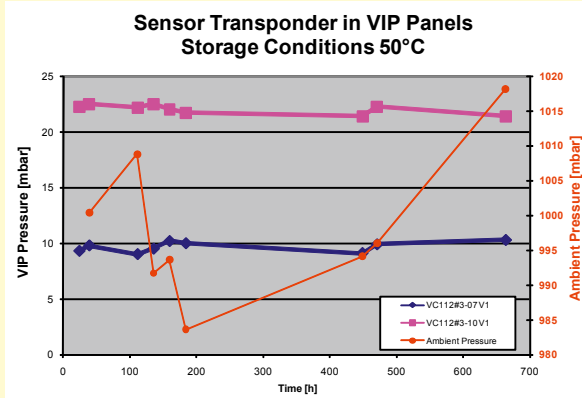


Figure 4: Long term measurement of embedded sensor transponders

5 Summary and Outlook

Measurement of the absolute pressure inside the panel down to some few mbar with an accuracy (1 sigma) of better than 1 mbar is achieved. The wireless transmission can even be achieved through the gas-tight enclosure including a thin metallic coating. The results demonstrate that the pressure sensor transponders presented here are as tiny as necessary for the integration into a thin vacuum insulation panel. It has also been verified that the power consumption of the system is as low as required for an inductive transmission of power and data without the need to incorporate a battery into the vacuum insulation panel. This wireless monitoring technique of the intra-panel pressure will allow a safe and more reliable use of vacuum insulation panels.

In next steps the long term measurements and environmental tests will be completed, evaluated and documented. These tests are executed in cooperation with partners in research and VIP manufacturers. It is planned to equip buildings with “smart” VIPs, which means VIPs with built-in sensor transponders, in the near future.

In a current research project the use of sensor transponders for the estimation of energy efficiency aspects is evaluated. In this approach sensor transponders are used not only for the monitoring of VIPs, but also in specific places within the building envelope. By measuring temperatures it is possible to determine the heat flow and to derive exact thermal transfer coefficients. This allows a comparison with data from the planning process.

6 References

- [1] T. Brockmann, R. Herr, S. Rössing, Vakuumisolationspaneele in der Baupraxis, Bundesinstitut für Bau-, Stadt- und Raumforschung (BBSR) Bonn, Germany (2011)
- [2] U. Heinemann, Vakuumdämmung in der praktischen Anwendung – Ergebnisse der wissenschaftlichen Begleitforschung, ZAE Bayern – Universität Würzburg, Workshop on vacuum insulation in construction, Bundesinstitut für Bau-, Stadt- und Raumforschung (BBSR) Bonn, Germany (2011)
- [3] G. vom Boegel, Technologische Trends bei RFID-Systemen für den Einsatz im Internet der Dinge in: H.-J. Bullinger, M. ten Hompel (Eds.), Internet der Dinge (Internet of Things), Springer, Berlin, 2007, pp. 157–178
- [4] K. Finkenzeller, RFID-Handbook, Fundamentals and Applications in Contactless Smart Cards, Radio Frequency Identification and Near-Field Communication, 3rd edition, Wiley & Sons LTD (2010)
- [5] H.-K. Trieu: Surface micromachined pressure sensor technologies, in : Proceedings Sensors Expo & Conference Fall 2002, Boston, MA, September 23-26, 2002, pp. 111–122
- [6] N. Koenig, M. Wuerth, G. vom Boegel, Potenziale von RFID-Technologien im Bauwesen – Kennzahlen und Bauqualität. Forschungsinitiative Zukunft Bau (2743), Dezember 2009, Fraunhofer IRB Stuttgart

A NEW INDOOR LOCALIZATION SYSTEM WITH IMPROVED MULTIPATH MITIGATION

M. Marx

Introduction

Localization or positioning is the process of determining the physical position of a device. Popular examples for outdoor applications include global navigation satellite systems like GPS and GALILEO, which are generally not suitable to establish indoor locations. However, there is an increasing demand for robust and accurate positioning, for instance in healthcare management (the tracking of persons and equipment) and inventory tracking in logistics.

A wide range of technologies can be used for localization: Video-based environment detection has fundamental problems with changing environments and requires, just like LIDAR-based technologies, a direct line of sight. Ultrasonic-based solutions are generally unable to penetrate walls and exhibit small operating ranges. Techniques using inertial sensing or odometry suffer from accumulated errors and therefore are subject to drift. For many applications, only localization technologies based on radio wave propagation are adequately suited.

State of the art

A variety of techniques have been developed for RF-based localization: A first distinction can be made between techniques based on exploiting received signal strength (RSS) measurements, angle of arrival (AOA) information or estimating the time of flight (TOF). RSS-based localization solutions exhibit rather low investments cost at the expense of positioning accuracy (typical errors around 3–30 meters [1]), whereas implementing AOA solutions requires rather complex antenna arrays [2]. TOF based localization systems can be distinguished between systems using the ultra wide bands (UWB) and the industrial scientific medical (ISM) bands. UWB-TOF based systems generally achieve better localization accuracy at the expense of small operating ranges, whereas ISM-based systems achieve larger operating ranges. RF-based localization systems usually consist of mobile devices, tagged to the objects to be localized, and base stations at fixed and known positions. In this context, the operating range is the maximum distance of the mobile device to a base station

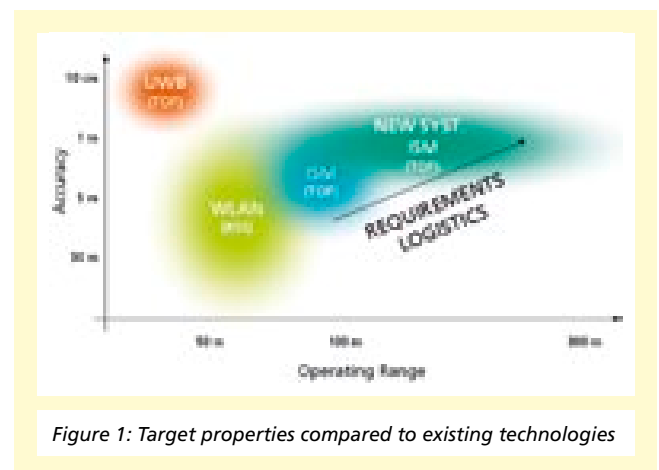


Figure 1: Target properties compared to existing technologies

while still achieving satisfactory positioning accuracy. Fig. 1 shows the typical positioning performance of these regarding operating range and accuracy.

There are many applications, especially in the field of logistics, requiring positioning of a large number of objects in a relatively large area with an accuracy of better than 1 meter. Currently, this demand in accuracy is only met by UWB-based systems. Due to the relatively short operating range of those systems, the coverage of larger areas may require the installation of several tens or hundreds of base stations, making this solution rather uneconomical. This issue is even reinforced by the fact that UWB-based localization systems generally require a direct line of sight between mobile devices and base stations.

Conventional systems do not provide a satisfactory solution for these applications.

A new localization system

In order to meet these challenging demands, a new localization system has been developed, that achieves positioning accuracy better than 1 meter, even in non-line-of-sight situations and through walls, at an operating range of at least 250 meters. To satisfy economic demands of applications with a large number of objects, special attention has been paid to

minimize costs of the mobile devices, while the system concept allows for the inexpensive deployment of base stations without extra installation.

For localization the time-difference-of-arrival (TDOA) method is used to compute the positions. The objects to be localized are tagged by a small battery powered mobile transmitter. To determine its 3D-position, the times of arrival at the fixed base stations are measured using a common time base. The start of transmission is a fourth unknown, therefore at least four base stations are required to establish and solve the system of equations. The position of the transmitter is calculated at a central localization server.

Low cost mobile devices and long range operation

Estimating the times of arrival based on the received signals and calculating the position of the mobile devices requires a considerable amount of processing power. Using the TDOA method, these complex calculations are performed on the base stations, whereas the mobile devices are only required to transmit a simple signal, which is readily generated using simple hardware or software.

To achieve a range of at least 250 meters even through obstacles and walls, while operating on the ISM band at 2.4 GHz, a spectrum spreading technique is used. That way, the operating range can be adjusted by choosing the appropriate sequence length for the spreading codes.

Multipath mitigation

The key to accurate localization in all TOF-based localizations systems is to measure the time of arrival of the radio signal arriving from the direct-line-of-sight (DLOS) path. However, indoors and in urban areas, the transmitted signal propagates over multiple non-line-of-sight (NLOS) paths in addition to the DLOS path. Conventional measurement techniques may not be able to differentiate the time of arrival of the direct line of sight signal from the reflection signal (NLOS) in these situations, resulting in considerable positioning errors. The new system employs an innovative algorithm for high-resolution delay

estimation on the signal received at the base stations, exploiting statistical information contained within the received signal [3]. With this post-processing, the time of arrival of the direct line of sight signal can be estimated with high resolution, even if the DLOS signal is distorted due to early reflections. Together with an approach for efficient implementation, this technique constitutes the core innovation of the new localization system.

Proof-of-concept demonstrator

To demonstrate the feasibility of processing the received signals in real-time, an appropriate hardware has been developed. Fig. 2 shows the main functions implemented in the base stations. The high frequency (HF) front-end converts the radio signal down to baseband. Subsequently, code acquisition and frequency synchronization is performed at the beginning of each localization cycle. After despreading the

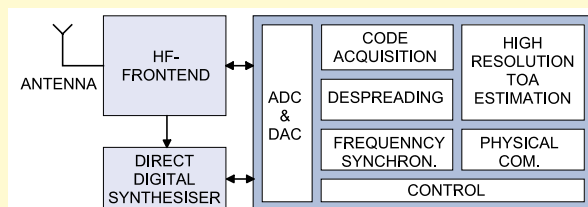


Figure 2: Implemented functions in the base stations



Figure 3: Demonstrators base stations

WIRELESS CHIPS AND SYSTEMS

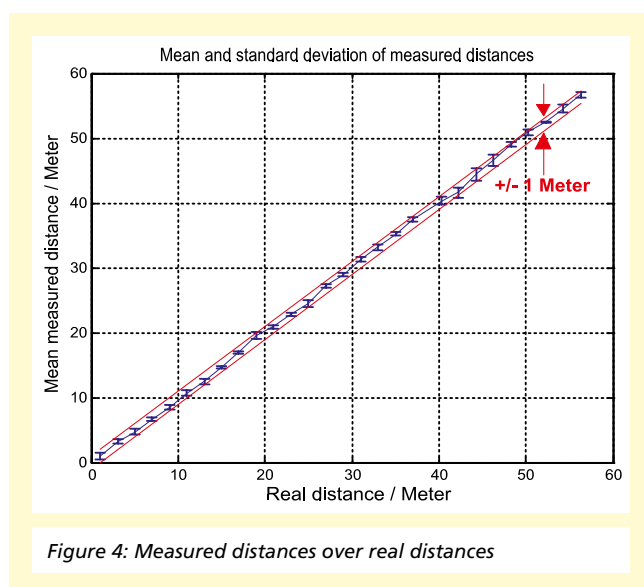
A NEW INDOOR LOCALIZATION SYSTEM WITH IMPROVED MULTIPATH MITIGATION

baseband signal, high resolution delay estimation and post-processing is performed. The resulting high-resolution TOA estimate is then used for ranging or localization. Fig. 3 shows a picture of the base stations.

Results and further work

To evaluate the ranging accuracy achievable in typical indoor situations, extensive measurements have been conducted using the demonstration hardware. Fig. 4 shows measured range versus actual range for several measurement situations with distances up to 60 meters, carried out in the institute building. For each measurement situation and distance, a series of 20 range measurements has been made. Error bars indicate the standard deviation and are centered on the mean.

In further work, the base stations will be implemented as a fully embedded solution, and small and low-power mobile devices will be developed. The devices and measurement procedure will be optimized to improve localization accuracy and performance.



References

- [1] Vossiek, M. ; Wiebking, L. ; Gulden, P. ; Wieghardt, J. ; Hoffmann, C. ; Heide, P.: Wireless local positioning. In: Microwave Magazine, IEEE 4 (2003), dec., Nr. 4, S. 77–86
- [2] Gezici, S ; Tian, Z ; Giannakis, G B. ; Kobayashi, H ; Molisch, A F. ; Poor, H V. ; Sahinoglu, Z: Localization via ultra-wideband radios. In: IEEE Signal Processing Mag (2005), Nr. 22, S. 70–84
- [3] Marx, M., System issues for time synchronization in Real Time Localization Systems with multi path mitigation. In: European Wireless Conference, Lucca, Italy: IEEE, 2010, pp. 596–601

BUILDING AUTOMATION: BUILDING AND INFRASTRUCTURE SERVICES

H.-J. Schliepkorte

Internationally mandatory goals of climate control have been a subject of discussion for more than a decade. The international attempts finally led to the Kyoto Protocol which came into effect in 2005. Moreover, the European Union (EU) attempts to play a leading role in the international climate policy by following ambitious goals to limit global climate change to 2 C° (in comparison to the pre-industrial level)¹. The European Commission took an important step on March 8, 2011, when it passed the programs “EU-roadmap for a low-carbon economy by 2050”² and “Energy Efficiency Plan 2011”³, which are highly relevant for the European climate and energy policy. They target the reduction of emissions by 25 percent until the year 2020 (in comparison to 1990). The climate protection scenarios, which were analyzed in the context of the program “Intelligent Energy Europe” – as presented in figure 1 – include the reduction of the CO₂ emission to 550 ppm or 450 ppm and show that a necessary measure for reaching the respective goal is the increase of

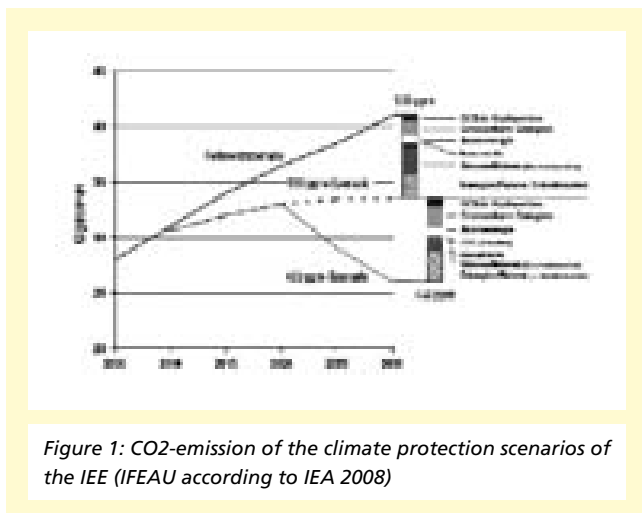


Figure 1: CO₂-emission of the climate protection scenarios of the IEE (IEFAU according to IEA 2008)

energy efficiency. This is considered as similarly important as the development of renewable energy sources.

Particularly the energy efficiency of the buildings sector⁴ is of importance due to its share of 40 percent⁵ of all energy consumption. Even though advanced building material and installation engineering help reducing energy consumption, the entire potential can only be fully drawn on by means of integrated building automation, which allows for the consideration of the building user. While energy efficiency is of high priority in the initial construction, it is successively replaced by user satisfaction as the construction process continues. Everything is done to satisfy the user disregarding energy consumption, which – as a result – exceeds all previous calculations and simulations. Furthermore, sensors for an energy-efficient and user-centered automation, which were not built-in due to the non-existing focus on building users, are missing.

User behavior – such as the changing of room temperature, the control of solar protection or the opening and closing of doors and windows – has a significant influence on building operations and, in this, also on energy consumption. Different sources estimate that the energy consumption directly linked to user behavior adds up to about 20 percent of all energy consumption of buildings (cf. Stadler 2001, p. 3⁶).

According to Stadler, user expectations of their workplace focus on two main points (cf. Stadler 2001, p. 16⁶).

1. a consistent, convenient and activity-adapted condition of their surroundings
2. the opportunity to directly influence the condition of the surroundings according to individual preference and condition [37].

⁴ This includes, among others, houses, public and private office buildings, shops and other buildings.

⁵ in 2008, cf. “Energy, transport and environment indicators”, Eurostat 2010

⁶ “Dialogfähige Energiemanagementsysteme im Kontext von Energieverbrauch und Nutzerverhalten”, Ingo Stadler, Dissertation, Kassel, 2001

¹ Communication from the European Commission of 10.01.20007: KOM (2007) 2

² Communication from the European Commission of 08.03.2011 IP/11/271

³ Communication from the European Commission of 08.03.2011 IP/11/272

SYSTEMS AND APPLICATIONS

BUILDING AUTOMATION: BUILDING AND INFRASTRUCTURE SERVICES

The first point underlines the central importance of building automation in the context of users' comfort conditions in their workplace. Convenience and space comfort are notably influenced by the following eight factors:

1. social factors
2. interior design
3. design of the workplace
4. air quality and odor
5. temperature
6. user-friendliness
7. lighting
8. acoustic and sounds

While the first three bear no connection to building automation, the last five may be – depending on the respective facilities – influenced directly through building automation. Optimal working surroundings enhance not only satisfaction with the workplace, but also bring along economic advantages. Various studies⁷ conclude that productivity may be increased by 15 percent. Building automation is the basis to reach those optimal conditions in an energetically best possible way. In addition, the appointed and legal guidelines⁸ can be controlled and kept.

The second point, that is, direct user influence, indicates the limits of building automation. An increase in automation, as illustrated in figure 2, does enhance energy efficiency, but it also reduces the user's opportunity to influence the condition of the surroundings, so that the dissatisfaction with and acceptance of technical solutions and automation decreases (REFERENZ). Users lose the authority over the room conditions and feel patronized. Moreover, they often do not understand why the automation triggers certain actions.

⁷ BOSTI Research Team – Buffalo Organization of Social and Technological Innovation

⁸ DIN, ISO, EN, ASR and ASV

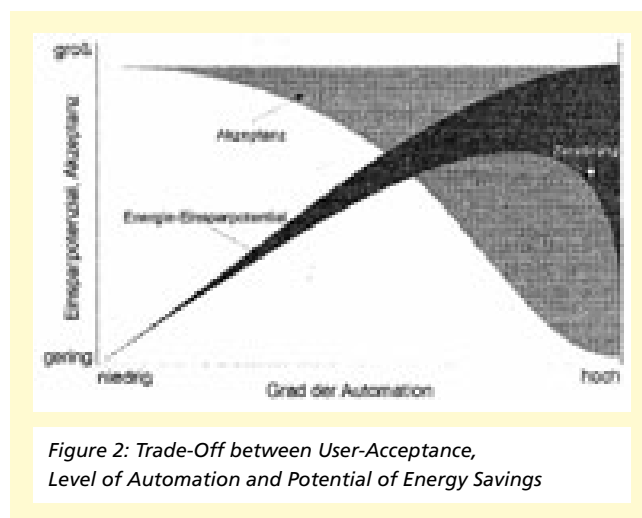


Figure 2: Trade-Off between User-Acceptance, Level of Automation and Potential of Energy Savings

The most important challenges in new and innovatively equipped buildings is the consideration of the trade-off between the level of automation, user acceptance and potential of energy savings, as well as the inclusion of users as early as possible.

The newly constructed enlargement of IT.NRW, whose building equipment is seen as a blueprint for the future of North-Rhine Westphalia, was built to meet the challenges listed above, using the experience of the Fraunhofer-inHaus-Center in Duisburg.

The Newly-Constructed Enlargement of IT.NRW

The newly-constructed enlargement of the Landesbetrieb Information und Technik Nordrhein-Westfalen (IT.NRW) in Düsseldorf, at the corner Ross- and Bankstraße, was modeled according to the design of RKW architects of the Building and Infrastructure Services (trans. "Bau- und Liegenschaftsbetrieb" BLB). The eight-story office building has a gross floor area of 15,565 square meters (excluding the underground garage) and accommodates four office floors, a cafeteria, a printing plant and further utility rooms.



Figure 3: The Newly-Constructed Enlargement of IT.NRW in Düsseldorf (Source: IT.NRW)

The primary heat supply of the building is covered by an electric heat pump which is fed by a field of 50 geothermal probes, which reach 130 meters deep into the earth. In order to cover the peak demand, heat supply via district heating is also enabled. The building is cooled with the help of two cooling compressors and with additional free cooling. Raumlufttechnische Geräte (RLT) take care of ventilation and air-conditioning, relying on heat recovery, air humidification and dehumidification and constant volume flow rate.

The office areas on the lower five floors use air-conditioning combined with heat recovery and thermal activation. The individual offices are additionally equipped with floor convectors arranged in a four-wire-system, built into the cavity below the window. This allows the individual adjustment of the room temperature.

Here, the Feldbus Local Operation Network (LON) was used for the implementation of assistant technology in office space. The automation allows for individual single room regulation to foster user comfort and energy efficiency. The room can be switched to either one of the three pre-defined scenarios:

1. occupied – automation with a focus on user comfort
2. un-occupied – automation with a focus on energy saving
3. standby – automation turned off

In order to detect reliably whether or not the room is occupied, window contacts and occupancy detectors are used to trigger switching between the different modes. Opening a window automatically switches the room into stand-by and room occupancy switches to the user-comfort-mode.

The rooms are linked to a subordinate timer software to determine the operating time and the best start-sequence, so that the room is precisely pre-coordinated in the mornings. The in-house weather station's luxmeter provides a command variable for the automatic control of the interior lighting and the solar protection. The threshold can be set individually for each room. In addition, the azimuth and elevation angles further allow for a fine-grained control of the solar protection.

Despite the room automation, the room user has full control over the room at all times: Manual control dominates automation, so that the room can be switched to the occupied-mode, which enables the manual setting via light- and blind-switches. With the help of the room operating devices the room temperature can be adjusted with an accuracy of ± 3 Kelvin of the parameterized index value. Thereby, the room user's individual comfort zone is taken account of.

Energy Consumption IT.NRW

The calculated demand of primary energy amounts to 142.3 kWh/m²a and falls below the permitted demand ac-

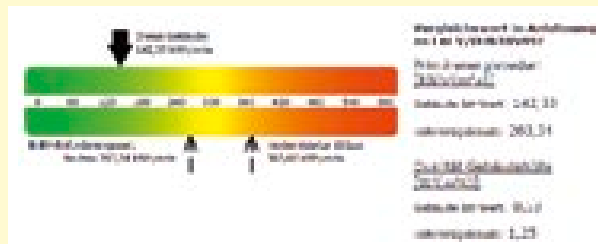


Figure 4: Classification of the Demand of Primary Energy per heated floor space

**BUILDING AUTOMATION:
BUILDING AND INFRASTRUCTURE
SERVICES**

According to EnEV 2007 by 46 percent. Similarly, the calculated [Wärmetransmissionstransferkoeffizient] of the building shell amounts to 0.53 W/m²K, that is, 58 percent below the permitted value.

The user-dependent energy consumption of buildings is monitored by Fraunhofer IMS. In addition, both the functionality of the introduced features and user acceptance are analyzed. The built-in actuating elements and sensor technology in the offices of IT.NRW aim to increase the comfort of office users while simultaneously keeping the user-dependant energy consumption low. The reduction of the energy demand is triggered by the absence of the user or the opening of a window. The following figure shows individual measurements during one day in one of the rooms of the IT.NRW-building. The displayed course of the day is determined by both the automatically triggered functions and by user-interference. The first thing to notice is the decrease in the desired level of temperature during the night, that is, before 4 UCT. Between 4 and 5 UTC the desired standard level of temperature and the offset are pre-coordinated. What is also clearly discernible is the lowering of the room temperature in the morning, after the user has opened the window. It indicates the closure of the heating valve as a result of the automatically triggered

standby-mode. Furthermore, the room lighting turns on automatically upon re-entrance in the morning. This depends on the – also adjustable – light level outside. Upon closure of the windows at around 8.30 UCT, the room is readjusted to the desired temperature of 21 °C.

Particularly the connection between opening a window and the transition to the standby-mode is not intuitively discernible. Formerly, users grew accustomed to opening the heating or cooling valve when opening the window in order to keep the room temperature at the desired level. In the IT.NRW-building, extreme levels of room temperature are observable and can often be linked to the opening of windows. If windows are kept open for a longer period of time during the summer, the level of room temperature is notably higher, because the general cooling is shut off automatically. A further user-dependency becomes obvious with reference to the setting of the offset-temperature in individual offices. In most cases, users select extreme values between -3 and +3 Kelvin, or they leave it at the default-setting of 0 Kelvin. The following figure displays the course of a month of one floor of IT.NRW. A dark blue line symbolizes the offset-temperature, a green line an offset of 0 K and a red line

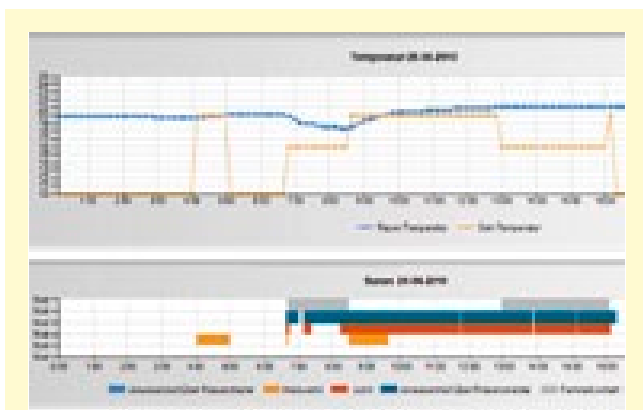


Figure 5: The level of temperature in relation to open windows and occupancy

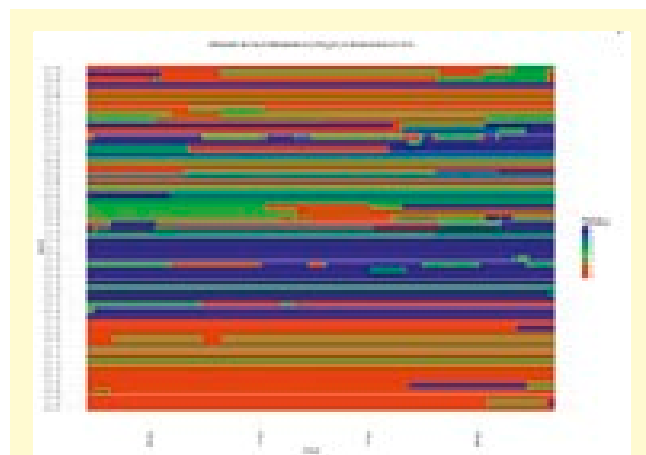
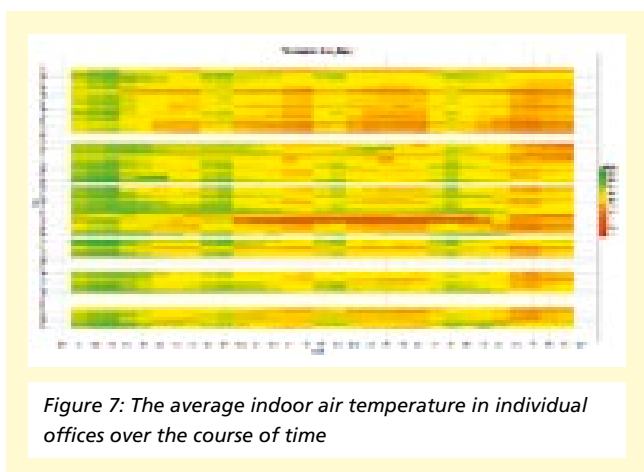


Figure 6: The user-dependency of the offset-temperature in individual offices over the course of time

an offset of +3 K. The figure reveals that only few offices use any of the intermediate stages.

Implementation Management

The installed sensory technology and actuating elements are not only used for the analysis of the user-dependent energy consumption but also for implementation management and performance tests. The display of the different levels of room temperature as a carpet-plot facilitates the detection of deviation from the desired levels. The following figure shows the different levels of room temperature during one month on one floor of the IT.NRW-building. Deviations of some offices from the others are clearly discernible. The red line in the middle of the plot, for instance, indicates a notably higher level of temperature in one of the rooms. The analysis of all rooms is very effective in comparison to the analysis of only individual rooms, because deviations are easily detectible.



Outlook

The introduced measures highlight the savings potential in the area of user-dependent energy consumption in office buildings. Automatic functions reduce energy consumption if the room is unoccupied or if the windows are opened. Exact figures indicating the savings potential of the introduced measures will be determined in the future to enable cost-benefit calculations for future buildings.

Furthermore, the analysis reveals that user behavior is closely linked to learned habits, which has some undesirable side-effects. The new features result in building behavior that differs from what users are accustomed to. This is particularly evident with reference to open windows and the setting of offset-levels in individual offices. The observed behavior suggests the necessity for the development of feedback mechanisms for users, because the building behavior does no longer correspond to the learned behavior.

Works Cited

Voss, K.; Löhnert, G.; Herkel, S.; Wagner, A.; Wambsganß, M., (2006), Bürogebäude mit Zukunft, Fachinformationszentrum Karlsruhe, Solarpraxis, Berlin



LIST OF PUBLICATIONS AND SCIENTIFIC THESES 2011

List of Publications and Scientific Theses 2011

1. Monographs	88

2. Journals and Conference Papers	88

3. Oral Presentations	92

4. Patents	
4.1 Granted Patents	92
4.2 Laid Open Patent Documents	93

5. Theses	
5.1 Dissertations	94
5.2 Diploma Theses	94
5.3 Master Theses	94
5.4 Bachelor Theses	95

6. Product Information Sheets	96

1. Monographs

Müller, H.-C.:

SmartForest : Einsatz von Transponder-Technik und drahtlosen Sensornetzen in der Forstwirtschaft.

Schlussbericht; gefördert durch die Bundesanstalt für Landwirtschaft und Ernährung (BLE); Förderkennzeichen 28-1-53. F02-07. 2011

2. Journal and Conference Papers

Baer, E.; Paschen, U.; Lorenz, J.:

Prediction of etch bias for polysilicon etching based on coupled equipment- and feature-scale modeling.

(International Conference on Micro- and Nano-Engineering (MNE) <37, 2011, Berlin>).

In: 37th International Conference on Micro- and Nano-Engineering (MNE): Abstract Book, 2011, without pagination; [1 B.]

Cleven, N.; Woitok, A.; Görtz, M.; Götttsche, T.; Steinseifer, U.; Schmitz-Rode, T.:

Testing and improvement of a long-term monitoring system for hypertension patients.

(Biomedizinische Technik (BMT) <45, 2011, Freiburg>).

In: BMT 2011. Berlin [u.a.]: de Gruyter, 2011, without pagination (Biomedizinische Technik 56, Suppl. 1)

Dierk, S.; Ünlübayir, S.; Trieu, H.-K.; Vogt, H.; Köper, I.:

A new approach for detecting ionophore concentrations in tethered bilayer lipid membranes.

(Biomedizinische Technik (BMT) <45, 2011, Freiburg>).

In: BMT 2011. Berlin [u.a.]: de Gruyter, 2011, [P96]

(Biomedizinische Technik 56, Suppl. 1)

Durini, D.; Brockherde, W.; Fink, J.; Hochschulz, F.; Paschen, U.; Hosticka, B. J.:

Fast-response, low-noise, multiple shutter, non-destructive readout line sensor for spectroscopy applications based on lateral-drift-field photodiode principle.

(Workshop CMOS Image Sensor for High Performance Applications <2, 2011, Toulouse>).

In: CMOS Image Sensor for High Performance Applications 2011. Toulouse 2011, without pagination [2 Bl.]

Feldengut, T.; Marzouk, A. M.; Kolnsberg, S.; Kokozinski, R.:

A passive UHF transponder with readout circuits for external mechanical switches.

(RFID SystTech <7, 2011, Dresden>).

In: RFID SysTech 2011. Berlin [u.a.]: VDE-Verl., 2011, without pagination

Goehlich, A.; Jonville, C.; Klieber, R.; Mao, X.; Martens, K.; Jansen, T.; Trieu, H.-K.; Vogt, H.:

A novel mass sensitive sensor.

(Mikrosystemtechnik-Kongress <4, 2011, Darmstadt>).

In: Mikrosystemtechnik Kongress 2011. Berlin [u.a.]: VDE-Verl., 2011, pp. 54–57

Gözüyasli, L.; Dogangün, A.; Munstermann, M.; Haese, A.; Stevens, T.:

inKüche – Assistive Kochumgebung für Senioren.

(Kongress Ambient Assisted Living <4, 2011, Berlin>).

In: Demographischer Wandel - Assistenzsysteme aus der Forschung in den Markt. Berlin [u.a.]: VDE-Verl., 2011, Paper 4.1 [6 Bl.]

Grella, K.; Vogt, H.; Paschen, U.:

High temperature reliability investigations of EEPROM memory cells realised in Silicon-on-Insulator (SOI) technology.

(International Conference and Exhibition on High Temperature Electronics Network <2011, Oxford>).

HiTEN 2011. Washington, DC: IMAPS, 2011, pp. 238–242

Grey Oropeza, S.; Vom Bögel, G.; Meyer, F.; Grabmaier, A.:
Digital radio receiver for an UHF-RFID system with an undersampling digitalization scheme.

(RFID SystTech <7, 2011, Dresden>).

In: RFID SystTech 2011. Berlin [u.a.]: VDE-Verl., 2011, without pagination

Häfner, J.; Görtz, M.; Mokwa, W.:

Flexibles taktiles Sensorarray für Robotik- und Prothetik-anwendungen.

(Mikrosystemtechnik-Kongress <4, 2011, Darmstadt>).

In: Mikrosystemtechnik Kongress 2011. Berlin [u.a.]: VDE-Verl., 2011, pp. 358–361 [Paper 89]

Häfner, J.; Görtz, M. Mokwa, W.:

Tactile CMOS-based sensor array for applications in robotics and prosthetics.

(Sensor + Test <2011, Nürnberg>).

In: Sensor + Test Conference 2011.

Wunstorf: AMA Service GmbH, 2011

Hennig, A.; Vom Bögel, G.; Grabmaier, A.:

Sensortransponder-System zur Blutdruckmessung im Herzen.

(Design-&-Elektronik-Entwicklerforum Embedded Goes Medical <2011, München>).

In: Embedded goes medical. Poing: WEKA, 2011, without pagination [10 Bl.]

Hennig, A.; Vom Bögel, G.; Grabmaier, A.; Vogt, H.:

Telemetrisches Drucksensorsystem zur kontinuierlichen Blutdruckmessung im Herzen.

(WümeK <12, 2011, Würzburg>).

In: Kongress für Technologie in der Medizin und Energieeffizienz in Kliniken. Wetzlar: Euritim, 2011, pp. 53–60

Herbert, S.; Hochschulz, F.; Maryasov, A.; Danylyuk, S.:

Challenges of high-speed EUV mask blank inspection.

(WOCSDICE <35, 2011, Catania>).

In: WOCSDICE 2011. Catania: CNR IMM, 2011, pp.183–184

Hochschulz, F.; Dreiner, S.; Vogt, H.; Paschen, U.:

CMOS photodiodes for narrow linewidth applications.

(Conference on Sensors <10, 2011, Limerick>).

In: IEEE Sensors 2011.Piscataway, NJ: IEEE, 2011, pp. 1600–1603

Hochschulz, F.; Paschen, U.; Vogt, H.:

Multiphysics simulations for the optimisation of CMOS processes for high precision optical measurement applications.

(Fraunhofer Multiphysics Conference <1, 2010, Bonn>).

In: Multiphysics Simulations – Advanced methods for industrial engineering (2011), Special ed., pp. 239–249

Hochschulz, F.; Brockherde, W.; Vogt, H.; Paschen, U.:

Neue CMOS-Bildsensoren erweitern Einsatzmöglichkeiten.

In: Labor-Praxis 35 (2011), 5 , pp. 22–24

Klauke, S.; Görtz, M.; Rein, S.; Hoehl, D.; Thomas, U.;

Eckhorn, R.; Bremmer, F.; Wachtler, T.:

Stimulation with a wireless intraocular epiretinal implant elicits visual percepts in blind humans : results from stimulation tests during the EPIRET3 prospective clinical trial.

In: Investigative ophthalmology and visual science 52 (2011), 1, pp. 449–455

König, N.; Philipp, C.; Vom Bögel, G.; Hennig, A.:

Sensor-Transponder (RFID) für die Druck- und Temperaturüberwachung in Vakuum-Isolations-Paneelen (VIP) – Stand und Ausblick.

(Fachtagung Anwendung der Vakuumdämmung im Bauwesen <2011, Berlin>).

In: Fachtagung Anwendung der Vakuumdämmung im Bauwesen. Berlin, 2011, getr. Zählung ; [6] Bl.

- Lorenz, J. K.; Bär, E.; Clees, T.; Evanschitzky, P.; Jancke, R.; Kampen, C.; Paschen, U.; Salzig, C. P. J.; Selberherr, S.:
Hierarchical simulation of process variations and their impact on circuits and systems: results.
In: IEEE transactions on electron devices 58 (2011), 8, pp. 2227–2234
- Matheis, F.; Brockherde, W.; Grabmaier, A.; Hosticka, B. J.:
Modeling and calibration of 3D-Time-of-Flight pulse-modulated image sensors.
(European Conference on Circuit Theory and Design <20, 2011, Linköping>).
In: ECCTD 2011. Piscataway, NJ: IEEE [u.a.], 2011, pp. 426–429
- Müntjes, J.; Meine, S.; Görtz, M.; Mokwa, W.:
Aufbau- und Verbindungstechnik für intelligente Implantate am Beispiel eines Druckmesssystems für die Pulmonalarterie (COMPASS).
(Mikrosystemtechnik-Kongress <4, 2011, Darmstadt>).
In: Mikrosystemtechnik Kongress 2011.
Berlin [u.a.]: VDE-Verl., 2011, pp. 603–606 [Poster 4.26]
- Munstermann, M.; Luther, W.:
Automatic human autonomy assessment system.
(International Symposium on Ubiquitous Computing and Ambient Intelligence (UCAml) <5, 2011, Riviera Maya>).
In: UCAml 2011. Riviera Maya, 2011, without pagination; [4 Bl.]
- Scherer, K.; Schliepkorte, H.-J.:
Ambient Intelligence in Immobilien – Potenzial für neue Facility-Management-Nutzeffekte?
(Facility Management <2011, Frankfurt, Main>).
In: Facility Management 2011. Berlin [u.a.]: VDE-Verl., 2011
- Schmidt, A.; Marzouk, A. M.; Kappert, H.; Kokozinski, R.:
A robust SOI gain-boostered operational amplifier targeting high temperature precision applications up to 300 °C.
(International Conference and Exhibition on High Temperature Electronics Network (HiTEN) <2011, Oxford>).
In: HiTEN 2011. Washington, DC: IMAPS, 2011, pp. 238–242
- Sommer, S. P.; Paschen, U.; Figge, M.; Vogt, H.:
Light switched plasma charging damage protection device allowing high-field characterization.
In: IEEE transactions on device and materials reliability 11 (2011), 1, pp. 81–85
- Spickermann, A.; Durini, D.; Süß, A.; Ulfing, W.; Brockherde, W.; Hosticka, B. J.; Schwöpe, S.; Grabmaier, A.:
CMOS 3D image sensor based on pulse modulated Time-of-Flight principle and intrinsic lateral drift-field photodiode pixels.
(ESSDERC <41, 2011, Helsinki>).
In: ESSDERC ESSCIRC 2011. Piscataway, NJ: IEEE, 2011, pp. 111–114
- Stanitzki, A.; Marzouk, A. M.; Feldengut, T.; Kolnsberg, S.; Kokozinski, R.:
An 868 MHz passive temperature sensing transponder using a self-biasing UHF rectifier with –10.5 dBm sensitivity in low-cost 0.35 µm CMOS.
(Analog <12, 2011, Erlangen>).
In: ANALOG '11. Berlin [u.a.]: VDE-Verl., 2011, pp. 69–70 [Paper 12] (GMM-Fachbericht 70)
- Tavangaran, N.; Brückmann, D.; Feldengut, T.; Hosticka, B. J.; Kokozinski, R.; Konrad, K.; Lerch, R. G.:
Effects of jitter on continuous time digital systems with granularity reduction.
(EUSIPCO <19, 2011, Barcelona>).
In: EUSIPCO 2011. Barcelona, 2011, pp. 525–529

Urbaszek, A.; Görtz, M.; Traulsen, T.; Mokwa, W.; Schmitz-Rode, T.:

Implantable sensor for continuous pulmonary artery hemodynamic monitoring in heart failure patients (COMPASS).

(Biomedizinische Technik (BMT) <45, 2011, Freiburg>)

In: BMT 2011. Berlin [u.a.]: de Gruyter, 2011, without pagination (Biomedizinische Technik 56, Suppl. 1)

Utz, A.; Gendrisch, L.; Brögger, D.; Weiler, D.; Vogt, H.:

Bestimmung der NETD von Fern-Infrarot Imagern auf Wafer-Level unter Umgebungsdruck in der Serienproduktion.

(Mikrosystemtechnik-Kongress <4, 2011, Darmstadt>).

In: Mikrosystemtechnik Kongress 2011. Berlin [u.a.]: VDE-Verl., 2011, pp. 165–168 [Paper 37]

Utz, A.; Gendrisch, L.; Vogt, H.:

Simulating far-infrared scenarios with the radiance synthetic imaging system.

In: Computing in science & engineering 13 (2011), 4, pp. 98–103

Utz, A.; Gendrisch, L.; Weiler, D.; Kolnsberg, S.; Vogt, H.:

Simulation method for LWIR radiation distribution using a visual ray-tracer.

(NUSOD <11, 2011, Rom>)

In: NUSOD 2011. Piscataway, NJ: IEEE, 2011, pp. 57–58

Varga, G.; Süß, A.; Hosticka, B. J.:

A sequential method for noise estimation in switched-capacitor systems using a switching time-frequency domain.

(European Conference on Circuit Theory and Design <20, 2011, Linköping>).

In: ECCTD 2011. Piscataway, NJ: IEEE [u.a.], 2011, pp. 521–524

Vom Bögel, G.; Meyer, F.; Kemmerling, M.; Grabmaier, A.:

Radio frequency powering of microelectronic sensor modules.

(RFID SystTech <7, 2011, Dresden>).

In: RFID SystTech 2011. Berlin [u.a.]: VDE-Verl., 2011, without pagination

Vom Bögel, G.:

Self-sustaining sensor-transponders: a technology for cost-efficient realization for a multitude of applications.

(ID World <10, 2011, Milano>).

In: ID World 2011. Milano: Wise Media, 2011, without pagination

Vom Bögel, G.; Trieu, H.-K.; Görtz, M.; Grabmaier, A.:

Wireless integrated pressure sensor for quality control of vacuum insulation panel.

(International Vacuum Insulation Symposium (IVIS) <10, 2011, Ottawa>).

In: Vacuum insulation panels: advances in applications. Ottawa, 2011, pp. 22–26

Weiler, D.; Ruß, M.; Würfel, D.; Lerch, R. G.; Yang, P.; Bauer, J.; Heß, J.; Kropelnicki, P.; Vogt, H.:

Development of an uncooled 25 µm pixel-pitch VGA-IRFPA.

(Infrared Colloquium <40, 2011, Freiburg>).

In: 40th Freiburg Infrared Colloquium. Freiburg, 2011, Paper 5.2

Weiler, D.; Ruß, M.; Würfel, D.; Lerch, R. G.; Yang, P.; Bauer, J.; Kropelnicki, P.; Heß, J.; Vogt, H.:

A far infrared VGA detector based on uncooled microbolometers for automotive applications.

(International Forum on Advanced Microsystems for Automotive Applications (AMAA '11) <15, 2011, Berlin>).

In: Advanced Microsystems for Automotive Applications 2011. Berlin [u.a.]: Springer, 2011, pp. 327–334

Weiler, D.; Ruß, M.; Lerch, R. G.; Yang, P.; Bauer, J.; Heß, J.; Kropelnicki, P.; Vogt, H.:
Improvements of a digital 25µm pixel-pitch uncooled amorphous silicon TEC-less VGA IRFPA with massively parallel Sigma-Delta- ADC readout.
(Infrared Technology and Applications Conference <37, 2011, Orlando, Fla.>).
In: Infrared technology and applications XXXVII. Bellingham, Wash.: SPIE Press, 2011, pp. 80121F-1–80121F-7

Würfel, D.; Ruß, M.; Lerch, R. G.; Weiler, D.; Yang, P.; Vogt, H.:
An uncooled VGA-IRFPA with novel readout architecture.
In: Advances in radio science 9 (2011), pp. 107–110

3. Oral Presentations

Greifendorf, D.:
RFID in schwierigen Umgebungen.
Euro ID User Forum, Berlin, April 6, 2011

Grinewitschus, V.:
Energieeffizienz und Ambient Assisted Living als Treiber für die Gebäudesystemtechnik.
Messe Bau – Fachforum „Intelligent planen, errichten, nutzen“, München, January 19, 2011

Scherer, K.:
Ambient intelligence: neue Chancen für die Prozessoptimierung in Räumen und Gebäuden.
Elmos AG, Dortmund, June 16, 2011

Scherer, K.:
Intelligente Gebäude – Intelligente Stadt – Lebensräume der Zukunft?
BKU-Bundestagung, Aachen, October 8, 2011

Stevens, T.:
Assistenzsysteme für ältere Menschen mit Vergesslichkeit.
RehaCare Kongress, Düsseldorf, September 21, 2011

Stevens, T.:
Innovationspfade für das Krankenhaus der Zukunft.
Klinikkongress Ruhr, Dortmund, September 27, 2011

Vom Bögel, G.:
Chancen und Potenziale drahtloser Sensorik.
EC-Ruhr Workshop, Köln, February 2, 2011

4. Patents

4.1 Granted Patents

Boom, T. van den; Hosticka, B. J.; Trieu, H.-K.:
Vorrichtung und Verfahren zum geregelten Transport mikrofluidischer Proben.
September 22, 2011
DE102007018752 B4

Deiters, H.; Linnenberg, S.; Nachrodt, D.; Paschen, U.; Vogt, H.:
Thin-film resistor with a layer structure and method for manufacturing a thin-film resistor with a layer structure.
September 27, 2011
US8026788 B2

Durini Romero, D.; Brockherde, W.; Hosticka, B. J.:
Detektor und Verfahren zum Detektieren elektromagnetischer Strahlung und Computerprogramm zur Durchführung des Verfahrens.
January 13, 2011
DE102009020218 B3

Huppertz, J.; Hosticka, B. J.; Würfel, D.:

Device and method for detecting electromagnetic radiation.

February 8, 2011

US7884329 B2

Mokwa, W.; Trieu, H.-K.:

Endoskop zum Erfassen von optischen Bildinformationen an einem distalen Ende und zum Bereitstellen entsprechender elektronischer Bildinformationssignale an einem proximalen Ende :

May 5, 2011

DE102009036030 B3

Schrey, Olaf; Hosticka, Bedrich J.; Brockherde, W.:

Image sensor, method for operating an image sensor, and computer program using a time-delayed integration.

December 27, 2011

US8085327 B2

Schrey, Olaf; Hosticka, Bedrich J.; Brockherde, W.:

Detection of optical radiation using a photodiode structure.

May 24, 2011

US7947939 B2

Trieu, H.-K.; Wiebe, P.; Klieber, R.:

Apparatus and method for controlling and monitoring the pressure in pressure line or pipes.

September 6, 2011

US 8011250 B2

Trieu, H.-K.; Wiebe, P.; Klieber, R.:

Vorrichtung und Verfahren zur Kontrolle und Überwachung des Druckes in Druckleitungen bzw. Rohren.

March 16, 2011

EP2091596 B1

4.2 Laid Open Patent Documents

Hennig, A.; Vom Bögel, G.:

Antennenanordnung und Transponderlesegerät.

August 11, 2011

DE102010028993 A1

Hennig, A.; Vom Bögel, G.:

Antennenvorrichtung, Transponderlesegerät, Induktionsherd.

November 17, 2011

DE102010028992 A1

Hennig, A.; Vom Bögel, G.:

Passiver Transponder für ein RFID-System und Verfahren zum Übertragen von Daten von/zu einer Datenquelle eines solchen Transponders.

June 9, 2011

DE102010028991 A1

Marx, M.; Kokozinski, R.:

Vorrichtung und Verfahren zum Bestimmen eines Referenzempfangszeitpunkts eines Referenzsignals.

January 5, 2011

DE102009009693 A1

Spickermann, A.; Brockherde, W.; Hosticka, B. J.:

Konzept zur optischen Abstandsmessung.

March 2, 2011

EP2290393 A2

Spickermann, A.; Brockherde, W.; Hosticka, B. J.:

Konzept zur optischen Abstandsmessung.

May 12, 2011

DE102009037596 A1

Vogt, H.; Trieu, H.-K.; Goehlich, A.; Debusmann, K.:
Drucksensor und Verfahren zu dessen Herstellung.
October 27, 2011
DE102010028044 A1

5. Theses

5.1 Dissertations

Betz, W.:
Flexible mikroelektromechanische Implantate für den chronischen Einsatz: Verkapselungskonzepte und Testverfahren für die Materialcharakterisierung.
Duisburg, Essen, Univ., Diss., 2011

KiBler, S.:
Untersuchung einer neuen Methode zur Integration von angebundenen Doppellipidschichten in CMOS-Strukturen zur Realisierung bioelektrischer Sensoren.
Duisburg, Essen, Univ., Diss., 2011

Marx, M.:
Entwurf eines laufzeitbasierten Ortungssystems.
Duisburg, Essen, Univ., Diss., 2011

Utz, A.:
Entwicklung einer automatischen Testumgebung für FIR-Bauelemente
Duisburg, Essen, Univ., Diss., 2011

5.2 Diploma Theses

Deja, D.:
Aktivitätserkennung und Erinnerungsunterstützung in einer intelligenten Wohnumgebung.
Duisburg, Essen, Univ., Dipl.-Arb., 2011

Haese, A.:
Evaluating the effectiveness of an electronic memory assistant – Does the “InBad” decrease memory failure?
Düsseldorf, Univ., Dipl.-Arb., 2011

Kricke, B.:
Entwurf einer Datenbank zur automatischen Sicherung, Aufbereitung und Auswertung von Simulationsergebnissen am Fraunhofer Institut (IMS) Duisburg.
Bonn, Univ., Dipl.-Arb., 2011

Osenberg, Hendrik:
Konzeption und Implementierung eines Verfahrens zur Messdatenübertragung über mobiles Internet unter Verwendung Bluetooth angebundener Mobiltelefone.
Siegen, Univ., Dipl.-Arb., 2011

Yazici, N.:
Konzeption und Implementierung eines Sensorik-Moduls für ein mobiles Gleichgewichts-Trainingssystem zur Behandlung von Störungen des vestibulären Systems.
Gelsenkirchen, Fachhochschule, Dipl.-Arb., 2011

5.3 Master Theses

Blei, D.:

Konzeptionierung und Entwurf einer digital gesteuerten Trägerunterdrückung für UHF RFID Lesegeräte.

Krefeld, Hochsch., Master Thesis, 2011

Kotrache, Sami:

Aufbau und Weiterentwicklung eines Sensorsystems zur Erfassung von Vital- und Aktivitätsparametern im Bett.

Gelsenkirchen, Fachhochsch., Master Thesis, 2011

Li, X.:

Rauschcharakterisierung fortschrittlicher CMOS Bauelemente in einem 0,35 µm-Prozess.

Siegen, Univ., Master Thesis, 2011

Mocheva, B.:

Channel coding for a HF sensor transponder system in medical applications.

Duisburg, Essen, Univ., Master Thesis, 2011

Saxler, M.:

Konzeptionierung der Regelparameter und Realisierung eines Systems zur automatischen Trägerunterdrückung in RF Transceivermodulen und RFID Lesegeräten.

Duisburg, Essen, Univ., Master Thesis, 2011

Schubert, C.:

Entwicklung und Charakterisierung einer Funktionalisierung von Enzymelektroden mit Lactat Oxidase zur amperometrischen Bestimmung von Lactatkonzentrationen in biosensorischen Mikrosystemen.

Gelsenkirchen, Fachhochsch., Master Thesis, 2011

Subbiah, I.:

Design of a low noise bandgap reference circuit for image sensor applications.

Hamburg-Harburg, Techn. Univ., Master Thesis, 2011

Zhang, J.:

A SDR based receiver for a HF transponder reader and analysis of a symbol synchronisation technique.

Duisburg, Essen, Univ., Master Thesis, 2011

5.4 Bachelor Theses

Droste, D.:

Auswahl eines NMOS-Digital-Transistors für eine hochtemperatur taugliche 0,35µm SOI-Dünnschicht-Technologie.

Düsseldorf, Fachhochsch., Bachelor Thesis, 2011

Jakimovska, B.:

Analysis of thermal indoor comfort and building performance employing data mining concept with rapid miner toolset.

Duisburg-Essen, Univ., Bachelor Thesis, 2011

Kitanovski, S.:

Activity recognition in smart homes using ambient sensor technology.

Duisburg-Essen, Univ., Bachelor Thesis, 2011

Mehlich, M.:

Entwurf und Konzeptionierung eines FPGA basierten Signalverarbeitungsmoduls für Software-Defined-Radio basierte Transponder-Lesegeräte.

Krefeld, Hochsch., Bachelor Thesis, 2011

Salem, S. I. G. M:

Digital base-band signal synthesizer for a UHF transponder interrogator based on a FPGA platform.

Duisburg, Essen, Univ., Bachelor Thesis, 2011

Volkmer, C.:

Entwicklung eines Messprogramms für Hot Carrier Messungen an Feld-Effekt-Transistoren (MOSFET) auf Silicon-On-Insulator (SOI).

Düsseldorf, Fachhochsch., Bachelor Thesis, 2011

Vüllings, M.:

Entwicklung und Charakterisierung von Mikroelektroden in der Biosensorik für medizintechnische Anwendungen.

Remagen, Fachhochsch., Bachelor Thesis, 2011

Youssef, Z.:

Evaluierung von kryptographischen Verfahren zur authentifizierten Datenübertragung auf Mikrokontrollern mit begrenzter Rechenleistung.

Köln, Fachhochsch., Bachelor Thesis, 2011

6. Product Information Sheets

Biohybride Systeme – Wir bringen Biologie und Elektronik zusammen

IMS-Duisburg, 2011

Crash-Sensor erhöht Sicherheit in Lagerhallen

IMS-Duisburg, 2011

Drahtlose Fensterkontakte

IMS-Duisburg, 2011

Far Infrared Detektor for Thermal Imaging

IMS-Duisburg, 2011

IMS LS-3580 CMOS Linear Photosensor Array 1 x 3580 pixel

IMS-Duisburg, 2011

Ihr Weg zu innovativen MEMS-Bauteilen – Das IMS MST Lab&FAB

IMS-Duisburg, 2011

In-Situ-Sensorik für die Überwachung von Lithium-Polymer-Batterien

IMS-Duisburg, 2011

Neues Mikrosystemtechnik Lab&Fab

IMS-Duisburg, 2011

Universal Sensor for Allergens and Biomarkers

IMS-Duisburg, 2011

CHRONICLE 2011

Chronicle

Preis des Bundespräsidenten „Ort der Idee 2011“	98
The Opening of the new Microsystems Technology Lab	99
Messen Conlife and Rehacare	100
IVAM Round Table	101
The user Forum for Wireless Sensor Technology	102
Fairs and Exhibitions	103
inHaus-Forum 2011	104



PREIS DES BUNDESPRÄSIDENTEN „ORT DER IDEE 2011“

April 6, 2011: Fraunhofer-inHaus-Center Receives Award as “Ort im Land der Ideen 2011” for Its Inventiveness, Passion and Strength of Implementation

Since 2006, the initiative “Deutschland - Land der Ideen”, in cooperation with the Deutsche Bank and under the patronage of the Federal President, has been awarding 365 landmarks each year with the title “Ort im Land der Ideen” (trans.: “Landmark in the Land of Ideas”). An independent jury chooses those who show exceptional inventiveness, passion and strength of implementation.

Coinciding with the inHaus’s ten-year-anniversary in April, which was celebrated with more than 200 sponsors, partners and friends, the award underlines the inHaus-Center’s story of success. For ten years, Fraunhofer-inHaus-Center has been guided by the vision to jointly implement integrated room and building systems with strong application benefits.

*Professor Grabmaier and
Professor Vogt open the
MST Lab&Fab*



*from right to left:
Professor Buller,
Ministerin Schulze,
Professor Vogt,
Professor Grabmaier*

THE OPENING OF THE NEW MICROSYSTEMS TECHNOLOGY LAB & FAB

On June 22nd 2011 Mrs. Svenja Schulze, NRW-Minister for Innovation, Science and Research and Thomas Rachel, Parliamentary State Secretary, inaugurated the new Microsystems Lab&Fab. Many representatives from companies, scientific institutions and politics came to the opening ceremony in order to congratulate and to learn more about the high-tech opportunities which open the way for innovative products.

"In our already existing labs we firstly manufacture the CMOS-Chips, which contain the whole electronic of the sensors", explains Prof. Dr. Holger Vogt, deputy director of the IMS and now director of the MST-Lab. "These CMOS-Chips then will be extended by the sensory functions, for example by elements which detect the heat radiation". The application fields of e.g. bolometers are widely spread: concerned parents could measure contact-free the body temperature of their febrile children without waking them up. In factory buildings bolometers can monitor facilities in the production line: Are there areas which become too hot? And could these high temperatures point to

defective areas? In the car, the sensors can extend the driver assistance systems by the detection of the heat radiation of pedestrians and animals.

The new lab enables the scientists to work with a variety of materials, for example biological protective layers could be deposited. These layers can be deposited on pressure sensors which can be implanted in the human body without causing a rejection. This is helpful for patients who are exposed to a higher risk of heart attack. If the cardiac pressure rises up, the sensor perceives it and the patient is able to take timely some pharmaceuticals or to alarm the doctor.

Bioactive layers on CMOS, which react highly specific with analytes, are the basis for sensitive bio sensors that e.g. can detect markers in the blood, which point to diseases. With the start of the new Lab, Fraunhofer IMS plans to considerably enlarge this forward-looking topic.



CONLIFE AND REHACARE

Fraunhofer-inHaus-Center as Fair Exhibitor at the ConLife Cologne and the REHACARE 2011

The market for home networking systems and connected lifestyles has been gaining importance. This trend was also evident at the ConLife in Cologne, June 29 to June 30, 2011, a technical exhibition focussing on the areas of consumer electronics, ambient assisted living and energy efficiency. Fraunhofer-inHaus-Center took part as an exhibitor with a large joint stand, presenting different projects concerning ambient assisted living and energy efficiency. Furthermore, Prof. Dr. Viktor Grinewitschus (Management Fraunhofer-inHaus-Center, Technology & Innovation) participated in the opening plenary on “Connected Life as a Global Market - Germany’s position in 2011”.

This year’s REHACARE, September 21 to September 24, 2011, offered experience reports, practical examples, current scientific insights and a broad selection of products and services

with a focus on “Self-determined Living and Care at Home”. The business area Health and Care of Fraunhofer-inHaus-Center participated as an exhibitor with a large stand of 50 m². In cooperation with Fraunhofer IMS, Fraunhofer, ISST, Pressalit, Mauser, Villeroy & Boch and Sozialwerk St. Georg, it presented assistance systems for a safe and self-determined life at home later in life. Besides various solutions for bathrooms (viClean shower-toilet-combination (“washlet”), a height-adjustable toilet, a stretcher for shower and care support, the plunge-detecting shower Squaro and the inBath), the project JUTTA as well as the Daily Care Journal (IT-supported documentation tool for care networks) were presented to the public. In addition, three employees of Fraunhofer IMS and the business area Health and Care participated in the series of lectures on “Living safely and conveniently at Home”.



IVAM ROUND TABLE

On February 10th the IVAM-RoundTable took place at the Fraunhofer IMS with approximately 40 participants from research and industry. The RoundTable gave the opportunity to get information about latest developments in the field of CMOS technology. Amongst others, manufacturing solutions which make it possible to process CMOS Wafer on top by Postprocessing have been presented. By adding further layers, structures or devices like additional chips (FlipChip Technology) novel integrated sensor solutions become real. These are applicable e.g. in medical engineering where smallest pressure sensors can be implanted in various parts of the human body.

Another aspect was the use of ICs in rough environments as they are used in automotive and aerospace engineering. Special CMOS production processes enable the use of devices at temperatures up to 250 °C or with voltages up to 600 V. With a following clean room tour the participants gained insight into the high-tech lines of the institute which are able to produce more than 70,000 wafers per year on a surface of 1300 m². Additionally, the participants visited the inHouse Innovation Centre areas SmartHome and SmartBuilding where they experienced new system solutions for rooms and buildings.



THE USER FORUM FOR WIRELESS SENSOR TECHNOLOGY

The user forum for wireless sensor technology in industry and logistics brought together partners from industrial application and from research and development for an exchange of information and experiences.

Transponder systems – especially sensor transponder systems – and sensor networks offer an excellently applicable technological basis for the wireless collection of identification and sensor data. Especially in such application fields in which – because of technical or economic reasons – wired sensory technology is not practicable or even impossible e.g. at rotating machine

pieces. By wireless communication and energy supply new application fields open up. Furthermore, wireless technologies can be used in the locating of mobile objects e.g. in storage or in the controlling of transport processes.

Recent research and development results were presented by lectures and demonstrations which afforded the opportunity for discussions and prospective cooperations. In his speech Dr. vom Bögel pointed out the importance and possibilities of Fraunhofer sensor transponders for logistics and quality control.



FAIRS AND EXIBITIONS

It is a long lasting tradition at Fraunhofer IMS to take part in well-known trade fairs. We take these opportunities to strengthen existing alliances and to establish new contacts and to bridge the gap between science and industry. This year we presented our latest research results and projects at the following fairs: the Euro ID in Berlin, the Sensor + Test in Nürnberg, the Laser in München and the Vision in Stuttgart.

The **Euro ID** is the international trade fair and science forum for new trends in the automatic identification. The department "Transponder Systems and Sensor Networks" demonstrated it's Crash Sensor which raises the security in warehouses. Furthermore we showed a new method which gives information on the periodic maintenance of machines and last but not least we presented a method to measure humidity by wireless transponders and sensor nodes.

The **Sensor + Test** in Nürnberg again attracted numerous visitors and company representatives. Fraunhofer IMS was represented by the departments "Circuit Design and Wireless Systems", "Transponder Systems and Sensor Networks" and "Integrated Actuators and Sensors".

The **Laser World of Photonics** in München is the world's leading trade fair for the laser and photonics sector and focuses on optical technologies. As in the years before Fraunhofer IMS took part and presented its new CMOS image sensors, infrared sensors and X-ray detectors.

The **VISION** in Stuttgart is an annual fair which focuses on machine vision technologies. It attracts numerous representa-

tives of companies belonging to the automotive, medical and consumer sector. Fraunhofer IMS demonstrated its 3D CMOS-camera, the application specific CMOS image sensors and the outstanding uncooled far infrared sensors.

Fraunhofer IMS participated at the stand of the Fraunhofer Microelectronics Alliance during the **SEMICON** in Dresden. Fraunhofer IMS presented its services with regard to semiconductor processes which require stability and know-how.

At the congress on **High Temperature Electronics** which took place in Essen specialists from research and industry discussed on new technologies and application fields for High Temperature electronics. On the stand Fraunhofer IMS presented the technology for integrated circuit design for High Temperature Applications up to 250°C. These ASICs and Standard-ICs suit for harsh environments which are to be found in the following applications: Oil & gas exploration, Geothermal Energy, Aerospace, Process control, Power Electronics and Automotive.

The **Nano-Conference** in Dortmund underlined the important role of nanotechnology in the key sectors: energy management, mobility and health. Fraunhofer IMS as developer of microelectronic and microsystems technologies plays an important role with regard to new systems and products which enable us to live healthier, more environmental friendly and energy-saving. Fraunhofer IMS showed transponder systems and sensor networks for different applications.



INHAUS-FORUM 2011

November 10, 2011: Fraunhofer-inHaus-Forum 2011 “Energy Turnaround in Buildings – Trends and Solutions for Energy Systems of the Future”

Currently, our buildings consume – and, thus, also waste – about 40 per cent of all primary energy, which is far more than in any other segment. Current research, new developments and pilot projects aim at an economical implementation of the newest findings. Fraunhofer-inHaus-Center and its partners have been taking a share in this development since 2001, contributing new material, innovative technical building equipment and integral coordination of application processes and services.

This year’s Fraunhofer-inHaus-Forum, organized in cooperation with the initiative win² of the Lower-Rhenish Chamber of

Industry and Commerce (IHK) provided information on this up-to-date topic. 160 participants listened to lectures researchers had prepared with special reference to the field of energy efficiency. Keynotes by well-known representatives of the field framed the event. The day ended in a panel discussion of leading experts.

As it has become common to the establishment of the inHaus-Forum, visitors had the chance to take a look at the laboratories. Further insights into the six business areas and their research focus were offered in the form of screens installed throughout the publicly accessible exhibition area.

PRESS REVIEW

Neue Form der Laufzeit-Messung

3D-Time-of-Flight-Technologie mit indirektem Pulslaufzeit-Verfahren

In unserer dreidimensionalen Welt müssen Sensor-Systeme zukünftig in der Lage sein, alle drei Dimensionen zu erfassen - und zwar in Echtzeit. Das ermöglichte jetzt neuartige 3D-Bildsensoren auf Basis der Time-of-Flight-Technologie. Ein patentiertes Pulslaufzeit-Verfahren vermeidet zudem Mehrdeutigkeiten und unterdrückt störendes Hintergrundlicht.

3D-Messsysteme können helfen für jeden Punkt eines 3D-Gegenstands ein 3D-Kamera gehen einen Schritt weiter und liefern zudem Tiefeninformationen für jeden Punkt oder für bestimmte Punkte im Raum. Die Qualität der Tiefeninformationen hängt dabei vom gewählten 3D-Messverfahren ab. Welches Messverfahren angewendet wird, bestimmt die Kundenanwendung. Das Spektrum der 3D-Messverfahren ist groß: Es reicht von Triangulationsverfahren wie Stereokameras oder Stereobildsensoren über Radar und Ultraschall bis hin zu optischen Time-of-Flight-Verfahren.

Triangulations-Verfahren
Klassische Triangulationsverfahren für das Nahbereich liefern sehr genaue Messungen im Millimeterbereich. Sie arbeiten sehr gut bei bekannten Lichtverhältnissen. Bei wechselnden Umgebungslichtbedingungen können jedoch Ungenauigkeiten in der Messung auftreten. Meist werden geometrische Beobachtungen wie Laserlinien in Kombination

mit anderen Sensoren gleicher Bauart verwendet. Ein großer Vorteil bei Radar ist die weitgehende Unempfindlichkeit gegenüber Schmutz, Schnee, Regen, in denen die Messung zur Abgrenzung zu Wetterbewerten unterstützt werden soll, sind immer über ein physikalisches Gitternetz der Verfahren. Die Tiefenmessung kann bei ähnlichen Bedingungen unter 1 cm liegen.

Time-of-Flight-Verfahren
Optische Time-of-Flight (ToF)-Technologien stellen einen in der nahen Zukunft sehr wichtigen Zweig von 3D-Messverfahren dar. Die Verfahren sind günstig, einfach zu integrieren, innovativ und in sehr vielen Anwendungen einsetzbar. Drei Time-of-Flight-Verfahren in vierer Sensoren und Kundenanwendungen Verwendung:
Continuous-Wave (CW)-Verfahren, direkter Pulsverfahren, indirekter Pulsverfahren von TriDCam.

In der Praxis kann die Tiefenmessung daher anwendungspassend unter 1 cm liegen.

sich mehrere Sensoren gleicher Bauart verwenden. Ein großer Vorteil bei Radar ist die weitgehende Unempfindlichkeit gegenüber Schmutz, Schnee, Regen, in denen die Messung zur Abgrenzung zu Wetterbewerten unterstützt werden soll, sind immer über ein physikalisches Gitternetz der Verfahren. Die Tiefenmessung kann bei ähnlichen Bedingungen unter 1 cm liegen.

Indirekter Pulsverfahren
Die Besonderheit der TriDCam-Sensoren ist das patentierte, einseitige Verfahren der Time-of-Flight-Messung, einem einseitigen, indirekten Pulsverfahren und die Produktion in einem ersten CMOS-Prozess. Die hohe Ausbeuteerbringung des TriDCam-Zellenarrays machte viele Applikationen möglich.

Abbildung 1 zeigt die Prinzip-Skizze einer TriDCam Time-of-Flight-Messung. Ein einzelnes Lichtpulss wird auf das zu messende Objekt geschossen. Nach einer Zeit T zurück kehrt der Puls zum Sensor zurück und wird dort mit zwei Integrationskammern gleichzeitig

CMOS-Sensoren lernen Blau zu sehen

CMOS-Chips sind in manchen Bereichen farbenblind, das ihre Schicht lässt UV-Licht nicht durch. Ein neuer Fertigungsprozess erlaubt Forscher des Fraunhofer-Instituts für Mikroelektronische Schaltungen und Systeme IMS verschiedene Arten, macht die Schicht transparent - und die Sensoren für Spezialanwendungen tauglich.



KonstruktionsPraxis, März 2011

Bei dem neuen Fertigungsprozess wird die Schutzschicht in den Schichten entfernt. Damit benötigt das Licht oder Infrarot Energie in der UV-Licht, um vom Material abstrahlt zu werden - der Sensor im Bereich für das blaue und das UV-Bereich transparent gemacht. Mit dieser Strukturierung können vor allem UV-geladene optische Methoden revolutionieren. (Infrastruktur-Gesellschaft, Tel. +49(0)281 13055)

Nachtsichtgeräte für jedermann

Spezialer der Fraunhofer-Gesellschaft sollen neue Infrarotsensoren sein

Infrarotsensoren sehen heute mehr als sonst: Jege, denn die letzten Weiterentwicklung ermöglichen, bei denen der empfindliche Schicht muss jedoch der Sensor geteilt werden. Fraunhofer-Ingenieure haben nun einen Baustein entwickelt, der bei Zimmertemperaturen arbeitet.

Einmal, heute, und eine in mehreren Varianten. Die Leistungsfähigkeit ist ein weiterer Schritt, um die Leistungsfähigkeit zu erhöhen. Die Leistungsfähigkeit ist ein weiterer Schritt, um die Leistungsfähigkeit zu erhöhen.

Die Leistungsfähigkeit ist ein weiterer Schritt, um die Leistungsfähigkeit zu erhöhen. Die Leistungsfähigkeit ist ein weiterer Schritt, um die Leistungsfähigkeit zu erhöhen.

Die Leistungsfähigkeit ist ein weiterer Schritt, um die Leistungsfähigkeit zu erhöhen. Die Leistungsfähigkeit ist ein weiterer Schritt, um die Leistungsfähigkeit zu erhöhen.

Die Leistungsfähigkeit ist ein weiterer Schritt, um die Leistungsfähigkeit zu erhöhen. Die Leistungsfähigkeit ist ein weiterer Schritt, um die Leistungsfähigkeit zu erhöhen.

Die Leistungsfähigkeit ist ein weiterer Schritt, um die Leistungsfähigkeit zu erhöhen. Die Leistungsfähigkeit ist ein weiterer Schritt, um die Leistungsfähigkeit zu erhöhen.

Die Leistungsfähigkeit ist ein weiterer Schritt, um die Leistungsfähigkeit zu erhöhen. Die Leistungsfähigkeit ist ein weiterer Schritt, um die Leistungsfähigkeit zu erhöhen.

INSPECT, Juni 2011

Mehr Durchblick dank Infrarot

Bisher mussten Sensoren ständig aufwendig gekühlt werden / Jetzt reicht sogar die Raumtemperatur

Infrarotkameras sehen mehr als die bloße Auge und können beispielsweise den Wärmehaushalt sicherer machen. Bei Kameras für den humanen Infrarotbereich muss die Sensor jedoch ständig gekühlt werden, was aufwendig und kostspielig ist. Ein neuartiger Detektor funktioniert nun auch bei Raumtemperatur.

Nachteile unterwegs auf der selbstbestimmten Landstraße. Die hier vige Strecke ist schwer einsehbar, auch dass es so toll. Demnach entsprechend vornehmlich über der Autofahrt - und nicht die Rolle auf der Straße dennoch ist, als es fast so gut ist. Mit einer Vollbremsung verbunden es im besten Moment eines Zwischenfalls mit dem Tier, Infrarotkameras können so für mehr Sicherheit sorgen. Diese Objekte, die empfindliche Körperempfinden haben, brauchen im besten Fall einen Wellenlängenbereich von 10 Mikrometern von sich aus. Detektoren in der Kamera nehmen diese Wärmestrahlung auf und übersetzen sie in Wärmebilder. Dadurch können der Fahrer Menschen oder Tiere erkennen, lange bevor die Augenblicke sie erfassen. Andere Verkehrsteilnehmer werden durch die unabhangige Infrarotstrahlung nicht beeinflusst.

Das Problem Infrarotkameras für den Wellenlängenbereich oberhalb von fünf Mikrometern liegt an Infrarot - der Sensor muss ständig auf etwa minus 193 Grad Celsius heruntergekühlt werden. Zwar gibt es auch heute schon gekühlte Infrarot für den humanen Infrarotbereich, allerdings werden diese überwiegend im militarischen Bereich eingesetzt und sind am europaischen Markt kaum verfügbar. Das will sich ändern. Forschern aus dem Fraunhofer-Institut für Mikroelektronische Schaltungen und Systeme IMS in Duisburg ist es gelungen, einen selbstkühlenden Sensor für den humanen Infrarotbereich zu fertigen, der bei Raumtemperatur funktioniert. „Der Durchblick wissen wir die neuen, die eine solche Technologie anerkennen“, sagt Dr. Erik Weiler, Wissenschaftler am IMS.

Insbesondere der IMEPA-Sensoren (Active Pixel Array) ist ein Mikrosensoren - ein temperaturunempfindlicher Detektor, der langwelliges Infrarotlicht absorbiert. Um ein zweidimensionales Bild zu erzeugen, sind mehrere Mikrosensoren zusammengefasst. Nimm man ein Mikrosensoren Licht von einer Wärmequelle auf, führt das zu einem Temperaturanstieg in seinen Bereich

und ändert seinen elektrischen Widerstand. Ein Ausdehnung wandelt dieses Widerstandsänderung dann direkt in ein elektrisches Signal um. Auch das war bisher nicht ohne einen weiteren Zwischenschritt möglich. Normalerweise wandelt der elektrische Impuls zuerst in ein analoges Signal über und anschließend mit Hilfe eines Komparators digitalisiert.

„Wir setzen bei unserem Infrarot einen ganz spezifischen Konverter, einen Sigma-Delta-Wandler, ein. So ist es möglich, direkt ein digitales Signal zu erzeugen“, erklärt Wissenschaftler Dr. Dirk Weiler. „Da die empfindlicher und kostengünstiger Kaltung nicht mehr nötig ist, eröffnet sich weitere Anwendungsmöglichkeiten. „Vor allem im Bereich von mehreren Centimeter stufen sich einen best“, ist Weiler sicher. Denn ohne Kaltung können sich nicht nur nur Camcorder sparen. Auch die Automobilindustrie und die Luftfahrtindustrie sind wichtige Bereiche für die Kaltung wegfällt. Ein patentiertes Einzelobjekt für mobile Infrarotkameras ist der Baustein, etwa ein verstellbarer Infrarot-empfangs- oder -emissions- in verschiedenen Geometrien zu realisieren.

Hannu-Post, Mai 2011

Saarbrücker Zeitung, März 2011

Fraunhofer IMS liefert die CMOS-Fertigungsprozesse an einer neuen Prozesslinie

UV-transparente Schutzschicht für CMOS-Bildsensoren

CMOS-Bildsensoren sind in manchen Bereichen farbenblind, was an ihrer Schutzschicht liegt. Die UV-Licht nicht durchlassen. Ein neuer Fertigungsprozess macht die Schutzschicht transparent - und die Sensoren für Spezialanwendungen tauglich.

Die Leistungsfähigkeit ist ein weiterer Schritt, um die Leistungsfähigkeit zu erhöhen. Die Leistungsfähigkeit ist ein weiterer Schritt, um die Leistungsfähigkeit zu erhöhen.

Die Leistungsfähigkeit ist ein weiterer Schritt, um die Leistungsfähigkeit zu erhöhen. Die Leistungsfähigkeit ist ein weiterer Schritt, um die Leistungsfähigkeit zu erhöhen.

Die Leistungsfähigkeit ist ein weiterer Schritt, um die Leistungsfähigkeit zu erhöhen. Die Leistungsfähigkeit ist ein weiterer Schritt, um die Leistungsfähigkeit zu erhöhen.

Die Leistungsfähigkeit ist ein weiterer Schritt, um die Leistungsfähigkeit zu erhöhen. Die Leistungsfähigkeit ist ein weiterer Schritt, um die Leistungsfähigkeit zu erhöhen.

Die Leistungsfähigkeit ist ein weiterer Schritt, um die Leistungsfähigkeit zu erhöhen. Die Leistungsfähigkeit ist ein weiterer Schritt, um die Leistungsfähigkeit zu erhöhen.

Die Leistungsfähigkeit ist ein weiterer Schritt, um die Leistungsfähigkeit zu erhöhen. Die Leistungsfähigkeit ist ein weiterer Schritt, um die Leistungsfähigkeit zu erhöhen.

Markt und Technik, März 2011



Maschinen mit Köpfchen

Mehrere Tausend in der Produktion arbeitende Maschinen für die Weiterentwicklung smarterer Fertigungsanlagen sorgen für intelligente, vernetzte Maschinen und effiziente, energieoptimierte Produktion.

Das Experimentierfeld auf dem Dornwerder Flugplatz findet am 23. Mai im Rahmen der MST-Regionalkonferenz von 10 bis 12. Oktober an der Messe (Pav.) Geschäftsleiter der Mittelschulen (Pav.), Geschäftsleiter der Mittelschulen (Pav.) und System (Pav.) werden für 1000 Karten haben werden im Handy.

Die Verbindung von IT-Lösungen, Highspeed-Produktion und Mikrosystemtechnik ist die Zukunftsfähigkeit für zahlreiche Anwendungen, insbesondere in der Fertigungstechnik. Diese Fertigungstechnik kann heute nicht ohne die intelligente Vernetzung und Steuerung der Prozesse in ein intelligentes, vernetztes Produktionssystem sein. Prof. Helmut Vogt vom Fraunhofer-Institut für Mikroelektronische Schaltungen und Systeme (IME) vertritt die Dornwerder Unternehmensgruppe.

Prof. Helmut Vogt und Prof. Dr. Ingrid Isenhardt präsentieren IT-Lösungen für die Produktion. Das 5. MST-Regionalforum wird von der Dornwerder Unternehmensgruppe im Rahmen der Produktion der MST-Region durchgeführt. Das komplette Programm und weitere Informationen unter www.stm-technik.de/veranstaltungen.

Ruhr Nachrichten, Mai 2011

Forschung an Zukunftsvisionen

Das Fraunhofer-Institut eröffnet ein neues Reinheitslabor. Gut geschützt vor kleinsten Staubpartikeln kann dort an Mikrochips geforscht werden. Bis Ende 2012 sollen insgesamt 16 Millionen Euro in das Projekt fließen.

Das Fraunhofer-Institut für Mikroelektronische Schaltungen und Systeme (IME) in Duisburg hat ein neues Reinheitslabor eröffnet. Das Labor ist für die Herstellung von Mikrochips für die Automobilindustrie und die Halbleiterindustrie geeignet. Das Labor ist für die Herstellung von Mikrochips für die Automobilindustrie und die Halbleiterindustrie geeignet. Das Labor ist für die Herstellung von Mikrochips für die Automobilindustrie und die Halbleiterindustrie geeignet.



Das neue Reinheitslabor des Fraunhofer-IME in Duisburg. Von links: Prof. Dr. Ingrid Isenhardt, Prof. Dr. Helmut Vogt, Prof. Dr. Ingrid Isenhardt, Prof. Dr. Helmut Vogt, Prof. Dr. Ingrid Isenhardt, Prof. Dr. Helmut Vogt.

Rheinische Post, Juni 2011

Kleine Teile leisten Großes

Fraunhofer-Institut eröffnet neues Reinheitslabor für 16 Mio Euro. Halbleitertechnik: Teilchen für Auto in Arbeit

Im Jahr 2011 wird ein neues Reinheitslabor für die Halbleitertechnik eröffnet. Das Labor ist für die Herstellung von Mikrochips für die Automobilindustrie und die Halbleiterindustrie geeignet. Das Labor ist für die Herstellung von Mikrochips für die Automobilindustrie und die Halbleiterindustrie geeignet.

Das neue Reinheitslabor des Fraunhofer-IME in Duisburg. Das Labor ist für die Herstellung von Mikrochips für die Automobilindustrie und die Halbleiterindustrie geeignet. Das Labor ist für die Herstellung von Mikrochips für die Automobilindustrie und die Halbleiterindustrie geeignet.

Das neue Reinheitslabor des Fraunhofer-IME in Duisburg. Das Labor ist für die Herstellung von Mikrochips für die Automobilindustrie und die Halbleiterindustrie geeignet. Das Labor ist für die Herstellung von Mikrochips für die Automobilindustrie und die Halbleiterindustrie geeignet.

NRZ Duisburg, Juni 2011

Forschung an Zukunftsvisionen

Das Fraunhofer-Institut eröffnet ein neues Reinheitslabor. Gut geschützt vor kleinsten Staubpartikeln kann dort an Mikrochips geforscht werden. Bis Ende 2012 sollen insgesamt 16 Millionen Euro in das Projekt fließen.

Das Fraunhofer-Institut für Mikroelektronische Schaltungen und Systeme (IME) in Duisburg hat ein neues Reinheitslabor eröffnet. Das Labor ist für die Herstellung von Mikrochips für die Automobilindustrie und die Halbleiterindustrie geeignet. Das Labor ist für die Herstellung von Mikrochips für die Automobilindustrie und die Halbleiterindustrie geeignet.

Das Fraunhofer-Institut für Mikroelektronische Schaltungen und Systeme (IME) in Duisburg hat ein neues Reinheitslabor eröffnet. Das Labor ist für die Herstellung von Mikrochips für die Automobilindustrie und die Halbleiterindustrie geeignet. Das Labor ist für die Herstellung von Mikrochips für die Automobilindustrie und die Halbleiterindustrie geeignet.

Das Fraunhofer-Institut für Mikroelektronische Schaltungen und Systeme (IME) in Duisburg hat ein neues Reinheitslabor eröffnet. Das Labor ist für die Herstellung von Mikrochips für die Automobilindustrie und die Halbleiterindustrie geeignet. Das Labor ist für die Herstellung von Mikrochips für die Automobilindustrie und die Halbleiterindustrie geeignet.

Rheinische Post, Juni 2011

Mikrosysteme künftig "made in Duisburg"

Mikrosystemtechnik: Wärmesensoren, Drucksensoren im Gehirn, Schaltstellen für aktive Prothesen - im neuen Mikrosystemtechnik-Labor des Fraunhofer-Instituts für Mikroelektronische Schaltungen und Systeme IME in Duisburg werden Forscher künftig eine Vielzahl an Materialien verarbeiten und elektronischer Komponenten aus verschiedenen Sensorkonstruktionen erweitern.

VDI Nachrichten, Duisburg, 1.7.11, 11.

Das Fraunhofer-Institut für Mikroelektronische Schaltungen und Systeme (IME) in Duisburg hat ein neues Reinheitslabor eröffnet. Das Labor ist für die Herstellung von Mikrochips für die Automobilindustrie und die Halbleiterindustrie geeignet. Das Labor ist für die Herstellung von Mikrochips für die Automobilindustrie und die Halbleiterindustrie geeignet.

Das Fraunhofer-Institut für Mikroelektronische Schaltungen und Systeme (IME) in Duisburg hat ein neues Reinheitslabor eröffnet. Das Labor ist für die Herstellung von Mikrochips für die Automobilindustrie und die Halbleiterindustrie geeignet. Das Labor ist für die Herstellung von Mikrochips für die Automobilindustrie und die Halbleiterindustrie geeignet.

Das Fraunhofer-Institut für Mikroelektronische Schaltungen und Systeme (IME) in Duisburg hat ein neues Reinheitslabor eröffnet. Das Labor ist für die Herstellung von Mikrochips für die Automobilindustrie und die Halbleiterindustrie geeignet. Das Labor ist für die Herstellung von Mikrochips für die Automobilindustrie und die Halbleiterindustrie geeignet.

Das Fraunhofer-Institut für Mikroelektronische Schaltungen und Systeme (IME) in Duisburg hat ein neues Reinheitslabor eröffnet. Das Labor ist für die Herstellung von Mikrochips für die Automobilindustrie und die Halbleiterindustrie geeignet. Das Labor ist für die Herstellung von Mikrochips für die Automobilindustrie und die Halbleiterindustrie geeignet.

Das Fraunhofer-Institut für Mikroelektronische Schaltungen und Systeme (IME) in Duisburg hat ein neues Reinheitslabor eröffnet. Das Labor ist für die Herstellung von Mikrochips für die Automobilindustrie und die Halbleiterindustrie geeignet. Das Labor ist für die Herstellung von Mikrochips für die Automobilindustrie und die Halbleiterindustrie geeignet.

Das Fraunhofer-Institut für Mikroelektronische Schaltungen und Systeme (IME) in Duisburg hat ein neues Reinheitslabor eröffnet. Das Labor ist für die Herstellung von Mikrochips für die Automobilindustrie und die Halbleiterindustrie geeignet. Das Labor ist für die Herstellung von Mikrochips für die Automobilindustrie und die Halbleiterindustrie geeignet.

VDI Nachrichten, Juli 2011

CMOS-Sensoren und Mikrolinsen machen 3-D-Blick ins Körperinnere möglich

Fraunhofer-Forscher können mit CMOS-Bildsensoren und speziellen Mikrolinsen in den menschlichen Körper blicken. Mit diesem System sollen künftig chirurgische Eingriffe präziser erfolgen.

Ein Chirurg ist darauf angewiesen, präzise in das Innere des menschlichen Körpers vorzudringen. Dank moderner Endoskope ist es möglich, auf große Schritte zu verzichten.

Dabei hilft eine 3-D-Optik und ein spezieller Bildsensor, der einen perfekten Tiefeneindruck des Körperinneren ermöglicht.

Den perfekten 3-D-Blick ins Körperinnere haben Forscher des Fraunhofer-Instituts für Mikroelektronische Schaltungen und Systeme IMS in Duisburg zusammen mit dem Projektpartner im EU-Projekt «Minisurg» entwickelt.

CMOS-Bildsensoren wie in Spiegelreflexkameras

Während bisher nur CCD-Bildsensoren mit einer geringen Auflösung zur Verfügung standen, ist es jetzt dem Wissenschaftlern gelungen, CMOS-Bildsensoren, die beispielsweise auch in Spiegelreflexkameras verbaut sind, für diese Spezialanwendung tauglich zu machen.

Dazu haben die Forscher spezielle Mikrolinsen entwickelt. Über jeweils zwei Spalten des Sensors, auf denen die Pixel angeordnet sind, ist eine zylindrische Mikrolinse angebracht. Über ein

davorliegendes Objektiv fällt das Licht auf die Linse, die es auf die Pixel bündelt.

Die Besonderheit dabei ist, dass das Objektiv zwei Blendenöffnungen hat. Diese funktionieren ähnlich wie das rechte und das linke Auge.

Stereoskopie beim CMOS-Sensor

Mit anderen Worten: Zwei Lichtstrahlen fallen auf die Linse. Das Licht des «linken Auges» fällt von links ein und wird auf die rechte Sensorspalte gebündelt, und umgekehrt. Unterhalb der Linse kreuzen sich die beiden Lichtstrahlen.

Das Ergebnis: Wie das Gehirn die Daten vom linken und rechten Auge verarbeitet, erhält der CMOS-Sensor zwei verschiedene Bildinformationen. Eine Software rechnet diese auseinander und verarbeitet sie getrennt. Je nach System bekommt der Arzt dann den dreidimensionalen Eindruck direkt auf dem Bildschirm zu sehen, oder aber er nutzt eine Polarisationsoberfläche.

Spezielle Mikrolinsen bündeln die Lichtstrahlen

Damit die Lichtstrahlen präzise auf den Sensor gebündelt werden, sind spezielle

Mikrolinsen notwendig. Vor deren Herstellung berechneten die Fraunhofer-Ingenieure zunächst die optimale Form mit Hilfe von Simulationen.

Das war notwendig, um Störlichter zu eliminieren. So muss die Linse etwa garantieren, dass rechter und linker Kanal scharf voneinander getrennt sind. Das heißt, dass nicht mehr als fünf Prozent von einem Lichtstrahl auf den Sensorspalt des anderen Kanals einfallen die Experten nennen das «Übersprechen».

Chip mit einem Durchmesser von 7,8 mm

Anschließend passten die Forscher die üblichen Herstellungsverfahren für Mikrolinsen an die errechnete Linseform an. Zudem mussten sie bei der Fertigung der Miniatürkameras bestimmte Anforderungen erfüllen.

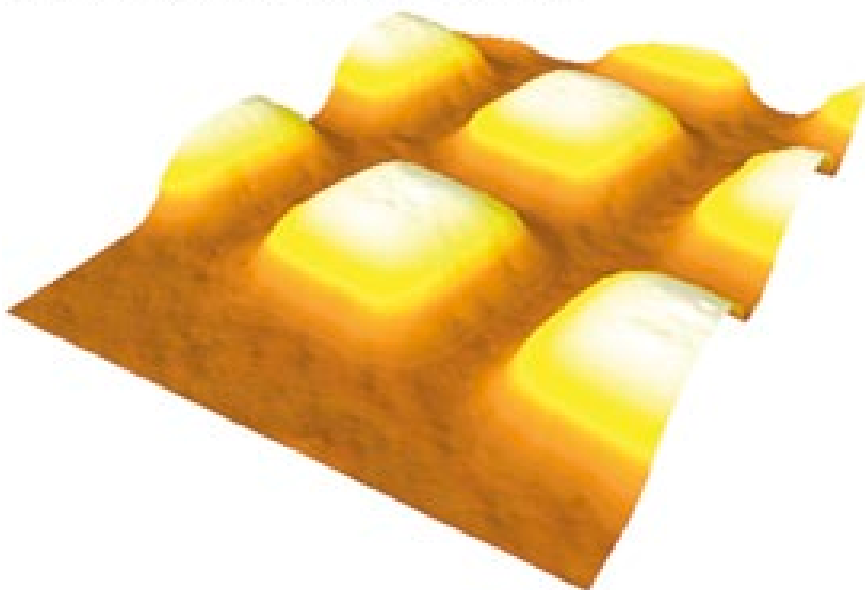
Mit Erfolg: Der Chip ist so winzig, dass er in ein Rohr von gerade mal 7,8 mm Durchmesser passt. Zusammen mit dem Glasfaserbündel, das als Lichtquelle dient, misst das Endoskop 10 mm im Durchmesser.

ÄTZEN MIT GASEN

Mikroelektromechanische Systeme bieten vielseitige Funktionalität auf mikroskopisch kleinem Raum. Ein möglicher Einsatzbereich sind Sicherheitssysteme für den Straßenverkehr. Um die mechanischen Teile dieser Systeme auf Halbleiter aufzubringen, sind Ätzverfahren nötig – Probleme mit herkömmlichen Methoden verhinderten aber bisher die Herstellung im industriellen Maßstab. Ein neues Verfahren mit ätzenden Gasen soll Abhilfe schaffen. Entwickelt wurde es am Fraunhofer-Institut für Mikroelektronische Schaltungen und Systeme in Duisburg.

In der Herstellung von Mikrosystemtechnik kommen drei Schichten zum Einsatz: ein Substrat, eine Opferschicht als Abstandshalter und die Funktionsschicht. Da viele mechanische Teile von Mikrosystemen eine freitragende Struktur erfordern, muss unter diesen hindurch die Opferschicht weggeätzt werden. Das ist mit herkömmlichen Verfahren nicht möglich. So besteht zum Beispiel beim Ätzen mit Flüssigkeiten die Gefahr, dass während des Trocknens Funktionsteile am Substrat festkleben. Der Einsatz ätzender Gase umgeht dieses Problem und ermöglicht nun die Herstellung im großen Maßstab.

DENNIS HUGST



Mehr Sicherheit in Lagerhallen

Um Arbeitssicherheit zu gewährleisten, müssen Regale in Lagerhallen regelmäßig auf ihre Stabilität überprüft werden. Doch Kontrollgänge kosten Zeit und liefern nur eine Momentaufnahme. Einem effizienteren und preiswertigeren Schritt nennt ein neues Monitoring-System, das Forscher aus dem Fraunhofer-Institut für Mikroelektronische Schaltungen und Systeme IMS in Zusammenarbeit mit der FWS Handling Control entwickelt haben. Mittels eines drahtlosen Sensornetzwerks lässt sich

denen der Zustand jeder einzelnen Stange rund um die Uhr überwachen. Überdies werden die Regalstützen mit einer Art Luftkissen als Antifallvorkehrung versehen, die die Wucht von Stößen abfedern soll. Die Fraunhofer-Forscher haben in diese Schutzvorrichtung Sensoren integriert, die den Druck innerhalb der Luftkissen messen. Wird ein Luftkissen angepöpselt, registriert der Sensor die dadurch verursachte Druckerhöhung und meldet sie über eine Funkstrecke an eine Kontrollstation. Diese befindet sich etwa

im Büro des Lagerleiters. An weiteren Stellen in der Lagerhalle installierte Regalstützen nehmen die Meldungen der Sensoren entgegen und geben sie an die Kontrollstation weiter. Der Lagerleiter muss nur noch einen Blick auf das Display der Rechnerstation werfen, um zu wissen, wann und wo er in der Halle anhalten zu einer Kontrolle kam. Dabei zeigt ihm das System automatisch an, ob er sich an einem harmlosen, mittelstarken oder schweren Aggressiv handelt. www.ims.fraunhofer.de



Sensornetz
Wald-Mikroklima drahtlos überwacht

Auswirkungen der Klimaveränderung auf die Wälder sowie den Grad der Schadstoffbelastung überwacht ein drahtloses Sensornetz des Fraunhofer IMS. Damit lassen sich relevante Parameter innerhalb eines Ansatz an vielen Positionen gleichzeitig messen. Man erhält ohne großen Installationsaufwand ein detailliertes Bild über die Umweltbedingungen vor Ort. Je nachdem, welche Werte sie messen sollen – etwa den Durchdringungswinkel des Bodens, die Lufttemperatur oder die Blattfeuchte – werden die verschiedenen Sensorknoten in

Waldböden oder an Zweigen gebracht. Bei Bedarf können Messpositionen ohne großen Aufwand verändert werden. Die intelligenten Mini-Computer vernetzen sich selbstständig und steuern den Transport von Messdaten innerhalb dieses Netzes. Per Mikrokabel werden die Ergebnisse eine zentrale Baumbestandsdatenbank übertragen.

Technische Details

- Mobilfunkmodem
- Batteriekapazität über 1 Jahr
- Fraunhofer IMS

Fraunhofer www.ims.fraunhofer.de

Green Energy Technology, August 2011

F&H Fördern und Heben, Mai 2011

Fensterkontakte – drahtlos, autark und wartungsfrei

Sensorenkontaktlose Fensterkontakte melden an, welche Fenster im Haus offen oder geschlossen sind. Forscher haben jetzt ein besonders kontaktloses und autarkes System entwickelt, das ohne Kabel oder Batterien auskommt.

Hilft alle wichtigen Stellen im Haus zu erkennen, um alle Durchdringungswinkel des Bodens, die Lufttemperatur oder die Blattfeuchte zu messen. Man erhält ohne großen Installationsaufwand ein detailliertes Bild über die Umweltbedingungen vor Ort. Je nachdem, welche Werte sie messen sollen – etwa den Durchdringungswinkel des Bodens, die Lufttemperatur oder die Blattfeuchte – werden die verschiedenen Sensorknoten in Waldböden oder an Zweigen gebracht. Bei Bedarf können Messpositionen ohne großen Aufwand verändert werden. Die intelligenten Mini-Computer vernetzen sich selbstständig und steuern den Transport von Messdaten innerhalb dieses Netzes. Per Mikrokabel werden die Ergebnisse eine zentrale Baumbestandsdatenbank übertragen.

Wichtig waren drahtlose Module, die sich an Stellen, die für den Menschen unzugänglich sind, leicht integrieren lassen. Ein solches System wurde entwickelt, das ohne Kabel oder Batterien auskommt. Die Forscher haben ein besonders kontaktloses und autarkes System entwickelt, das ohne Kabel oder Batterien auskommt. Die Forscher haben ein besonders kontaktloses und autarkes System entwickelt, das ohne Kabel oder Batterien auskommt.



Deutsches Handwerksblatt, Oktober 2011

Crash-Sensor erhöht Sicherheit in Lagerhallen

Um Arbeitssicherheit zu gewährleisten, müssen Regale in Lagerhallen regelmäßig auf ihre Stabilität überprüft werden. Doch Kontrollgänge kosten viel Zeit und liefern nur eine Momentaufnahme. Fraunhofer-Forscher haben ein drahtloses sensorbasiertes System entwickelt, das den Zustand der Regale kontinuierlich überwacht.

An Ende eines langen Arbeitstages möchte der Lagerist noch schnell die letzten Punkte überprüfen. Ein wenig zu schmerzvoll bricht er das Geländegerüst zum Regal und fährt dabei eine Stange an. Eine alltägliche Situation in großen Lagerhallen, in denen die Mitarbeiter mit einer Zerknirschung die Ware durch enge Gänge manövrieren müssen. Auch **harmlose Stöße können Regalstützen destabilisieren**.

Doch selbst harmlose Stöße sind nicht ohnebedeutend, denn ein Lösen an einem der Regalstützen destabilisiert. Im schlimmsten Fall droht ein Einsturz der Hochregale eine erhebliche Gefahr für die Angestellten. Daher müssen die Stützen regelmäßig auf Schäden kontrolliert werden. Bildung integriert ein

Schutzsystem ein kontaktloses Monitoring-System, das Forscher aus dem Fraunhofer-Institut für Mikroelektronische Schaltungen und Systeme (IMS) in Duisburg in Zusammenarbeit mit der FWS Handling Control entwickelt haben. Mittels eines drahtlosen Sensornetzwerks lässt sich damit der Zustand jeder einzelnen Stange rund um die Uhr überwachen.

Die Anforderungen an den Betrieb von Regalsystemen haben sich mit Einführung der Europäischen Norm DIN EN 15670 erheblich erhöht. Regelmäßige Überprüfungen sind verpflichtend geworden, so Dr. Werner, Geschäftsführer von FWS Handling.

Display zeigt an, wann und wo ein Aggressiv getroffen hat

Fragesteller an IMS. Wird ein Luftkissen angepöpselt, registriert der Sensor die dadurch verursachte Druckerhöhung und meldet sie über eine Funkstrecke an eine zentrale Kontrollstation. Diese befindet sich etwa im Büro des Betriebsleiters. An weiteren Stellen in der Lagerhalle installierte Regalstützen nehmen die Meldungen der Sensorknoten entgegen und geben sie an die Kontrollstation weiter. Der Betriebsleiter muss nur noch einen Blick auf das Display der Rechnerstation werfen, um zu wissen, wann und wo er in der Halle anhalten zu einer Kontrolle kam. Dabei zeigt ihm das System automatisch an, ob er sich an einem harmlosen, mittelstarken oder schweren Aggressiv handelt.

Das System zeigt ihm, wann und wo er sich an einem harmlosen, mittelstarken oder schweren Aggressiv handelt.



Drahtlose Fensterkontakte – wartungsfrei, energieautark

UNTERSCHIEDLICHE FENSTERKONTAKTE NEHMEN VIEL, WEIL DIE STRICHEN IN KASSE OFFEN ODER GESCHLOSSEN SIND. FÜR DIESEN HABEN SIE EIN DRABLOS KOMFORTABEL UND AUSREICHENDS SYSTEM ENTWICKELT, DAS SICH KEINEM WARTUNGSAUFWAND UNTERZIEHT.

Handwerk ist ein Beruf, der sich nicht nur um die Produktion von Gütern, sondern auch um die Erhaltung dieser Güter kümmert. In der Fensterbranche ist dies besonders wichtig, da Fenster oft über Jahrzehnte hinweg in Gebrauch sind. Ein System, das die Fensterkontakte wartungsfrei und energieautark macht, ist daher ein wichtiger Schritt in der Entwicklung moderner Fenstertechnik.



Deutsches Handwerksblatt, Oktober 2011

Die Entwicklung dieser Kontakte ist ein Prozess, der viel Zeit und Mühe erfordert. Die Kontakte müssen nicht nur die mechanische Belastung standhalten, sondern auch die elektrischen Anforderungen erfüllen. Ein System, das diese Anforderungen erfüllt, ist ein wichtiger Bestandteil moderner Fenstertechnik.

Die Kontakte sind ein wichtiger Bestandteil moderner Fenstertechnik. Sie ermöglichen eine zuverlässige Überwachung des Fensterstatus, ohne dass Wartung oder Energiezufuhr erforderlich sind.

Die Entwicklung dieser Kontakte ist ein Prozess, der viel Zeit und Mühe erfordert. Die Kontakte müssen nicht nur die mechanische Belastung standhalten, sondern auch die elektrischen Anforderungen erfüllen.

Die Kontakte sind ein wichtiger Bestandteil moderner Fenstertechnik. Sie ermöglichen eine zuverlässige Überwachung des Fensterstatus, ohne dass Wartung oder Energiezufuhr erforderlich sind.

Anwenderforum drahtlose Sensorik bringt Industrie und Forschung zusammen

Mit einem Anwenderforum drahtlose Sensorik am 8. November in Dusseldorf will das Fraunhofer Institut für Mikroelektronische Systeme IMS die wichtigen Player aus Industrie und Forschung bei einem für den Industriestandort Deutschland wichtigen Thema an einen Tisch bringen.

Deutschland ist ein Hochtechnologie- und Hochleistungsland mit einer hohen Automatisierungsrate in Fertigung und Logistik. Um diese Vorteile zu nutzen, ist es wichtig, drahtlose Sensorik zu integrieren, um die Produktion zu optimieren.

- Diskutieren technischer Möglichkeiten
- Definition von Fertigungs- und Logistikprozessen
- Abstimmung von Partnerschaften und Kooperationen

Neben der Fachbeiträge werden ebenfalls Expertenreferate und Diskussionsrunden angeboten. Es besteht die Gelegenheit für Diskussionsrunden, um die Herausforderungen zu diskutieren.



Process Online, August 2011

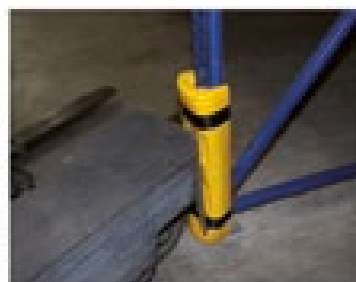
Crash-Sensor erhöht Sicherheit in Lagerhallen

Produktion Nr. 20-18, 2011

Ein vom Fraunhofer-Institut für Mikroelektronische Schaltungen und Systeme IMS entwickeltes Monitoring-System bietet einen verbesserten Schutz in Hochregallagern.

Entstehung (18). Am Ende des Arbeitstages werden die Lagerregale oft nicht vollständig entleert. Dies kann zu Schäden an den Regalen führen, wenn diese überlastet werden. Ein System, das dies verhindert, ist ein wichtiger Bestandteil moderner Lagerhaltungstechnik.

Die Entwicklung dieses Systems ist ein Prozess, der viel Zeit und Mühe erfordert. Das System muss nicht nur die mechanische Belastung standhalten, sondern auch die elektrischen Anforderungen erfüllen.



Das System ist ein wichtiger Bestandteil moderner Lagerhaltungstechnik. Es ermöglicht eine zuverlässige Überwachung des Lagerstatus, ohne dass Wartung oder Energiezufuhr erforderlich sind.

Für die Entwicklung dieses Systems ist ein Prozess, der viel Zeit und Mühe erfordert. Das System muss nicht nur die mechanische Belastung standhalten, sondern auch die elektrischen Anforderungen erfüllen.

Die Entwicklung dieses Systems ist ein Prozess, der viel Zeit und Mühe erfordert. Das System muss nicht nur die mechanische Belastung standhalten, sondern auch die elektrischen Anforderungen erfüllen.

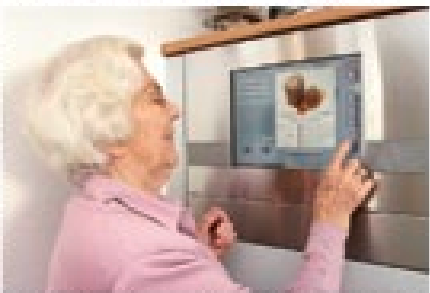
Feldtest in größerem Warenlager ist geplant

Die voraussichtliche Ende März werden die Warenlager einen

Bewohner am Bildschirm: Brauche Brot!

Das Fraunhofer IPT hat ein Prototypen-System entwickelt, das die Lebensqualität von älteren Menschen verbessern soll. Die interaktive Kommunikation wird durch Touchscreens ermöglicht und kann über ein Smartphone gesteuert werden.

„Die Idee ist, dass ältere Menschen über ein Touchscreen mit einem virtuellen Assistenten kommunizieren können. Dieser Assistent kann ihnen helfen, wichtige Informationen zu finden, Termine zu vereinbaren oder einfach nur mit ihnen zu plaudern.“



Das Fraunhofer IPT hat ein Prototypen-System entwickelt, das die Lebensqualität von älteren Menschen verbessern soll.

99 Die Idee ist, dass ältere Menschen über ein Touchscreen mit einem virtuellen Assistenten kommunizieren können.

Fränkischer Tag, Juli 2011

Der Helfer im Spiegel

Wohnungen werden künftig «wiser», was ihre Bewohner an. Gesucht sind Ingenieure, die diese das helfen können.

SPECIAL: INGENIEURE & TECHNIKER Ingenieurwissen wird zunehmend intelligenter. Ingenieure bauen zwar auch heute ganz handlich Brücken, Tunnel und Häuser (ausnahmslos auch der Superlative, siehe Seite 88), aber immer öfter stülzen sie die Digitalen, wie dieses Special zeigt. In Eigenregie werden Studieninteressierte heraus, was sich die nächsten Jahre bis. Am Ende können sie vielleicht auch hier ein Messerchen lassen (Seite 88). Tipprechtlich kamisch, dass sich nicht mehr Schulabgänger für technische Studiengänge mit festen Jahresarbeitsverträgen entscheiden (Seite 88).

Die Idee von Michael Beale ist ein wie eine digitale Wohnung. Die Möbel sind aus festen Holz und aus Glas, werden Oberflächen verändert, große Fenster lassen viel Licht herein, ein Fernseher zeigt im Hintergrund eine kleine Welt. Beale sagt: Die wichtigste Funktion ist es nicht, was die Wohnung tun kann, sondern dass sie ein intelligentes Haus ist, das die Bewohner mit sich selbst verbindet. Beale sagt: Die wichtigste Funktion ist es nicht, was die Wohnung tun kann, sondern dass sie ein intelligentes Haus ist, das die Bewohner mit sich selbst verbindet.

Beale sagt: Die wichtigste Funktion ist es nicht, was die Wohnung tun kann, sondern dass sie ein intelligentes Haus ist, das die Bewohner mit sich selbst verbindet. Beale sagt: Die wichtigste Funktion ist es nicht, was die Wohnung tun kann, sondern dass sie ein intelligentes Haus ist, das die Bewohner mit sich selbst verbindet.

Die Wohnung im Teil eines Projekts des Fraunhofer IPT ist in Dresden. Die wurde speziell für die alte und teilweise pflegebedürftige Menschen entwickelt. Die wichtigsten Funktionen sind: Ein virtuelles Teamwerk, was die Bewohner an wichtige Orte, erleichtert die Kommunikation innerhalb der Wohnung und ermöglicht es, die Bedürfnisse von Pflegepersonal zu berücksichtigen. Es soll es möglich machen, besser selbstständig in ihrer zu wohnen und Abhängigkeit von Pflegepersonal zu vermeiden. Diese Wohnungen ist es, die

Interaktivität (IPT) entwickelt. „Die Idee ist, dass ältere Menschen über ein Touchscreen mit einem virtuellen Assistenten kommunizieren können.“

Die Zeit, September 2011

Fraunhofer hofft auf den Preis des Publikums

Im Rahmen der Feierlichkeiten zum zehnjährigen Bestehen am 6. April wurde das Fraunhofer-Innovations-Zentrum als „Ausgewählter Ort 2011“ im Land der Ideen gekürt. In diesem Jahr hat die Publikumsstimme die Möglichkeit aus den 262 „Ausgewählten Orten 2011“ des Publikums zu wählen. Die Wahl startete am gestrigen Montag. Der Wettbewerb „262 Orte im Land der Ideen“ wird von der Bundesministerin für Wirtschaft und Innovationen, Ilse Aigner, in Kooperation mit der Deutschen

WAZ Duisburg, August 2011

Mobilität wird zunehmend rational

Automobil-Wissenschaftler beobachten einen Trend zu mehr Nüchternheit im Umgang mit der Mobilität. Nach ihren Einschätzungen wird der Pkw der Zukunft praktisch sein und elektronisch hochgerüstet. Darüber hinaus wird er nicht nur einem allein gehören. Das „eigene“ Auto tritt in den Hintergrund.

VDI Nachrichten, Duisburg, 26. 8. 11. „Für auf der ganzen Welt große der Pkw auf den Ruf eines Notrufsystems oder im Austausch der Personalität - noch. Nach Programmen von Marketingern und Soziologen könnte diese Aufgabe in einigen Jahren der Vergangenheit angehören. Denn die jüngere Generation legt auf den Besitz eines eigenen Autos keinen besonderen großen Wert mehr. Zwar wollen auch die Jungen von A nach B gelangen, doch über die Wahl der Verkehrsmittel entscheiden immer

wichtigen Faktoren eine große Rolle.“ Japan mit seinen überfüllten Städten ist für viele ein erhellendes Beispiel. „Die Mütter der 30- bis 40-Jährigen in Tokio haben kein Interesse an einem eigenen Auto, weil es keinen Sinn mehr hat.“ Anders sei das bei der Generation der 20er-Jahre. Die wollen sich ein eigenes Auto leisten. Für die Automobilindustrie sei der Abwärtstrend noch kein Problem. Der Absatz werde sogar leicht zunehmen, etwa durch Mieten in Osteuropa. „Aber in 20

Alte die Smartphons seien ein Beispiel dafür, dass die Technik zwar immer komplexer werde, die Anwendung aber immer simpler. Für Senioren könnte ein Verkehrsmittel für die Mobilität im Auto, das sich bald über Touchscreens bedienen lassen könnte und gleich über das Smartphone, mit dem der Fahrer das Klimateure, Musikanlage und vieles mehr steuern könnte. „Der Trend geht dahin, dass das Auto als Internet angeschaltet wird“, so Christophorus Scherer. Die technische Hochrüstung habe indes auch Grenzen.

VDI Nachrichten, Juni 2011

Der Internetspiegel für das Badezimmer

Nur für kein Badewasser, Toilettern kein Händewaschen und eine virtuelle Einkaufsberatung - das Entwicklungslabor der New York Times will das Internet im Badezimmer bringen. Bestellt wird das System per Sprache oder Geste.

Am 12.08.2011. „Was sich ereignet ist, ist das Badewasser, Toilettern kein Händewaschen und eine virtuelle Einkaufsberatung - das Entwicklungslabor der New York Times will das Internet im Badezimmer bringen. Bestellt wird das System per Sprache oder Geste.“

Das System ist ein Spiegel, der die Nutzer mit virtuellen Einkaufsberatung versorgt. Die Nutzer können über die Sprache oder Geste bestellen. Das System ist ein Spiegel, der die Nutzer mit virtuellen Einkaufsberatung versorgt.

Das System ist ein Spiegel, der die Nutzer mit virtuellen Einkaufsberatung versorgt. Die Nutzer können über die Sprache oder Geste bestellen. Das System ist ein Spiegel, der die Nutzer mit virtuellen Einkaufsberatung versorgt.

Das System ist ein Spiegel, der die Nutzer mit virtuellen Einkaufsberatung versorgt. Die Nutzer können über die Sprache oder Geste bestellen. Das System ist ein Spiegel, der die Nutzer mit virtuellen Einkaufsberatung versorgt.

Das System ist ein Spiegel, der die Nutzer mit virtuellen Einkaufsberatung versorgt. Die Nutzer können über die Sprache oder Geste bestellen. Das System ist ein Spiegel, der die Nutzer mit virtuellen Einkaufsberatung versorgt.

Das System ist ein Spiegel, der die Nutzer mit virtuellen Einkaufsberatung versorgt. Die Nutzer können über die Sprache oder Geste bestellen. Das System ist ein Spiegel, der die Nutzer mit virtuellen Einkaufsberatung versorgt.

Handelsblatt.com, September 2011

Imprint

Copyright 2011 by Fraunhofer-Gesellschaft
Hansastraße 27 c
80686 München

Annual Report
Fraunhofer-Institut für Mikroelektronische
Schaltungen und Systeme

Director: Prof. Dr. rer. nat. A. Grabmaier

Addresses:

IMS Duisburg
Finkenstraße 61
47057 Duisburg

Phone +49(0)2 03/37 83-0

Fax +49(0)2 03/37 83-2 66

E-mail martin.van.ackeren@ims.fraunhofer.de

Internet www.ims.fraunhofer.de

Editorial Staff: Martin van Ackeren

